UNIVERSIDADE ESTADUAL PAULISTA
"JÚLIO DE MESQUITA FILHO"
Campus de Botucatu

Instituto de Biociências de Botucatu - Unesp

PERFIL TRANSCRICIONAL DO SECRETOMA DO MICROAMBIENTE TUMORAL PARA IDENTIFICAÇÃO DE POTENCIAIS MEDIADORES DE CAQUEXIA.

SARAH SANTILONI CURY

BOTUCATU – SP

2022

UNIVERSIDADE ESTADUAL PAULISTA
"Júlio de Mesquita Filho"
INSTITUTO DE BIOCIÊNCIAS DE BOTUCATU

PERFIL TRANSCRICIONAL DO SECRETOMA DO MICROAMBIENTE TUMORAL PARA IDENTIFICAÇÃO DE POTENCIAIS MEDIADORES DE CAQUEXIA.

CANDIDATA: SARAH SANTILONI CURY

ORIENTADOR: PROF. DR. ROBSON FRANCISCO CARVALHO

Tese apresentada ao Instituto de Biociências, Campus de Botucatu, UNESP, como parte dos pré-requisitos necessários para obtenção do título de Doutor no Programa de Pós-Graduação em Ciências Biológicas (Genética).

BOTUCATU – SP

2022

Ficha catalográfica

FICHA CATALOGRÁFICA ELABORADA PELA SEÇÃO TÉC. AQUIS. TRATAMENTO DA INFORM.
DIVISÃO TÉCNICA DE BIBLIOTECA E DOCUMENTAÇÃO - CÂMPUS DE BOTUCATU - UNESP
BIBLIOTECÁRIA RESPONSÁVEL: ROSANGELA APARECIDA LOBO-CRB 8/7500

Cury, Sarah Santiloni.
Perfil transcricional do secretoma do microambiente tumoral para identificação de potenciais mediadores de caquexia / Sarah Santiloni Cury. - Botucatu, 2022

Tese (doutorado) - Universidade Estadual Paulista "Júlio de Mesquita Filho", Instituto de Biociências de Botucatu
Orientador: Robson Francisco Carvalho
Capes: 20205007

1. Biologia computacional. 2. Biologia de sistemas. 3. Caquexia. 4. Secretoma.

Palavras-chave: Bioinformática; Biologia de sistemas; Caquexia associada ao câncer.

Dedicatória

À Deus, Ademir Santiloni e aos pacientes, dedico.

Agradecimentos

Ao meu marido *Leandro Santos.*

Aos meus familiares, em especial minha mãe *Valquiria Santiloni*, meu irmão *Caio Santiloni Cury* e minha avó *Valquiria Cury*.

Aos meus parceiros de pós-graduação *Jakeline Oliveira, Amanda Schnepper, Victória Schmidt, Eliane Pilan, Jeferson Souza e Ana Luiza Bonaldo.* Aos parceiros de Laboratório de Biologia do Músculo Estriado (LBME) *Bruna Zanella*, *Jéssica Silvino*, *Érika Perez*, *Guilherme Gutierrez* e professora *Maeli Dal Pai*.

Aos colaboradores desse trabalho *Diogo de Moraes, Dra. Paula Paccielli Freire, Jakeline Oliveira, Dra. Érica Nishida Hasimoto, Dra. Patricia Pintor dos Reis e Dr. Miguel Batista.*

Aos pacientes que participaram deste estudo.

A todos os meus amigos e colaboradores.

Ao Departamento de Clínica Genética do Hospital de Vejle, Dinamarca. Em especial *à Dra. Silvia Rogatto, Dra. Luisa Matos do Canto* e *Naiade Calanca.*

Aos funcionários, docentes e alunos do Departamento de Biologia Estrutural e Funcional do Instituto de Biociências de Botucatu (IBB) – UNESP.

Aos membros da banca de avaliação da qualificação e tese do doutorado: *Dr. Otávio Marques, Dr. Dr. Luiz Araújo, Dra. Silvia Rogatto, Dra. Graziela Romagnoli, Dr. João Agostinho Machado Neto, Dra. Patricia Pintor dos Reis e Dr. Luis Fernando Barbisan.*

Ao programa de Pós-Graduação Ciências Biológicas (Genética) do Instituto de Biociências de Botucatu (IBB) - UNESP.

Ao Conselho Nacional de Desenvolvimento Científico e Tecnológico (CNPq) pelo auxílio financeiro (Processo: 141601/2019-1) cedido para execução deste trabalho.

Ao meu orientador professor *Robson Francisco Carvalho.*

Epígrafe

A Sabedoria é resplandecente e sempre viçosa. Ela é facilmente contemplada por aqueles que a amam, e se deixa encontrar por aqueles que a procuram. Ela até se antecipa, dando-se a conhecer aos que a desejam. Quem por ela madruga não se cansará, pois a encontrará sentada à sua porta. Meditar sobre ela é a perfeição da inteligência; e quem ficar acordado por causa dela em breve há de viver despreocupado. Pois ela mesma sai à procura dos que a merecem, cheia de bondade, aparece-lhes nas estradas e vai ao seu encontro em todos os seus projetos.

(Livro da Sabedoria 6,12-16)

Sumário

Resumo

A caquexia é uma síndrome metabólica comumente encontrada em pacientes com cânceres de pâncreas ou pulmão. É caracterizada pela perda de massa muscular, com ou sem perda de tecido adiposo, a qual não pode ser revertida por suporte nutricional, e que induz pior resposta aos tratamentos radio e quimioterápicos e menor sobrevida. Os pacientes com caquexia apresentam alterações funcionais em processos fisiológicos, metabólicos e imunológicos, que resultam em desequilíbrio energético e proteico. Mediadores plasmáticos circulantes (fatores indutores de caquexia; FICs) desempenham um papel crucial no desenvolvimento de alterações sistêmicas que ocorrem na caquexia associada ao câncer. Embora muitos fatores derivados do tumor já tenham sido implicados com a patogênese da síndrome, as associações foram geralmente baseadas em seus níveis plasmáticos ou no perfil de expressão gênica na massa tumoral, mas ainda não é conhecido perfil de expressão dos FICs em células específicas que compõe o microambiente tumoral (MAT). Além das células tumorais, o MAT é composto por células residentes e recrutadas e pelas moléculas secretadas por essas células (secretoma). O presente projeto tem como objetivos caracterizar: 1) o perfil transcricional do secretoma de células do MAT de pacientes com câncer de pulmão (carcinoma pulmonar de células não pequenas; CPCNP), e 2) o perfil de expressão de FICs secretados em células individuais de pacientes com câncer de pâncreas (adenocarcinoma ductal pancreático; ADP). Para isso, foram utilizados dados de expressão gênica global, disponíveis publicamente, de pacientes potencialmente caquéticos com CPCNP (determinados por análises tomográficas) e ADP, separadamente. Os dados transcriptômicos dos componentes do secretoma foram correlacionados com dados clínicos e de composição de células do sistema imune do MAT. Finalmente, avaliamos computacionalmente a potencial ação sinérgica de FICs, selecionados do secretoma, e sua interação com tecidos e órgãos afetados na caquexia através de predições de ligantes e receptores. Nossa estratégia permitiu identificar que pacientes caquéticos com CPCNP apresentam altos níveis de expressão de citocinas pró-inflamatórias derivadas principalmente de células T CD8. Além disso, esses pacientes apresentam um aumento de células exauridas em seu MAT. Para a análise dos pacientes com câncer de pâncreas, foi possível caracterizar o perfil celular de mediadores centrais da caquexia em resolução de células única, e predizer suas interações com receptores de tecidos-alvo na caquexia. Esses mediadores foram detectados como expressos em altos níveis pelas células neoplásicas pancreáticas. Dessa forma, nossos achados caracterizam o perfil de expressão de FICs secretados por células específicas do MAT em tumores de pulmão e pâncreas, bem como suas interações com o músculo esquelético, fígado e tecido adiposo. Em conjunto, nossos resultados servirão de base para o desenvolvimento de futuras estratégias

terapêuticas visando à minimização da perda de massa muscular, aumentando, assim, a sobrevida e a qualidade de vida dos pacientes com caquexia associada aos cânceres de pulmão e pâncreas.

Abstract

Transcriptional Profile of Tumor Microenvironment Secretome for Identification of Potential Cachexia Mediators.

Cachexia is a metabolic syndrome commonly found in pancreatic and lung cancer patients. It is characterized by loss of muscle mass, with or without loss of adipose tissue, which cannot be reversed by nutritional support, which induces worse response to radio and chemotherapy and lower survival. Cachectic patients have functional changes in physiological, metabolic, and immunological processes that result in energy and protein imbalance. Circulating plasma mediators (cachexia inducing factors; CIFs) play a crucial role in the development of systemic alterations that occur in cancer-associated cachexia. Although many tumor-derived factors have already been implicated in the pathogenesis of the syndrome, the associations were generally based on their plasma levels or gene expression profile in bulk tumor tissues, but the CIFs expression profile in single cells within the tumor microenvironment (TME) is not yet known. In addition to cancer cells, TME is composed of resident host cells and recruited cells, the products secreted by these cells (secretome). This project aims to characterize: 1) the secretome transcriptional profile of the TME cells from patients with lung cancer (non-small cell lung carcinoma; NSCLC), and 2) the expression profile of secreted CIFs in single cells of patients with pancreatic cancer (ductal adenocarcinoma). pancreatic; PDAC). Publicly available global gene expression data from potentially cachectic patients with NSCLC (determined by CT scans) and PDAC were individually evaluated. Transcriptomics data of secretome factors were correlated with clinical data and tumor immune composition of TME. Finally, we computationally evaluated the potential synergistic action of CIFs, selected in the secretome, and their interactions with tissues and organs affected in cachexia using predictions of ligands and receptors. Our strategy allowed us to identify NSCLC cachectic patients with high expression of pro-inflammatory cytokines mainly derived from CD8 T cells. In addition, these patients showed an increase in exhausted cells in their TME. In pancreatic cancer, it was possible to identify a core of pro-cachectic mediators, in single-cell resolution, able to interact with receptors in cachexia target tissues. These mediators are expressed at high levels by pancreatic neoplastic cells. Thus, our findings point to cachexia mediators secreted by specific TME cells in lung and pancreatic tumors with the potential to interact with muscle, liver, and adipose tissue. Taken together, our results may contribute as a basis for the development of future therapeutic strategies aiming to decrease muscle mass loss, thus increasing the survival and quality of life of patients with cancer cachexia.

1. *Introdução*

Caquexia associada ao câncer

A caquexia é definida como uma síndrome metabólica complexa caracterizada pela perda de massa muscular, com ou sem perda de tecido adiposo, a qual não pode ser revertida por suporte nutricional[1]. Os pacientes com essa síndrome apresentam alterações funcionais em processos fisiológicos, metabólicos e imunológicos que resultam em desequilíbrio energético e proteico[2]. A caquexia pode estar associada com resistência à insulina, anorexia e inflamação[1].

Existe uma variedade de condições agudas ou crônicas associadas à caquexia. A síndrome é observada em pacientes após extensa lesão traumática e sepse[3]. Doenças infecciosas, como AIDS, malária e tuberculose, assim como doenças crônicas como fibrose cística, cirrose hepática, doença de Crohn, artrite reumatoide, acidente vascular cerebral, doenças degenerativas neurológicas, doença renal crônica, doença pulmonar obstrutiva crônica, insuficiência cardíaca crônica e o câncer também estão frequentemente associadas a caquexia[3–6].

A caquexia associada ao câncer é uma síndrome multifatorial que afeta até 80% dos pacientes em estágios avançados da doença, e representa a causa direta de morte de até 20% de todos os pacientes oncológicos[7]. A caquexia está altamente associada a tipos específicos de tumores, como o de pâncreas, esôfago, estômago, fígado e pulmão e, da mesma forma, os pacientes com essas neoplasias têm o mais alto grau de perda de peso[8–13]. Em contrapartida, os pacientes acometidos por câncer de tireoide, mama, melanoma ou próstata apresentam um menor risco em desenvolver a síndrome (20-30% dos pacientes)[14]. A etiologia da caquexia associada ao câncer nos diferentes tipos tumorais envolve interações complexas e específicas entre o tumor e o hospedeiro que ainda não estão completamente elucidadas.

A característica clínica mais proeminente da caquexia associada ao câncer é a perda de peso nos adultos, a qual pode ser corrigida pela retenção fluídica[15]. A caquexia no câncer emerge a partir

de alterações metabólicas induzidas pela presença do tumor, a qual acarreta perda de apetite (anorexia), anemia, baixos níveis de testosterona e de outros hormônios anabólicos[15]. A diminuição na ingestão do alimento e a anorexia acentuam a perda de massa muscular e corpórea, resultando numa condição de astenia, fraqueza, imobilidade e insuficiência cardíaca ou respiratória[16]. O estado caquético no câncer representa prognóstico desfavorável, e diminuição da qualidade de vida e da resposta aos tratamentos radio e quimioterápicos[17,18]. A caquexia afeta uma proporção considerável de pacientes com câncer de pulmão[19], com até 80% dos pacientes apresentando alto risco de desenvolver a síndrome dependendo do estágio tumoral[14].

Caquexia associada ao câncer de pulmão

O câncer de pulmão é o mais comum no mundo - mais de 2 milhões de novos casos foram diagnosticados em 2020 - e é o que mais leva ao óbito, sendo responsável por mais de 1 milhão de mortes[20]. Segundo o INCA (Instituto Nacional de Câncer, 2020, http://www.inca.gov.br/), no Brasil, são estimados 17.760 novos casos de câncer de traqueia, brônquios e pulmão entre os homens, e 12.440 novos casos entre as mulheres[21]. O câncer de pulmão é uma das principais causas de morte evitáveis, pois é geralmente diagnosticado em estágios mais avançados da doença[22]; a sobrevida média em um total de cinco anos varia entre 13 a 21%, em países desenvolvidos, e entre 7 e 10%, nos países em desenvolvimento[21]. O câncer de pulmão apresenta-se em duas formas principais, que são classificadas de acordo com sua característica histológica: câncer pulmonar de células pequenas (CPCP, da sigla, em inglês, SCLC, *Small-Cell Lung Cancer*), que representa cerca de 15% de todos os tipos de câncer de pulmão, e o câncer pulmonar de células não pequenas (CPCNP, da sigla, em inglês, NSCLC, *Non-Small-Cell Lung Cancer*), que prevalece em cerca de 85% dos casos[22,23]. Os CPCNP mais frequentes são de três subtipos: adenocarcinoma, carcinoma de células escamosas (*Squamous-cell carcinoma*, em inglês) e carcinoma de grandes células (em inglês, *Large-cell Lung Cancer*)[23], sendo o adenocarcinoma e o carcinoma de células escamosas os mais comumente encontrados na população[23,24]. O fumo ou

exposição passiva ao tabaco estão associados à 90% dos casos de câncer de pulmão[25]. Fumar pode causar todos os tipos de câncer, porém, está fortemente relacionado com CPCP e carcinoma de células escamosas; e o adenocarcinoma é o tipo mais comum em pacientes não fumantes[23]. Além dos diferentes fatores de riscos envolvidos com a etiologia de cada subtipo, sabe-se que o subtipo pode determinar o melhor tratamento[26]. Os subtipos de CPCNP possuem distinções moleculares importantes: mutações em *EGFR* e translocações em *ALK* são aberrações gênicas frequentemente encontradas em pacientes com adenocarcinoma pulmonar[27]. As terapias personalizadas para essas alterações em adenocarcinomas mostraram-se eficazes para o tratamento da doença quando comparado à quimioterapia padrão[28]. Esses achados, além de modificar a forma de tratar esses pacientes, mudou também a classificação histopatológica do câncer de pulmão, pois a terminologia CPCNP não abrange essas especificidades. Em 2015, o termo CPCNP foi revisto e excluído, determinando-se os adenocarcinomas e carcinomas de células escamosas como os mais prevalentes tipos histológicos de tumores pulmonares epiteliais[26]. Entretanto, a prevalência de caquexia é geralmente reportada para CPCNP e CPCP, sem distinção dos subtipos[26]. Estima-se que 83% dos pacientes com CPCNP apresentam a síndrome, enquanto 61% dos pacientes com CPCP possuem caquexia-anorexia[29]. Pacientes com os subtipos mais prevalentes de CPCNP (adenocarcinomas e carcinomas de célula escamosas) apresentam caquexia em frequências similares[30]. Considerando-se que a caquexia tem maior prevalência em CPCNP do que em CPCP, e ainda, que o risco de desenvolvimento de caquexia é similar para os subtipos de CPCNP, este presente estudo busca ampliar a compreensão da caquexia considerando os pacientes com CPCNP, com enfoque em dados de adenocarcinoma e carcinomas de células escamosas combinados.

Embora existam avanços no diagnóstico precoce e tratamento padrão, o câncer de pulmão é frequentemente diagnosticado em um estágio avançado e tem prognóstico desfavorável[23]. Dentre as causas desse prognóstico desfavorável do câncer de pulmão, destaca-se o desenvolvimento de caquexia em muitos pacientes, o que contribui para maior mortalidade da doença; estima-se que apenas 20%

dos pacientes em risco de desenvolvimento da caquexia sobrevivem até 5 anos após o diagnóstico[14,31–33]. A perda de massa muscular esquelética na caquexia associada ao câncer de pulmão pode levar a uma substancial perda de peso e diminuição do índice de massa corporal (IMC), os quais estão associados a pior evolução em pacientes com CPCNP[31,34,35].

Estudos utilizando imagens de tomografia computadorizada (TC) revelaram perda de massa muscular oculta em pacientes com CPCNP com peso corporal estável[19,36]. Além disso, em pacientes com CPCNP, tanto a perda de massa muscular bem como a detecção, por imagens de TC, de uma menor área muscular (muscularidade) têm sido associadas a um menor tempo de progressão do tumor, maior risco de toxicidade por quimioterapia e menor sobrevida[19,36–41]. A perda de massa muscular, detectada por imagens de TC, também afeta negativamente o estado funcional e a qualidade de vida desses pacientes[42,43]. A detecção de uma área muscular através de imagens de TC tem sido associada à alterações nas concentrações de marcadores de inflamação (albumina sérica e proteína C-reativa) [revisado por Collins et al., [44]]. Estudo recente desenvolvido por nosso grupo de pesquisa demonstrou que a área dos músculos peitorais é um importante preditor de caquexia associada ao CPCNP, pois pacientes com baixa muscularidade apresentam aumento na expressão gênica de citocinas pró-inflamatórias, como IL-8, IL-6 e CSF3, no tecido tumoral, as quais estão associados a uma menor sobrevida[30]. **Entretanto, ainda não são totalmente conhecidos os mecanismos moleculares e as principais células tumorais que contribuem para a produção dessas citocinas nos carcinomas pulmonares.**

O câncer de pulmão é relevante para o estudo da caquexia e identificação de potenciais marcadores moleculares e alvos terapêuticos, pois é possível separar pacientes com câncer que desenvolvem a síndrome dos que não são acometidos, e investigar suas diferenças. ~~Entretanto,~~ a síndrome é ainda mais relevante no câncer de pâncreas, pois acomete 80-90% dos pacientes[13], portanto,

resultados identificados em câncer de pâncreas também podem auxiliar na compreensão da síndrome. Veremos isso com maiores detalhes no tópico abaixo.

Caquexia associada ao câncer de pâncreas

O tipo histológico de câncer de pâncreas mais comum é o adenocarcinoma, o qual se origina no tecido glandular (tumores na região exócrina), e podem surgir a partir do epitélio ductal ou de células acinares [45]. O adenocarcinoma ductal do pâncreas (ADP) representa 80-90% dos tipos histológicos[46]. Apesar de não ser um dos tipos de câncer mais incidente entre homens e mulheres - pois é responsável por cerca de 2% dentre todos os tipos de câncer diagnosticados - o câncer de pâncreas é agressivo e de difícil detecção, apresentando, portanto, alta taxa de mortalidade[21]. Estima-se que menos de 8% dos pacientes com câncer de pâncreas sobrevivem até cinco anos após o diagnóstico [47]. No Brasil, em 2018, cerca de 5.497 homens e 5.601 mulheres foram à obtido pela doença, de acordo com os dados publicados pelo INCA[21]. Mundialmente, o câncer de pâncreas, é a sétima principal causa de morte[48], mas projeta-se que futuramente o câncer de pâncreas irá ultrapassar o câncer de mama como a terceira principal causa de morte na Europa [49]. Em 2020, 495.773 novos casos foram diagnosticados no mundo e 466.003 pacientes foram a óbito, destacando-se, mais uma vez, a alta mortalidade do câncer de pâncreas[20]. Mesmo considerando a dificuldade de determinar quantas dessas mortes resultam diretamente da caquexia, é bastante evidente que a caquexia contribui significativamente para as altas taxas de mortalidade do câncer de pâncreas[50].

A caquexia associada ao ADP apresenta a maior prevalência dentre todos os tipos de câncer, sendo encontrada em 80 a 90% dos pacientes[13], podendo ocorrer até mesmo em pacientes em estágios iniciais da doença, em que a ressecção cirúrgica do tumor ainda é possível[51]. Por essa razão, o ADP é o câncer mais amplamente estudado na busca de biomarcadores da caquexia e de mecanismos moleculares pela qual a síndrome se estabelece[52–56]. Entretanto, ainda há certa discordância entre alguns achados. Embora IL-6, IL-1β, TNF-α, INF-γ sejam amplamente utilizados como biomarcadores

circulantes de caquexia capazes de induzir alterações morfofisiológicas no músculo esquelético[57], Talbert e colaboradores demonstraram baixos níveis séricos dessas citocinas inflamatórias em pacientes com ADP, as quais não se associaram à caquexia nas condições investigadas, mas outros fatores como leptina, GM-CSF e MCP-1 foram associadas à sindrome[52]. Esses resultados reforçam a necessidade de se estudar mais profundamente os fatores indutores de caquexia em pacientes com ADP para se atingir um consenso. Ainda assim, é evidente que a inflamação é extremamente relevante no câncer de pâncreas. De fato, nosso grupo de pesquisa demonstrou recentemente que o ADP apresenta aumento na expressão gênica de significativa parte dos mais conhecidos fatores indutores de caquexia, enquanto tumores menos associados à síndrome regulam positivamente apenas uma pequena parcela desses fatores[58]. Além disso, tumores pancreáticos com baixa pureza tumoral, ou seja, com baixa quantidade de células neoplásicas e alta quantidade de infiltração de células normais (como células imunes, fibroblastos, etc.) também expressam, em maiores proporções, os fatores que induzem caquexia[58]. Esses resultados demonstram que a inflamação derivada do microambiente tumoral tem um papel chave no desenvolvimento de caquexia. **Todavia, a caracterização das células que promovem a baixa pureza tumoral encontrada nos tumores de pâncreas, e por consequência, seus mecanismos moleculares que contribuem para o processo inflamatório, necessitam maiores investigações**.

Considerando a relevância da caquexia para o câncer de pulmão e de pâncreas, e ainda, a urgência de se compreender a influência do microambiente imune tumoral na indução de alterações imunológicas que contribuem para o estado caquético nesses pacientes, este estudo busca entender a origem da inflamação derivada de tumores de pulmão e pâncreas, como também investigar se os mecanismos imunológicos são semelhantes ou distintos em cada um dos tipos tumorais. Entretanto, a relevância da inflamação na caquexia é evidente para ambos os cânceres de pulmão e pâncreas.

Inflamação derivada do tumor na caquexia associada ao câncer

A etiologia da caquexia associada ao câncer no câncer de pâncreas e pulmão envolve interações tumor-hospedeiro muito complexas e específicas que ainda precisam ser completamente elucidadas. A ação combinatória de mediadores solúveis (fatores indutores de caquexia) secretados por células cancerosas e do microambiente tumoral[58], incluindo muitas citocinas pró-inflamatórias, contribuem para a inflamação sistêmica, e atuam diretamente no músculo esquelético induzindo a perda de massa muscular[13,18,59,60]. Consequentemente, os esforços para identificar mediadores e biomarcadores estão centrados nos níveis desses fatores caquéticos no plasma[52,61–65]. Muitos desses fatores que circulam no sangue são derivados de células cancerosas e do microambiente tumoral[58]. Entretanto, ainda não está claro quais são as principais células tumorais responsáveis pela produção desses fatores. Portanto, a caracterização do perfil de expressão gênica célula-específica tem o potencial de revelar padrões transcricionais que contribuem para compreensão dos mecanismos pelos quais ocorre o desenvolvimento de caquexia no câncer de pulmão e pâncreas.

Dentre as citocinas pró-inflamatórias associadas à caquexia, as interleucinas (IL-1β, IL-6), o fator de necrose tumoral (TNF-α) e o interferon (INF-γ) tem uma grande importância pois atuam sistemicamente para o desenvolvimento de alterações celulares e moleculares que resultam na perda de função e massa muscular[13,18,59]. Esses fatores caquéticos podem ser produzidos e secretados pela célula tumoral ou pelas células do microambiente tumoral (MAT)[13,66]. De forma geral, as citocinas pró-inflamatórias são liberadas na circulação sanguínea e induzem uma inflamação sistêmica que afeta principalmente o cérebro, fígado, e os tecidos adiposo e muscular esquelético, com consequente indução de anorexia, aumento da produção de proteínas de fase aguda, perda de tecido adiposo e massa muscular[18,67] (**Figura 1**). No entanto, a detecção dos níveis circulantes destas citocinas pró-inflamatórias geralmente são realizadas em pacientes com doença avançada, incluindo muitos pacientes submetidos à segunda ou terceira linhas de tratamento quimioterápico.

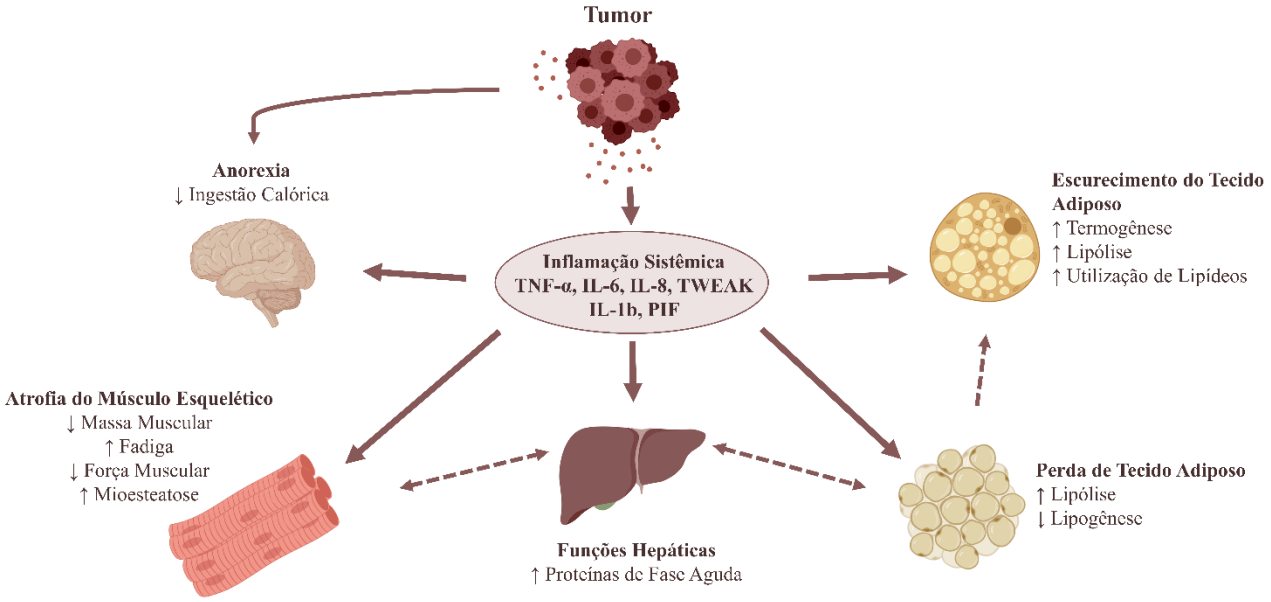

Figura 1. Alterações metabólicas em tecidos-alvo induzidas pelo secretoma tumoral durante a caquexia associada ao câncer. Citocinas pró-inflamatórias e fatores solúveis são secretados pelo microambiente tumoral e induzem alterações metabólicas em diversos órgão e tecidos: modificação do controle neuroendócrino do apetite no sistema nervoso central; escurecimento e perda do tecido adiposo; aumento da síntese de proteínas de fase aguda no fígado; e redução da massa muscular (adaptado de Tsoli & Robertson[18]).

A IL-6 também apresenta-se aumentada no soro de pacientes caquéticos em estágios iniciais e tardios da doença, e tem se mostrado essencial na atrofia muscular em diversos modelos experimentais de caquexia associada ao câncer[68,69]. A inibição da STAT3, um de seus alvos, atenua a perda de massa muscular, demonstrando o potencial dessa citocina como alvo farmacológico no tratamento da caquexia[70]. Os níveis circulantes de IL-6 também estão elevados em diversos modelos experimentais de caquexia associada ao câncer, nos quais apresenta um envolvimento direto na perda de massa muscular[71–74]. Medicamentos anti-IL-6 estão atualmente em desenvolvimento, sendo o anticorpo monoclonal humanizado clazakizumabe (ALD518) o único agente anti-IL6 específico que foi avaliado em ensaios clínicos para o tratamento da síndrome[75]. O ensaio clínico em fase II utilizando-se desse tratamento foi conduzido em uma população de 124 pacientes com CPCNP incuráveis, diagnosticados com caquexia definida por perda de peso corporal maior que 5% nos últimos 3 meses[76]. O clazakizumabe inibe a IL-6, é bem tolerado, e melhora a anemia e caquexia nesses pacientes[76,77], mas

não induz reversão do quadro e não altera a sobrevida global dos pacientes[78]. Inibidores de TNF-α e IL-1a também estão sendo testados em estudos clínicos de fases II e III. A talidomida (inibidor de TNF-α com ação anti-inflamatória) mostrou-se eficaz em aumentar o apetite e reduzir a perda de peso e massa magra em pacientes com caquexia associada ao câncer de pâncreas, e o MABp1 (anticorpo anti-IL-1a) aumentou significativamente a sobrevida e reduziu perda de massa muscular de pacientes com câncer colorretal (revisado por Cao et. al., [78]). Mais estudos são necessários para confirmar a eficácia dessas e outras drogas no tratamento da caquexia, pois ainda não há protocolo atual ou intervenção bem-sucedida para o tratamento da caquexia associada o câncer[78]. O único medicamento disponível atualmente para o tratamento da caquexia é a anamorelina – um agonista do receptor da grelina[79]. O medicamento foi aprovado, até o momento, para alguns tipos de câncer (CPCNP e cânceres gastrointestinais), somente no Japão[80]. Estudos clínicos de fase II e III demonstram que a anamorelina contribui para diminuição da perda de peso, recuperação de massa muscular, apetite e qualidade de vida, embora não tenha eficácia na recuperação da função muscular (força) e, tampouco, aumenta a sobrevida dos pacientes [78].

Outra importante citocina pró-inflamatória mais recentemente estudada na caquexia é a interleucina-8 (IL-8). A expressão de IL-8 nos tecidos tumorais está associada ao estado caquético e ao pior prognóstico em câncer de pâncreas[81,82]. Os pacientes caquéticos com alta expressão de IL-8 nos tecidos tumorais apresentaram menor sobrevida global ou sobrevida livre de doença[82]. Além disso, existe uma associação entre o aumento no nível de expressão de IL-8 em amostras de tumor pareadas com amostras de soro e o tamanho do tumor desses mesmos pacientes[82]. Também já foi demonstrado uma associação entre o aumento da IL-8 no microambiente tumoral e sistêmico com o aumento da perda de peso e massa muscular em camundongos induzidos à caquexia pelo xenotransplante de tumores pancreáticos de pacientes caquéticos[81]. Além disso, nosso grupo de pesquisa demonstrou que pacientes com câncer de pulmão que possuem menor área de músculos peitorais apresentam um

aumento de expressão gênica de *IL8* no tecido tumoral[30]. Ainda, nesse mesmo estudo, demonstramos que a IL-8 recombinante é capaz de induzir diretamente a atrofia em C2C12 miotubos "in vitro".

Essas informações demonstram que a caquexia associada ao câncer está extremamente relacionada com inflamação sistêmica, a qual parece ser provocada pelos efeitos do aumento de citocinas pró-inflamatórias e outros fatores solúveis produzidas pelo paciente em resposta ao tumor, ou ainda pelo tumor em si, em especial por fatores secretados por células do MAT (como revisado por Tsoli et al.,[18]). De fato, macrófagos ativados infiltrados no MAT de ratos caquéticos são responsáveis por secretar citocinas que podem contribuir para o desequilíbrio metabólico observado na caquexia[66]. Portanto, a análise do perfil de expressão de genes que codificam proteínas preditas como secretadas no MAT de pacientes com caquexia associada ao câncer de pulmão e pâncreas, bem como a determinação das células do MAT responsáveis pela secreção dessas moléculas, pode contribuir para a identificação de mediadores e biomarcadores da síndrome.

Microambiente tumoral na caquexia associada ao câncer

O MAT é composto por células tumorais e não tumorais que podem compreender: células neoplásicas, células hospedeiras residentes e recrutadas, produtos secretados dessas células (tais como citocinas e quimiocinas) e pelos componentes não celulares dispostos na matriz extracelular[83,84]. O MAT contém células do sistema imunológico, células de vasos sanguíneos e linfáticos, bem como fibroblastos, células epiteliais, pericitos e, eventualmente, adipócitos[85] (**Figura 2**). As células não tumorais do MAT têm uma função dinâmica e frequentemente promotora de tumores em todos os estágios da carcinogênese[86]. A comunicação intercelular no MAT é impulsionada por uma rede complexa e dinâmica de citocinas, quimiocinas, fatores de crescimento, enzimas de remodelação de matriz e citocinas inflamatórias num meio com grandes perturbações nas propriedades físicas e químicas do tecido[84].

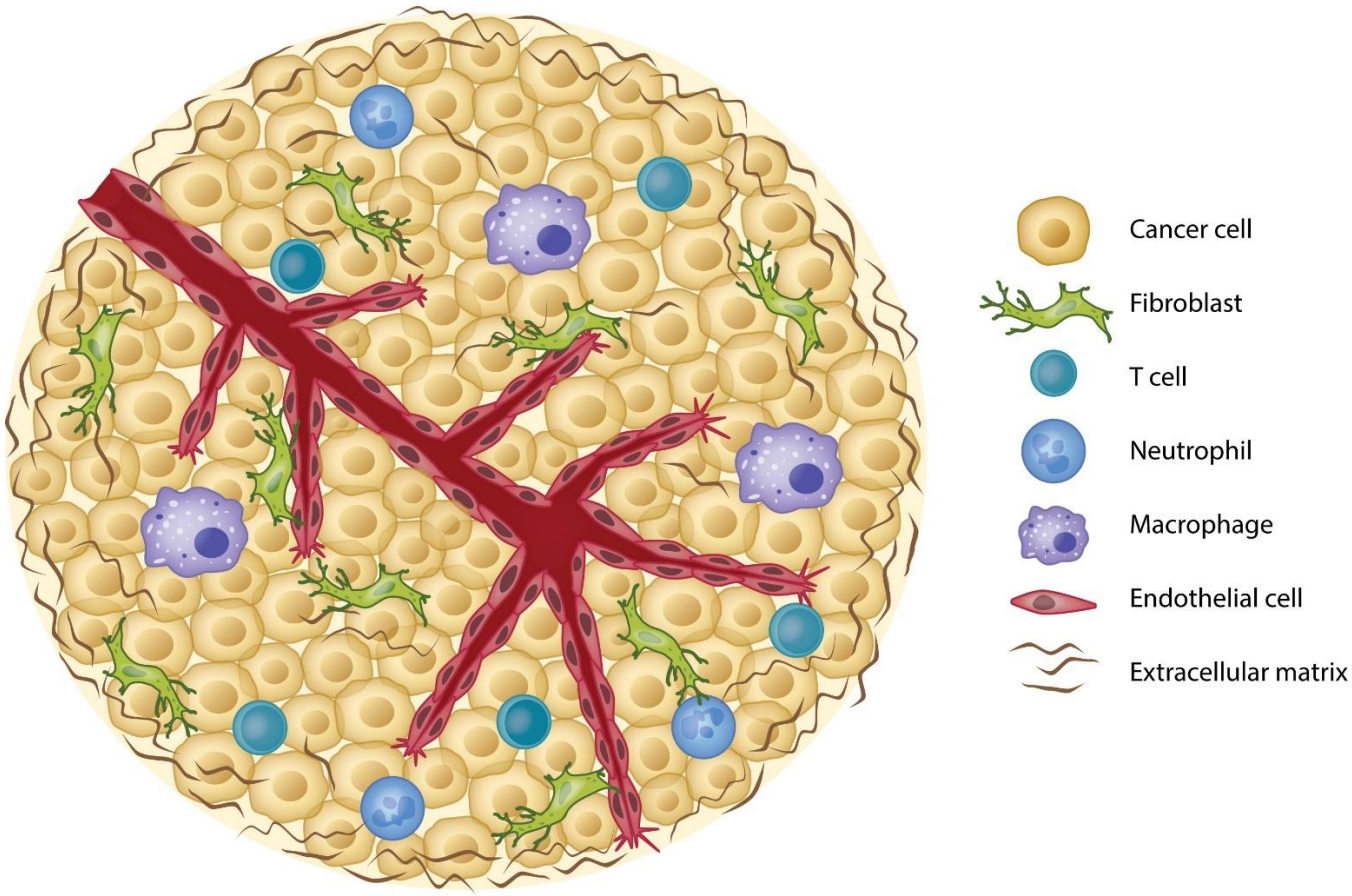

Figura 2. Esquema representativo da composição do microambiente tumoral, que pode consistir-se em: células neoplásicas, células estromais (fibroblastos e endoteliócitos), células imunes (células T, neutrófilos e macrófagos) e componentes acelulares da matriz extracelular. *Cancer cell*: célula neoplásicas; *Fibroblast*: fibroblasto; *T cell*: célula T; *Neutrophil*: neutrófilo; *Macrophage*: macrófago; *Endothelial cell*: células endoteliais; *Extracelullar matrix*: matriz extracelular. Ilustração criada por Lau and Vander Heiden, 2020 [87].

O MAT de diferentes órgãos é distinto e, portanto, intercomunicação entre células tumorais infiltrando um órgão específico e o microambiente desse órgão é diferente quando comparado com outros órgãos[83]. Dados genômicos e transcriptômicos derivados de amostras de massa tumoral têm sido utilizados para estudar o MAT; e as medidas de infiltração imune definem subtipos moleculares de câncer de ovário, melanoma e pâncreas[88–90], sendo a expressão de genes do sistema imune variável de acordo com o subtipo molecular em outros tipos tumorais[91]. A caracterização do microambiente

imune utilizando as assinaturas de expressão gênica, análise de receptores de células T, repertório de receptores de células B e análises para identificar alvos imunológicos neo-antigênicos, fornecem uma riqueza de informações em muitos tipos de câncer e têm valor prognóstico[92–100]. Uma extensa análise imunogenômica em mais de 10.000 casos, compreendendo 33 tipos diferentes de câncer, utilizando dados compilados do *The Cancer Genome Atlas* (TCGA) identificou seis subtipos imunes, classificados como: cicatrização de feridas, dominante de IFN-γ, inflamatório, depletado de linfócitos, imunologicamente silencioso e dominante de TGF-β. Esses subtipos foram caracterizados por diferenças nas assinaturas de macrófagos ou linfócitos, proporção de células Th1:Th2 e extensão da heterogeneidade intratumoral, aneuploidia, extensão da carga neo-antigênica, proliferação celular global, expressão de genes imunomoduladores e prognóstico[101]. Esse estudo demonstrou que o subtipo imunológico de cada tumor se associa ao desfecho clínico da doença, principalmente às taxas de sobrevida dos pacientes de acordo com seu subtipo.

Outro aspecto bastante relevante para compreensão do MAT é a pureza do tumor, determinada pela proporção de células malignas na composição heterogênea de tipos celulares que compõem o tumor. Até recentemente, a pureza do tumor era estimada por um patologista, principalmente por análise visual ou de imagem de células tumorais. Com o avanço das tecnologias genômicas, muitos novos métodos computacionais surgiram para inferir a pureza do tumor. Esses métodos fazem estimativas usando diferentes tipos de informações genômicas, como expressão gênica[102], variação de número de cópias somáticas[103–105], mutações somáticas[103,106] e metilação do DNA[103,107]. Aran *et al.* [108] realizaram uma análise *Pan-Cancer* utilizando 21 tipos tumorais do TCGA, a qual demonstrou que, independentemente do método utilizado, os padrões de pureza diferem por tipo de câncer, com alta pureza (acima de 90% de células neoplásicas) em carcinoma adrenocortical e glioma de baixo grau, e baixa pureza (<70% de células neoplásicas) em cânceres resultantes de exposições crônicas mutagênicas, como o adenocarcinoma de pulmão, carcinoma de células escamosas e carcinoma de células escamosas de cabeça e pescoço. Os tumores pancreáticos (principalmente) e pulmonares são

conhecidos por apresentarem a mais alta prevalência de caquexia[13,14], também apresentam baixa pureza tumoral, caracterizada por uma baixa celularidade neoplástica e uma alta fração leucocitária infiltrada no microambiente tumoral [101,109]. Além disso, os tumores de pâncreas classificados como de baixa pureza são aqueles que apresentam maior expressão de genes do secretoma associados à indução de caquexia[58].

Como a ação combinatória de mediadores solúveis secretados (secretoma) por células tumorais e células do microambiente tumoral, incluindo muitas citocinas pró-inflamatórias, contribui para a inflamação sistêmica e atua diretamente no músculo esquelético para induzir a perda de massa[13,18,59,60], a caracterização celular e molecular do MAT pode fornecer novos conhecimentos para compreensão da caquexia associada ao câncer. De fato, Matsuyama *et al.*[110] demonstraram que diferenças no microambiente onde as células tumorais se desenvolvem podem afetar a progressão e o fenótipo da caquexia associada ao câncer através de alterações em vários fatores circulantes derivados do microambiente tumoral. Além disso, a intercomunicação entre o tumor e tecidos periféricos é mais pronunciado em pacientes caquéticos, em comparação com pacientes com peso estável[111]. Portanto, embora ainda pouco explorada, a caracterização do perfil de expressão gênica de cada célula individual que compõe o MAT na caquexia do câncer é de fundamental relevância pois pode revelar mediadores de comunicação celular do MAT e gerar novos alvos para tratamento da caquexia e biomarcadores para diagnóstico precoce da síndrome.

A composição e função do MAT pode indicar a terapia mais adequada para pacientes oncológicos. A imunoterapia, por exemplo, tem como principal objetivo regular o microambiente tumoral reduzindo a presença de antígenos tumorais[112]. A evasão imunológica no MAT é mediada pela sinalização PD-L1 expresso pelas células neoplásicas e seu ligante PD-1 nas células T[113]. Inibidores de *checkpoint* imunológico dessas moléculas tem mostrado eficácia na restauração da citotoxicidade de células T[112]. Além disso, estudos recentes demonstram que pacientes com caquexia associada ao

câncer possuem maiores taxas de falha em monoterapia com pembrolizumabe (anti-PD-1) do que os pacientes com câncer não-caquéticos[114]. Portanto, a compreensão do MAT pode revelar novos potenciais tratamentos imunoterápicos para aumentar sua eficácia em pacientes com caquexia associada ao câncer.

Transcriptoma "single-cell" para análise do microambiente tumoral

O rápido desenvolvimento do sequenciamento de RNAs de células individuais (do inglês, s*ingle-cell transcriptome;* scRNA-seq) também tem oferecido oportunidades sem precedentes para o estudo da heterogeneidade molecular e celular do ecossistema do MAT de diferentes tipos de cânceres associados com a caquexia como, por exemplo, de pâncreas, cabeça e pescoço, fígado e pulmão[115–122]. Estudos com scRNA-seq em câncer de pulmão focam principalmente na caracterização do infiltrado inflamatório do tumor para avaliar a potencial resposta à tratamentos imunoterápicos, mostrando-se uma nova abordagem para estratificar os pacientes e revelar assinaturas imunes no câncer de pulmão[122,123]. Além disso, o scRNA-seq em carcinomas pancreáticos, embora ainda em menor extensão, tem sido realizado para caracterizar globalmente o perfil e composição de tumores pancreáticos[124,125].

Embora os diferentes tipos de células e tecidos tenham sido historicamente caracterizados pela sua morfologia e seu fenótipo, o recente desenvolvimento de métodos moleculares permitiu descrições cada vez mais precisas de suas propriedades, tipicamente medindo padrões de expressão de proteínas ou RNA mensageiro[126–128]. Os avanços tecnológicos também expandiram a multiplicação de medidas, de modo que o RNA-Seq pode agora enumerar praticamente todas as moléculas de RNAs mensageiros de uma única célula[129–134]. Essa nova abordagem forneceu *insights* sobre a biologia celular e composição de órgãos de vários organismos. A caracterização global de células T em CPCNP, através de scRNA-seq, revelou a existência de 16 subgrupos de células T CD4+ e CD8+ com diferentes estados

funcionais e dinâmica dentro do MAT, a qual se associou ao prognóstico dos pacientes, fornecendo, assim, novos parâmetros para estratificação do CPCNP[122].

Apesar de o scRNA-Seq ter surgido como uma técnica poderosa para caracterizar a heterogeneidade celular de tumores, atualmente é impraticável em coortes com grandes quantidades de amostras, e não pode ser utilizada com amostras coletadas e fixadas como parte do atendimento clínico de rotina. Entretanto, o perfil de expressão gênica de células individuais, obtido nesses experimentos de scRNA-Seq, pode ser utilizado como referência para dissecar *in silico* amostras tumorais complexas, estimando a abundância dos tipos celulares a partir dos dados do transcriptoma da massa tumoral. Vários algoritmos já foram desenvolvidos para predizer os tipos celulares a partir dados de expressão gênica de tecidos tumorais, incluindo EPIC[135], ESTIMATE[102], XCell[136], CIBERSORT[137] e CIBERSORTx[138]. Portanto, análises de transcriptomas obtidos por RNA-Seq podem ser utilizados para determinar os tipos celulares presentes nos tumores de pacientes caquéticos, comparando-se com o perfil de expressão gênica de células individuais obtidos por scRNA-Seq, a partir do mesmo tipo tumoral. Essa análise também tem o potencial de inferir o secretoma tumoral de cada uma das células que o compõe, auxiliando na identificação das células responsáveis pela secreção de fatores caquéticos no MAT.

Secretoma tumoral

Recentes avanços na genômica, transcriptômica e proteômica tem auxiliado a esclarecer o efeito do tumor em tecidos e órgãos adjacentes ou distantes através da análise do seu secretoma[59]. Secretoma representa o conjunto de macromoléculas secretadas por células, as quais permitem comunicação celular[139,140]. O termo secretoma foi cunhado por Tjalsma e colaboradores para denotar todos os fatores secretados por uma célula e, também, os constituintes da via secretória[141]. A definição de secretoma, então, foi revisada para incluir apenas proteínas secretadas no espaço extracelular[139,140].

O secretoma tumoral apresenta um papel importante em aspectos conhecidos do câncer, como proliferação celular, apoptose, angiogênese, alteração no metabolismo energético e desenvolvimento de resistência contra a terapias anticâncer[139]. O secretoma tumoral pode ser avaliado através de meio condicionado de linhagens celulares, líquidos intersticiais do tecido/tumor e fluídos corporais (revisado por Schaaij-Visser et al.,[142]). Portanto, a análise do secretoma tem grande potencial em revelar mediadores, biomarcadores e alvos para tratamento da caquexia. Muitas metodologias estão disponíveis para a identificação dos componentes do secretoma; entretanto, o uso de ferramentas ômicas (microarranjos, sequênciamento e espectometria de massas) tem se destacado nos últimos anos (revisado por Mukherjee et al.,[143]). Análises proteômicas revelaram que o secretoma de pacientes com câncer de pulmão, mama e colorretal possui biomarcadores relacionados ao aumento de sobrevida dos pacientes (revisado por Schaaij-Visser et al.,[142]).

As proteínas podem ser secretadas por uma célula através de vias de secreção clássica e não-clássica. As proteínas são, majoritariamente, secretadas pela via clássica, as quais são destinadas ao meio extracelular, em vesículas, pelo reticulo endoplasmático rugoso e complexo de Golgi [144]. Para ser destinada à essa via, é necessário que a proteína contenha em sua sequência de aminoácidos um peptídeo-sinal e um sítio de clivagem antes da região de sequência madura[145]. As proteínas secretadas por vias não-canônicas geralmente são localizadas no citoplasma ou núcleo células (proteínas com peptídeo-sinal também podem ser secretadas por outras rotas celulares) e podem ser secretadas através de microvesículas, exossomos, canais ou transportadores de membrana, lisossomos secretórios, etc[146]. Entretanto, independente da via de secreção, é possível predizer, através de ferramentas computacionais, a secreção de proteínas. A análise da sequência de peptídeos de uma proteína pode ser utilizada para estimar a presença do peptídeo-sinal[145] ou redes neurais podem predizer proteínas secretadas por vias não-clássicas[147]. O banco de dados *Human Protein Atlas* (HPA) possui a classificação mais atualizada do secretoma humano. Essa extensiva caracterização foi possível através das ferramentas computacionais anteriormente citadas e, também, pelo mapeamento e classificação da

localização subcelular em dezenas de milhares de imagens de microscopia confocal de alta resolução de proteínas humanas marcadas por imunofluorescência[148].

Algumas abordagens transcriptômicas têm sido utilizadas para desvendar o secretoma de uma célula ou de um tipo de tecido específico[149]. Em um estudo pioneiro de análise do transcriptoma utilizando microarranjos, Welsh *et al.* [150] descreveram o aumento da expressão de 74 genes que codificam proteínas secretadas em cânceres humanos. Apesar do número reduzido de genes preditos como codificadores de proteínas secretadas e do número relativamente baixo de amostras de tecido analisadas nesse estudo, uma fração significativa desses genes de secretoma, que apresentavam aumento da expressão em carcinomas, foi validada como desregulada no câncer ou com aplicações no diagnóstico e na terapia da doença. A utilização de dados transcriptômicos para predição de proteínas secretadas é vantajosa, pois as técnicas de sequenciamento de RNA possuem uma maior resolução quando comparadas às metodologias de proteômica. Além disso, o grande potencial da predição do secretoma através do transcriptoma foi amplamente explorado em nosso laboratório para assegurar sua aplicação. Recentemente, nosso grupo de pesquisa realizou uma análise computacional para predição do secretoma, a partir de dados do transcriptoma obtidos por tecnologia de microarranjos, para identificar proteínas potencialmente secretadas pelo tumor de pacientes com câncer retal localmente avançado[151] e câncer de laringe[152]. Essa estratégia foi efetiva, uma vez que as proteínas preditas como secretadas pelos tumores foram posteriormente validadas como apresentando níveis aumentados no soro[151] e plasma[152] em conjuntos independentes de pacientes.

Outra aplicação da análise do secretoma é a possibilidade de elucidar mecanismos de comunicação celular a partir dos dados de expressão gênica dos receptores dos fatores secretados em células ou tecidos alvo[153]. Os tumores e MAT são constituídos por complexas interações celulares que modificam as funções das células imunológicas locais. Estudar a comunicação célula-célula dentro desse contexto pode auxiliar e orientar o desenvolvimento de terapias ou imunoterapias eficazes contra

o câncer [153]. Ainda, considerando o caráter sistêmico da caquexia em que citocinas afetam diversos órgãos e tecidos distantes, a análise da comunicação entre fatores secretados pelo tumor e órgão-alvo também pode auxiliar em futuras terapias para reduzir os efeitos sistêmicos da caquexia.

Para nosso conhecimento, nenhum estudo explorou esses dados na busca de elementos do secretoma produzidos especificamente pelas células neoplásicas e células do MAT na caquexia e sua relação com tecidos alvo; em especial, pela dificuldade de obtenção de dados clínicos e moleculares de pacientes com caquexia (revisado por Penna et al.,[154]), principalmente de dados de sequenciamento *single-cell*. Entretanto, com o avanço de tecnologias para a análise de expressão gênica na última década, experimentos em larga escala, como de microarranjos e de novas metodologias de sequenciamento, tem gerado grandes quantidades de dados de que são depositados em bancos públicos (revisado por Rung et al.,[155]). Os dados públicos, geralmente, podem ser combinados com novos dados gerados pelos pesquisadores, ou então serem reanalisados para responder questões diferentes daquelas colocadas nos estudos originais[156]. A integração de dados ômicos disponíveis em bancos de dados é capaz de gerar *insights* biológicos, que, talvez, em estudos individuais não pudessem ser obtidos (revisado por Rung et al.,[155]). De fato, buscando melhor compreender o papel do secretoma tumoral na caquexia, reanalisando dados em larga escala de 12 tipos tumorais disponíveis no TCGA, demonstramos que o câncer de pâncreas – aquele com maior prevalência de caquexia – é também o que mais regula positivamente a expressão de genes do secretoma, sugerindo que o secretoma tumoral é essencial no desenvolvimento da caquexia e deve ser mais compreendido e explorado[58].

Reanálise de dados de transcriptoma tumoral para identificação de mediadores da caquexia

O uso de informações genéticas e clínicas disponíveis no banco de dados TCGA tem facilitado a obtenção desses dados para estudos em larga escala, estendendo sua avaliação para vários tipos tumorais (68 tipos de tumores primários estão inclusos no TCGA, englobando mais de 33 mil casos) [157]. Além disso, o portal *Genotype-Tissue Expression* (GTEx) possui dados de sequenciamento de

RNA de tecidos normais de indivíduos que não possuíam alterações neoplásicas, sendo o banco de dados mais completo para utilização como controles dos casos tumorais [128]. De maneira semelhante, o banco de dados *Cancer Cell Line Encyclopedia* (CCLE) também comporta dados genômicos globais de 1457 linhagens celulares de câncer e, tendo em vista que linhagens celulares de tumores humanos mantém muitas características da biologia tumoral, a análise do perfil global de expressão gênica de linhagens celulares pode auxiliar na descoberta de novos fármacos e mecanismos envolvidos em diferentes propriedades do desenvolvimento e progressão tumoral[158]. A correlação de dados transcriptômicos de linhagens celulares e do tecido tumoral pode revelar moléculas importantes para o câncer, em específico, nas alterações moleculares provenientes das células neoplásicas em si.

Os estudos globais que utilizam dados transcriptômicos inseridos em bancos de dados biológicos tem se mostrado de extrema importância para se extrair conhecimentos de impacto na pesquisa e tratamento do câncer. Robinson *et al.,* [159] realizaram uma análise *Pan-Cancer* (utilizando dados do TCGA) da expressão gênica de componentes do secretoma, a qual resultou em listas ordenadas de candidatos a biomarcadores diagnósticos detectáveis em fluidos biológicos. Essa investigação também revelou os padrões e as funções biológicas associadas às alterações na expressão de proteínas secretadas em diferentes tipos tumorais, focando principalmente em um conjunto específico de proteínas do secretoma. Essa estratégia reduziu a complexidade do secretoma ao estreitar a gama de moléculas secretadas necessárias para explorar questões fundamentais relacionadas à expressão alterada de genes que codificam proteínas do secretoma em diferentes tipos tumorais. No entanto, a complexidade do secretoma ainda está longe de ser completamente entendida e a seleção de diferentes estratégias metodológicas, ou de tipos específicos de tumores ou células do MAT, podem levar a novos *insights* sobre as funções biológicas do secretoma na caquexia. O secretoma produzido pelas massas tumorais dos cânceres associados à caquexia já foi globalmente caracterizado por nosso grupo de pesquisa [58]. Entretanto, demos maior foco nos fatores indutores de caquexia clássicos, como IL6, IFNG, IL8, etc. Por isso, ainda é necessário definir os fatores centrais do secretoma, relacionados

à inflamação e outras citocinas, a partir da expressão gênica, em resolução *single-cell*, de tumores com alta prevalência de caquexia, e que não são habitualmente explorados na caquexia. Portanto, o uso de dados públicos para análise do secretoma tumoral além de ser extremamente importante para a compreensão da biologia tumoral[142] pode, também, auxiliar na identificação de moléculas potencialmente responsáveis pela modulação do MAT. Para nosso conhecimento, não existem estudos que utilizam-se de informações de bancos de dados públicos e correlacionem globalmente dados de secretoma do MAT de pacientes caquéticos com dados de composição do microambiente tumoral para investigar mediadores da caquexia associada ao câncer.

Principais perguntas da tese

1) Qual é a composição celular do microambiente tumoral nos pacientes com câncer potencialmente caquéticos?
2) Qual é o perfil do secretoma das células malignas e células imunes do microambiente tumoral de pacientes com caquexia?
3) Quais são os mecanismos mediadores da interação tumor-hospedeiro na caquexia?

Hipótese

A hipótese deste estudo é de que a análise do perfil transcricional de tumores malignos de pulmão e pâncreas pode revelar a composição de células imunes no MAT de pacientes caquéticos. Além disso, os componentes do secretoma derivados dessas células podem atuar como mediadores da caquexia.

2. Objetivos

Objetivo Geral

Caracterizar o perfil transcricional do secretoma tumoral e de seu microambiente para identificar potenciais mediadores de caquexia.

Objetivos Específicos 1

1) Caracterizar e classificar a muscularidade dos pacientes com CPCNP, para identificação de pacientes potencialmente caquéticos;
2) Analisar dados transcriptômicos nos tecidos tumorais, linhagens celulares e células individuais de CPCNP;
3) Avaliar a composição do microambiente tumoral em CPCNP;
4) Definir o conjunto principal de componentes do secretoma tumoral que mais se correlacionam com a caquexia associada ao CPCNP;
5) Identificar as células responsáveis pela secreção de fatores indutores de caquexia no MAT de pacientes com CPCNP;
6) Correlacionar os dados clínicos com transcriptômicos dos pacientes com CPCNP;
7) Caracterizar a comunicação entre os componentes do secretoma tumoral e músculo esquelético.

Objetivos Específicos 2

1) Analisar dados transcriptômicos na massa tumoral, células individuais (*single-cell*) e linhagens celulares de ADP;
2) Identificar fatores centrais na indução de caquexia à partir do secretoma;
3) Avaliar a composição do microambiente tumoral em ADP;
4) Definir os componentes celulares do MAT de ADP responsáveis pela produção de fatores indutores de caquexia;
5) Caracterizar a comunicação entre os componentes do secretoma tumoral e tecidos afetados na caquexia, como o músculo, fígado e adiposo.

CAPÍTULO 1 - Lung cancer cachexia is associated with an inflammatory and immunosuppressive tumor microenvironment.

Sarah Santiloni Cury[1], Diogo de Moraes[1,2], Jakeline Oliveira[1], Paula Paccielli Freire[3], Patricia P Reis[4], Miguel Luiz Batista Jr[5,6], Érica Nishida Hasimoto[4], Robson Francisco Carvalho[1]

[1]Department of Structural and Functional Biology, Institute of Biosciences, São Paulo State University (UNESP), Botucatu, São Paulo, Brazil.
[2]Department of Biochemistry and Tissue Biology, University of Campinas, Rua Monteiro Lobato, 255, Campinas, São Paulo, 13083-862, Brazil.
[3]Department of Immunology, Institute of Biomedical Sciences, University of São Paulo, São Paulo, SP, Brazil.
[4]Department of Surgery and Orthopedics, Faculty of Medicine, São Paulo State University (UNESP), Botucatu 18618687, São Paulo, Brazil.

[5]Department of Biochemistry, Boston University School of Medicine, Boston, U.S.A.

[6]Department of Integrated Biotechnology, University of Mogi das Cruzes, São Paulo, Brazil.

Corresponding authors´ information:

Robson Francisco Carvalho

Department of Structural and Functional Biology

Institute of Biosciences, São Paulo State University (UNESP)

CEP: 18.618-689, Botucatu, São Paulo – Brazil

Telephone number: +55 14 3880 0473

robson.carvalho@unesp.br

Artigo submetido para o Journal of Cachexia, Sarcopenia, and Muscle (IF =12.063)
Minor revisions under review (JCSM-D-22-00221R1)

Abstract

Background

Cachexia is prevalent in patients with lung cancer. Studies demonstrated that cachexia-inducing factors (CIFs) derived from the tumor microenvironment (TME) are involved with the abnormalities that result in muscle atrophy. However, the TME characterization in lung cancer patients with cachexia remains to be explored. Therefore, we analyzed the cellular and molecular composition of the TME from cachectic patients with non-small cell lung cancer (NSCLC) by examining tumor RNA-sequencing.

Methods

We measured the muscularity of 211 treatment-naive NSCLC patients using computed tomographies available in The Cancer Imaging Archive (TCIA) database. The cutoffs to establish cachectic patients were selected by machine learning algorithms (Classification and Regression Tree - CART and Cutoff Finder) on pectoralis muscle area (PMA), clinical, and survival data. We evaluated the prediction model in an additional cohort of 36 NSCLC. Tumor RNA-Seq (GSE103584) was used to describe the transcriptomic profile and the cellular composition based on the digital cytometry tools and single-cell RNA-Seq (scRNA-Seq). We also analyzed tumor-muscle communication, and the inflammatory and immunosuppressive markers identified were further investigated in the LLC mice model.

Results

CART showed that lower PMA is associated with a high risk of death (hazard ratio:1.99). Cutoff Finder selected PMA cutoffs that separated low- from high-muscularity patients based on the risk of death (*P*-value=0.0026; CI=1.68-11.71; discovery set). The cutoff presented 84% of success in classifying cachexia, associated with high-risk in the additional cohort (*P*-value=0.09; CI=1.54-2.23; validation set). RNA-Seq revealed 90 upregulated secretome genes in low-muscularity compared to high-muscularity patients (FC>1.5; *P*-value<0.05). We found that muscle cells have receptors for the identified tumor secreted factors. Known CIFs such as *IL6*, *IFNG*, *LIF*, *CCL2*, and *CSF3* are highly expressed in tumors of low-muscularity patients. When considering all 332 upregulated genes, the tumor of low-muscularity patients enriched terms associated with leukocyte chemotaxis, cytokine/chemokine activity, and T cell activation. Digital cytometry analysis on these genes revealed that low-muscularity patients presented high proportions of CD8+T cells (*P*-value=0.03), specifically a subset of exhausted cells. scRNA-Seq analyses revealed CD8+T cells secreting CIFs and exhausted CD8 communicating with other T cells.

Conclusions

Our machine learning prediction identified patients with lower PMA and worse survival. Moreover, these patients showed an inflammatory and immunosuppressive TME enriched with CD8+T cells and highly expressing CIFs.

Keywords: non-small cell lung cancer, machine learning, computed tomography, transcriptomics, exhausted CD8+T cells

Introduction

Cachexia is a metabolic syndrome found in 50% of patients with lung cancer[1]. It is associated with worse survival rates in non-small cell lung cancer (NSCLC)[2], the most prevalent histological type of lung cancer[3]. Muscle mass loss in patients with advanced NSCLC is associated with pain and poor quality of life[4]. Therefore, early detection of cachexia is of utmost importance to predict NSCLC patient outcomes and guide better treatment decisions.

Multiple screening tools have been developed to measure muscle mass loss[5]. One feasible approach is computed tomography (CT) scans performed routinely for cancer diagnosis and follow-up[6]. CT-based muscle quantification at the third lumbar vertebra (L3) level is commonly used to assess cachexia in cancer patients[1]. However, CT-scans images of NSCLC patients usually do not include L3[7]. Studies overcame this limitation by analyzing the pectoralis muscle area (PMA)[8,9]. Our group demonstrated that PMA alone is a cachexia predictor in treatment-naive NSCLC patients[9]. PMA quantification in lung cancer patients is associated with clinical outcomes; however, each study used different calculations and cutoffs to select cachectic patients[8,9]. Although informative, the best PMA cutoff that classifies cachectic patients based on CTs remains to be defined.

Molecular markers also contribute to clinical classification of cachexia, however, none are yet approved for clinical use. Still, the synergic expression of tumor-derived cachexia-inducing factors (CIFs) is correlated with the prevalence of cachexia in different tumor types[10]. Lung cancer cachexia is characterized by increased expression of tumor-derived factors that ultimately induce skeletal muscle wasting[11]. NSCLC patients with low PMA muscularity present increased expression of *IL8*, *IL6*, and other critical CIFs genes[9]. Cell types in the tumor microenvironment (TME) contribute distinctively by secreting cytokines or other CIFs that act on the cell surface receptors of target tissues[12]. Cancer samples can be divided into clinically relevant immune subtypes depending on TME composition and gene expression profile[13]. Thus, computational deconvolution of the transcriptome from bulk tumor tissues using digital cytometry and scRNA-Seq data can help infer the cellular proportions and composition of TME. TME analysis also has the potential to enable the identification of cells within the TME of cachectic patients responsible for secreting CIFs.

We built a machine learning (ML) classification model based on PMA and clinical data to identify NSCLC patients with low muscularity and poor prognosis. We characterized the global secretome and TME immune fraction of these patients using tumor transcriptome. The predictive model determined the best PMA cutoffs to select potentially cachectic patients. We demonstrated that these patients have a pro-inflammatory state characterized by high tumor gene expression of CIFs. Based on computational deconvolution of the bulk tumor tissue transcriptomes, we also identified that patients with lower PMA and worse survival show a TME enriched with exhausted CD8+T cells. Furthermore, we demonstrated a slight increase of exhaustion markers in tumors of cachectic mice with lung cancer.

Material and Methods

Softwares, tools, and databases used herein are described in **Supplementary Material**.

NSCLC patients

CTs and clinical data were downloaded from The Cancer Imaging Archive (TCIA) database. The NSCLC-Radiogenomics collection containing 211 NSCLC patients[14,15] was selected as the discovery set. CTs were taken at diagnosis, and patients were treated with surgery. We included patients with primary tumors, presenting whole-body PET-CT before surgery, not subjected to chemo or radiotherapy, with arms raised during CT to avoid positioning bias, and overall survival data. Based on these criteria, 107 patients were included in the analyses. An independent validation set with 36 primary NSCLC patients (all gave their informed consent prior to their inclusion in the study) from the Faculty of Medicine, São Paulo State University (UNESP) - Botucatu, Brazil (2012-2019) was used to confirm the prediction model (approved by the Faculty of Medicine Research Ethics Committee REB#45723921.0.0000.5411), however, 32 patients had survival data available.

CT Imaging Analyses

We analyzed the pectoralis muscles using a single axial slice of the CT as previously described[9]. We also analyzed the total skeletal muscle cross-sectional area at the level of the L3 to classify cachectic patients based on pre-established skeletal muscle indexes (SMI; men<55 cm^2/m^2; women<39 cm^2/m^2)[4]. This classification was compared to the one generated by our model.

Building a cachexia classification model using a machine learning approach

Predictive analysis based on a non-parametric risk prediction model was performed by the Classification and Regression Tree (CART) method using the regression analysis available in "rpart" using RStudio. We performed pruning to generate the tree with minimum × error (prune function; cp =0.053). We used ten-fold cross-validation to assess the possibility of overfitting. We analyzed the age, tumor stage, PMA, and survival as variables. The Cutoff Finder package was independently applied to select the PMA cutoff that distinguishes patients' survival using R. Area Under the Curve-Receiver Operating Characteristics (AUC-ROC) analysis with 95% confidence interval (CI) via the easyROC web-tool was used to determine the diagnostic value of our PMA cut-offs for the prediction of cachexia. For this comparison, the cachexia phenotype was defined using L3 SMI cut-offs**.**

Tumor transcriptomic analysis

The tumor RNA-sequencing data (Illumina HiSeq 2500) of 130 subjects from NSCLC Radiogenomics collection were publicly available at GEO datasets (GSE103584). Of our 107 patients included, 46 had tumor transcriptomic data. We compared count data from LM (N=9) with HM (N=37) patients to perform differential gene expression analysis using the default setting of the Biojupies platform. The differentially expressed genes (DEGs) were selected according to fold change (FC)>|1.5| and *P*-

value<0.05. DEGs encoding secreted proteins were filtered based on the Human Protein Atlas (HPA database using the majority decision-based method for secreted proteins (MDSEC) list of 2943 secretory genes (**Table S1**). Principal component analysis (PCA) was performed using the ClustVis webtool.

Gene set enrichment and protein-protein interaction (PPI) network analyses

We used the EnrichR to perform functional enrichment analysis of the DEGs. We selected the top10 most enriched biological processes using gene ontology (GO) - 2018. PPI networks were conducted using the STRING tool. We considered experiments, databases, co-expression, neighborhood, and co-occurrence as active interaction sources. Only the highest confidence interactions were included (interaction score>0.9), and the disconnected nodes were omitted in the final network. A *P*-value<0.01 was considered statistically significant. PPI network data was visualized and annotated using Cytoscape. The network was analyzed using the CytoNCA plugin, which calculated each node's betweenness centrality.

Tumor-muscle crosstalk prediction

We used the ligand-receptor consensus list generated by Ramilowski et al., 2015[16] to test if the skeletal muscles express receptors for the tumor-derived factors identified. We validated the gene expression of each predicted muscle receptor in human primary muscle cells from the FANTOM5 project, 491 muscles tissues from the GTEx portal, muscle tissues from BioGPS website, and muscle tissues from GeneAtlas U133A, and gcrma human dataset. The alluvial diagram connecting the ligands to their respective receptors was generated using the SankeyMATIC tool.

Expression profile of secretome genes using the Cancer Cell Line Encyclopedia

To evaluate whether malignant lung cells themselves express the DEGs found in the tumor of LM patients, we used transcriptomic data from the Cancer Cell Line Encyclopedia (CCLE). We selected eight cell lines with a higher correlation with tumor tissues as an initial screening using the "TCGA-110CL Cell Line Panel". Considering that lung tumor organoids recapitulate the histology, gene expression, and genomic profile of the original tumor[17], we included lung tumor-derived organoids transcriptomic data available in the HCMI (Human Cancer Model Initiative) catalog (duplicates of the HCM-CSHL-0058-C34). The selected cell lines and organoids are described in **Table S2**.

Lung TME cellular composition and single-cell data analysis

To evaluate whether immune infiltrating cells express the DEGs found in the LM, we performed digital cytometry analysis using the CIBERSORTx tool to impute the immune cell fractions of 22 cell types (LM22 matrix signature) from the discovery bulk RNA-Seq data. We applied the default settings and batch-correction. We also performed a gene expression imputation analysis to verify whether the over-

expressed genes in potentially cachectic patients are expressed in the six major leukocyte subsets (B cells, CD4+T cells, CD8+T cells, NKT cells, NK cells, and monocytes) of patients with NSCLC derived from scRNA-Seq data[18]. Gene Expression Profile (GEP) were estimated using Fragments Per Kilobase of transcript per Million mapped reads (FPKM) from LM secretome genes data (discovery set) by CIBERSORTx group mode analysis. The specific state of T cells (naive, cytotoxic, and exhausted) was evaluated using Immune Cell Abundance Identifier (ImmuCellAI).

Ligand-receptor interactions from gene expression

We used the computational framework CellPhoneDB to predict cell-cell communication and better understand the interplay of tumor immune cells using its repository of curated ligand-receptor interactions for scRNA-Seq. We used the default setting to select the statistically relevant interaction (P-value < 0.05) between the NSCLC T cells using the expression profile enriched in LM patients. This analysis was performed by re-analyzing the publicly available scRNA-Seq data from Guo et al., 2018[19] (GSE99254).

Lewis Lung Carcinoma (LLC) mice model of cancer cachexia

Eight-week-old male C57BL/6J mice were obtained from Jackson Laboratory (#00066). Mice were housed on a 12 h light/dark schedule with free access to water and food. The Ethical Committee for Animal Research from the University of Mogi das Cruzes approved all the adopted procedures, which were carried out following the ethical principles by the Brazilian College of Animal Experimentation (CEUA#010/2019). Lewis Lung Carcinoma (LLC) tumor cells (LL/2: American Type Culture Collection) were used to induce cancer cachexia. LLC was injected subcutaneously into the right flanks (200 µl LLC cells; 3.5×10^5). Development of cachexia was monitored by tumor size and body weight over 28-day[20]. The impact of tumor growth and development of cachexia on animal welfare were considered, with appropriate measures to monitor and alleviate suffering implementation according to adopted endpoint criteria[21]. The animals were classified according to cachexia grading, considering the range of the body weight losses for 28 days. The following measure was considered; (final body weight (last experimental day) - the highest value of body mass measured during the experimental period [growth curve plateau]). Thus, the experimental groups were classified as Pre-Cachexia (PC), with a reduction of up to 5% of body mass, and Cachexia (CC), defined as a reduction of ≥5% to 20% of body mass, at the end of the experiments. Overnight-fasted mice were euthanized by decapitation without anesthesia. After euthanasia, the tumor mass was carefully dissected and weighed. Animals with metastasis in the lungs or other visceral organs were excluded. Bodyweight was measured daily, at the same time, over the 28-day experimental period on a precision scale (Ohaus®).

RT-qPCR

Total RNA samples (400 ng) were reverse transcribed into cDNA with the High-Capacity RNA-to-cDNA Master Mix (Thermo Fisher Scientific, USA). The qPCR reactions (15 µL) were performed with Power SYBR™ Green Master Mix (Thermo Fisher Scientific, USA), as described by the

manufacturer, using specific primers (listed in **Table S3**). The reactions were run on a QuantStudio™ 12 K Flex System (Thermo Fisher Scientific, USA) using 95°C for 10 min followed by 40 cycles of 95 °C for 15 s and 60 °C for 1 min as cycling conditions. The raw data were retrieved and imported into the Expression Suite Software v1.0.3 (Thermo Fisher Scientific, USA). Relative quantification of mRNA expression was evaluated using the $2^{-\Delta\Delta CT}$ method[22], and *Rpl13a* was used as a reference gene to normalize the mRNA expression data. This reference gene was selected based on geNorm calculations[23], and expression stability was further confirmed by comparing Ct values between groups (Coefficient of variation of 1%).

Results

Predictive models identify the best PMA cutoff that classifies cachectic patients

We included 107 patients with NSCLC with a mean age of 68.7 years old (42 to 87). Sixty-eight were male, and 39 were female. Sex differences were considered when analyzing the PMA. We also identified differences according to the age range, especially in women; the older ones (>65 years old) presented lower PMA than younger ones (≤65 years) (**Figure S1A**). PMA did not differ between young and older men (**Figure S1A**).

We z-score normalized PMA considering sex and age differences to make groups comparable (**Figure S1B**). CART analysis showed that patients with lower PMA are associated with a high-death risk followed by tumor stage (**Figure 1A**). Using the Cutoff Finder, the same muscularity cutoff separated patients with poor survival and low PMA (low-muscularity patients, LM; n = 22) from patients with better survival and high PMA (high-muscularity patients, HM; n = 85) (**Figure 1B**). Using the L3 SMI, we found that PMA classifies cachexia with an AUC value of 0.84 (95% CI: 0.7-0.98; P < 0.001; **Figure S1C**).

By transforming the PMA z-scored values into absolute values, we established the PMA cutoffs to select low-muscularity patients according to age and sex: young male = PMA<34.4 cm^2; old male = PMA<34.3 cm^2; young female = PMA<25.4 cm^2; and old female = PMA<18.6 cm^2. LM patients had lower body mass index (BMI) and SMI. We observed increased smokers' frequency, high tumor grade, pleural invasion, and tumor recurrence in the LM patients (**Table 1**). An independent group of low-muscularity NSCLC patients analyzed according to the PMA cutoffs generated during the discovery analysis confirmed the associations with poor prognosis (worse survival, recurrence, and smoking habits) (**Table 1 and Figure 1C**). Although not statistically significant, more LM patients (31.3%) had KRAS mutations when compared to HM (16.9%). Caucasians were the most common ethnicity in both groups from the discovery set, but Asians were prevalent in the HM group (not statistically significant; **Table 1**). Our validation set was composed of Brazilians that was self-declared as white (N=32, 89%), mixed (N=2, 5.5%), and black (N=2, 5.5%). Mixed and blacks were all classified as LM.

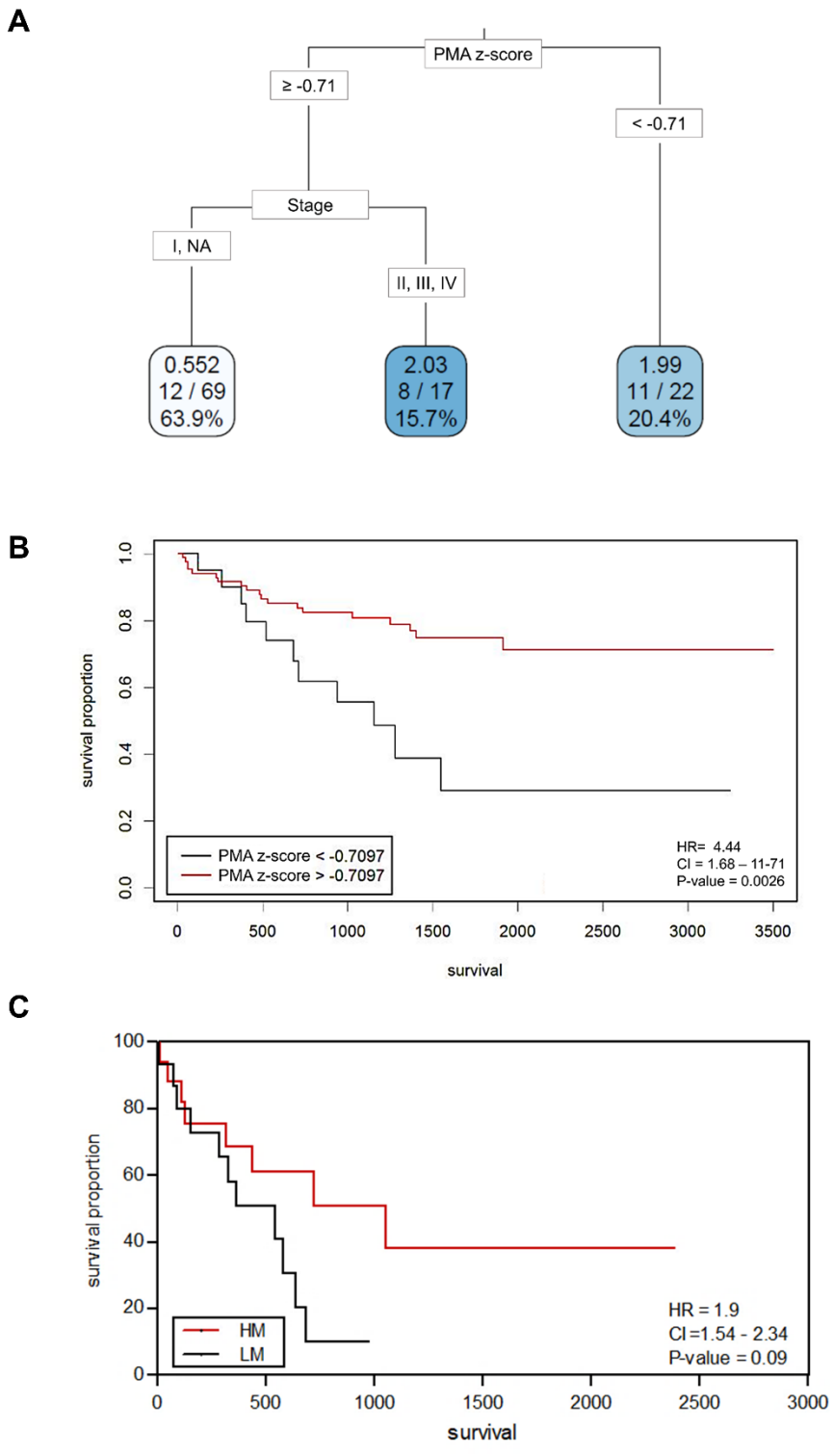

Figure 1. Cachexia classification models. A) Decision tree generated using Classification And Regression Trees (CART). Bottom boxes indicate hazard ratios, the number of patients at risk in each leaf, and the percentage of patients in each leaf. **B) K**aplan-Meier survival curve generated by CutoffFinder tool (red-curve: PMA>0.71and low-risk group; black-curve: PMA<0.71 and high-risk group). **C)** Kaplan-Meier survival curve comparing LM and HM (validation set). The resulting *P*-values for the log-rank test are shown. LM: low-muscularity; HM: high-muscularity. HR: hazard ratio; CI: 95% confidence interval.

Table 1. Clinical findings and skeletal muscle parameters of patients with NSCLC (non-small cell lung cancer) with low- and high-muscularity defined by pectoralis muscle cross-sectional area assessed using computed tomography and classification predictive model.

	Discovery set			Validation set			
	LM (PMA <-0.71) N=22	**HM (PMA >-0.71) N =85**	**p-value**	**LM N=19**	**HM N=17**	**p-value**	**Statistical test**
Age	68 ± 8.0	68.8 ± 9.2	0.71	64.2 ± 6.3	63.6 ± 9.5	0.82	T test
PMA (cm^2)	27.4 ± 6.3	36.9 ± 10.2	<0.0001	25.5 ± 5.6	33.2 ± 12.3	0.02	T test
BMI (kg/m^2)	23.1 ± 3.6	27.5 ± 5.2	<0.001	-	-	-	T test
SMI (cm^2/m^2)	44.1 ± 4.9	51.8 ± 8.9	0.017	-	-	-	T test
Gender (%)							
Male	72.7	61.2	0.32	68.4	35.3	0.047	chi-square
Female	27.3	38.8		31.6	64.7		
Ethnicity (%)							
Caucasian	72.7	55.3	0.27	-	-	-	chi-square
Asian	4.5	16.5		-	-		
African American	4.5	1.2		-	-		
Hispanic/Latino	0	3.5		-	-		
Native Hawaiian	4.5	1.2		-	-		
NA	13.6	22.3		-	-		
Smoking history (%)							
Current	36.4	10.7	0.0136	100	70.6	0.01	chi-square
Former	50	66.7		-	-		
Nonsmoker	13.6	22.6		0	29.4		
Histology (%)							
Adenocarcinoma	72.7	85.7	0.15	63.1	41.2	0.18	chi-square
Squamous cell carcinoma	27.3	14.3		36.8	58.8		
Stage (%)							
I-II	94.7	93.6	0.86	73.7	58.8	0.34	chi-square
III-IV	5.3	6.4		26.3	41.2		
Grade (%)							
G1	21	37.9	0.0082	23.5	42.8	0.25	chi-square
G2	47.4	56.1		70.6	51.2		
G3	31.6	6		5.9	-		
Lymphovascular invasion (%)							
Yes	11.8	5	0.32				chi-square
No	88.2	95		73.7	68.7	0.74	
Pleural invasion (%)				26.3	31.3		
Yes	31.6	12.3	0.047	58.8	40	0.29	chi-square
No	68.4	87.7		41.2	60		
Recurrence (%)							
Yes	36.4	14.3	0.0185	42.1	23.5	0.24	chi-square
No	63.6	85.7		57.8	76.5		
EGFR mutation status (%)							
Wildtype	82.3	71	0.3441	-	-	-	chi-square
Mutant	17.7	29		-	-		
KRAS mutation status (%)							
Wildtype	68.7	83.1	0.1973	-	-	-	chi-square

Mutant	31.3	16.9	-	-

N: number of patients; PMA: Pectoralis Muscle Area; LM: low-muscularity patients; HM: high-muscularity patients; BMI: body mass index; SMI: skeletal muscle index (L3 muscles). The data represent the mean ± standard deviation or the percentage.

Tumor tissues from low-muscularity patients present a pro-inflammatory profile

We included nine LM patients and 37 HM patients with RNA-Seq data availability for the expression analysis and observed a similar expression profile using the PCA (**Figure 2A**). These similarities resulted in DEGs with adjusted *P*-values (false discovery rate, FDR, corrected) that were not statically significant (> 0.8). Therefore, we considered *P*-values < 0.05 to select DEGs for further analysis. We also took into consideration the biological context of these DEGs to avoid misinterpretation due to false positives**.** We identified 682 DEGs (332 were up and 350 were downregulated) in LM (**Figure 2B** and **Table S4**). Enrichment analysis of the upregulated genes demonstrated leukocyte chemotaxis, cytokine/chemokine activity, and T cell activation as the most enriched terms in LM patients. The downregulated genes enriched terms associated with drug transport, cellular adhesion, and glucuronidation (**Figure 2C)**. We found 90 and 41 up and downregulated secretome genes in LM (**Table S4**). We failed to identify significant interactions among the downregulated secretory genes in the PPI. Therefore, we focused on the upregulated secretome genes that included several known cachexia mediators described in pan-cancer[10] and lung cancer[9] (**Table S5**), such as *IL6, IFNG*, *LIF*, *CCL2*, and *CSF3* (**Figure 2D**). IL6 presented the highest betweenness centrality and a central position in the network. *CCL2* (MCP-1) was the CIF with the highest abundance in LM tumors (**Figure 2E**).

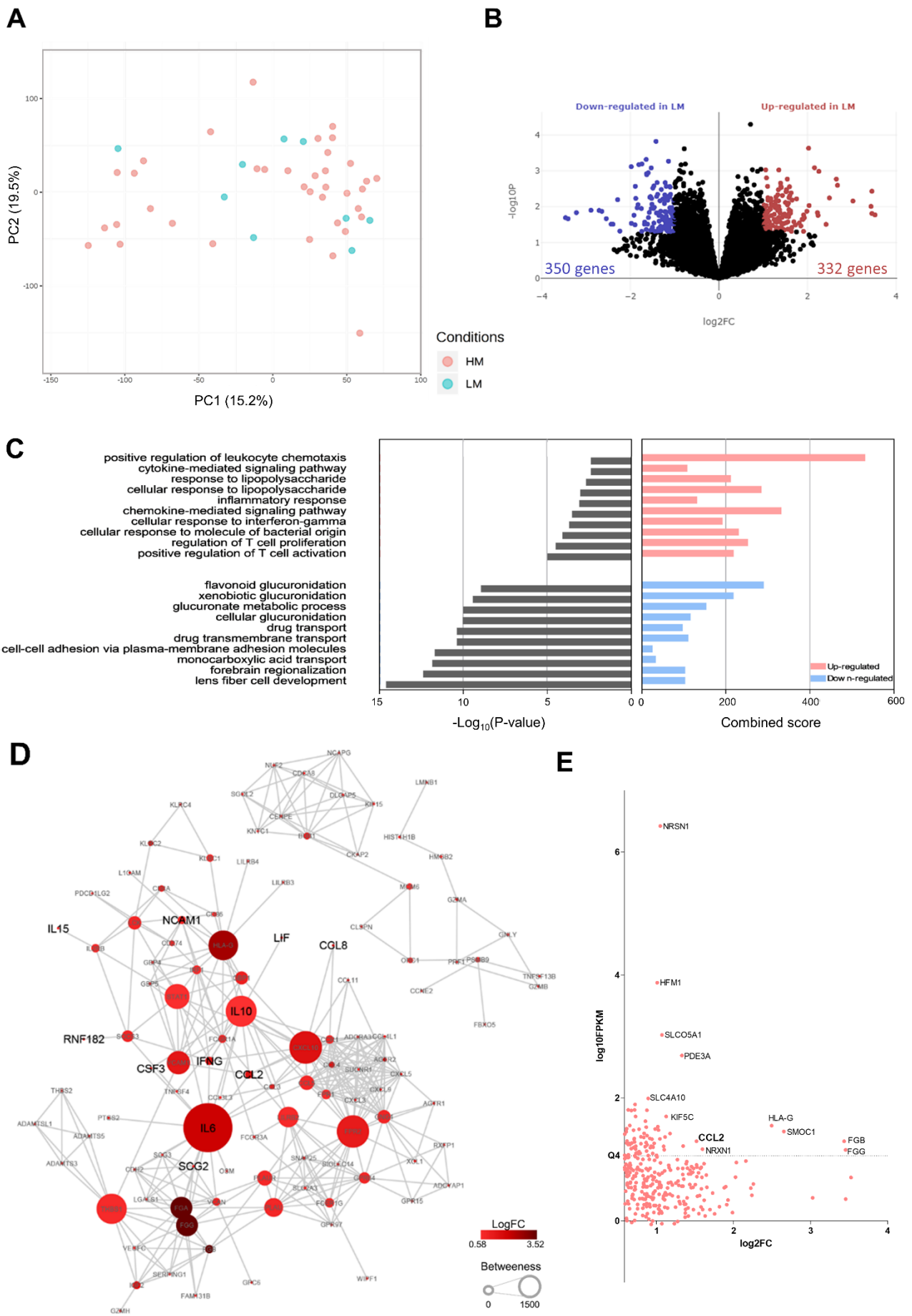
A
PC2 (19.5%)
PC1 (15.2%)
Conditions
HM
LM
B
Down-regulated in LM
Up-regulated in LM
350 genes
332 genes
-log10P
log2FC
C
positive regulation of leukocyte chemotaxis
cytokine-mediated signaling pathway
response to lipopolysaccharide
cellular response to lipopolysaccharide
inflammatory response
chemokine-mediated signaling pathway
cellular response to interferon-gamma
cellular response to molecule of bacterial origin
regulation of T cell proliferation
positive regulation of T cell activation
flavonoid glucuronidation
xenobiotic glucuronidation
glucuronate metabolic process
cellular glucuronidation
drug transport
drug transmembrane transport
cell-cell adhesion via plasma-membrane adhesion molecules
monocarboxylic acid transport
forebrain regionalization
lens fiber cell development
Up-regulated
Dow n-regulated
-Log10(P-value)
Combined score
D
NCAM1
IL15
LIF
CGL8
IL10
RNF182
CSF3
IFNG
CCL2
IL6
SOG2
LogFC
0.58
3.52
Betweeness
0
1500
E
NRSN1
HFM1
SLCO5A1
PDE3A
SLC4A10
KIF5C
HLA-G
SMOC1
CCL2
NRXN1
FGB
FGG
Q4
log10FPKM
log2FC

Figure 2. Tumors of patients with low-muscularity present a pro-inflammatory profile enriched with cachexia-inducing factors and mediators. A) Principal component analysis (PCA) demonstrating similar expression profiles between HM and LM patients. **B)** Volcano-plot demonstrating differentially expressed genes in LM (fold change > 1.5 and *P*-value <0.05). **C)** Enrichment analysis of top10 terms related to biological processes from 332 up (red) and 350 downregulated (blue) genes in LM. Bar graphs represent ranked -log10 *P*-values (Fisher exact test), from the least to the most significant according to EnrichR analysis. **D)** Protein-protein interaction networks of the ninety upregulated genes predicted to encode secreted proteins in LM patients. The larger the circles, the higher the betweenness centrality value of the node. Red intensities represent the gene expression fold change (logFC). Higher letter sizes indicate previously described cachexia-inducing factors in pan-cancer[10] and lung cancer[9]. Gray lines highlight the interactions. Interactions were visualized using Cytoscape v3.7.2. **E)** Scatterplot comparing abundance (log10 FPKMs, y-axis) and degree of expression (log2-fold change, x-axis) of upregulated genes in LM. LM: low-muscularity; HM: high-muscularity; FPKM: Fragments Per Kilobase Million.

Tumor-derived factors are predicted to interact with skeletal muscle

To verify how the secretome profile from tumors of LM is potentially altering the skeletal muscle morphology, we constructed a tumor-muscle connectome by identifying the gene expression of the ligands produced by the tumors and their corresponding receptors in skeletal muscle cells and tissues (**Figure 3**). We observed that several ligands have receptors expressed in abundance both in skeletal muscle cells and tissues. Interestingly, *LIF*, *IFNG*, and *IL6* were the cytokines presenting the receptors with high expression in the muscle cells compared with other cytokines, such as CCLs and CXCLs, in which the expression of the receptor is absent in muscle cell lines. Many receptors for CCLs and CXCLs are expressed in skeletal tissues, as demonstrated in the GTEx and BioGPS data, suggesting that these cytokines target the muscle tissue cells other than the myoblasts, myotubes, and satellite cells. This analysis ratifies that tumor-released factors may target skeletal muscle via specific receptors.

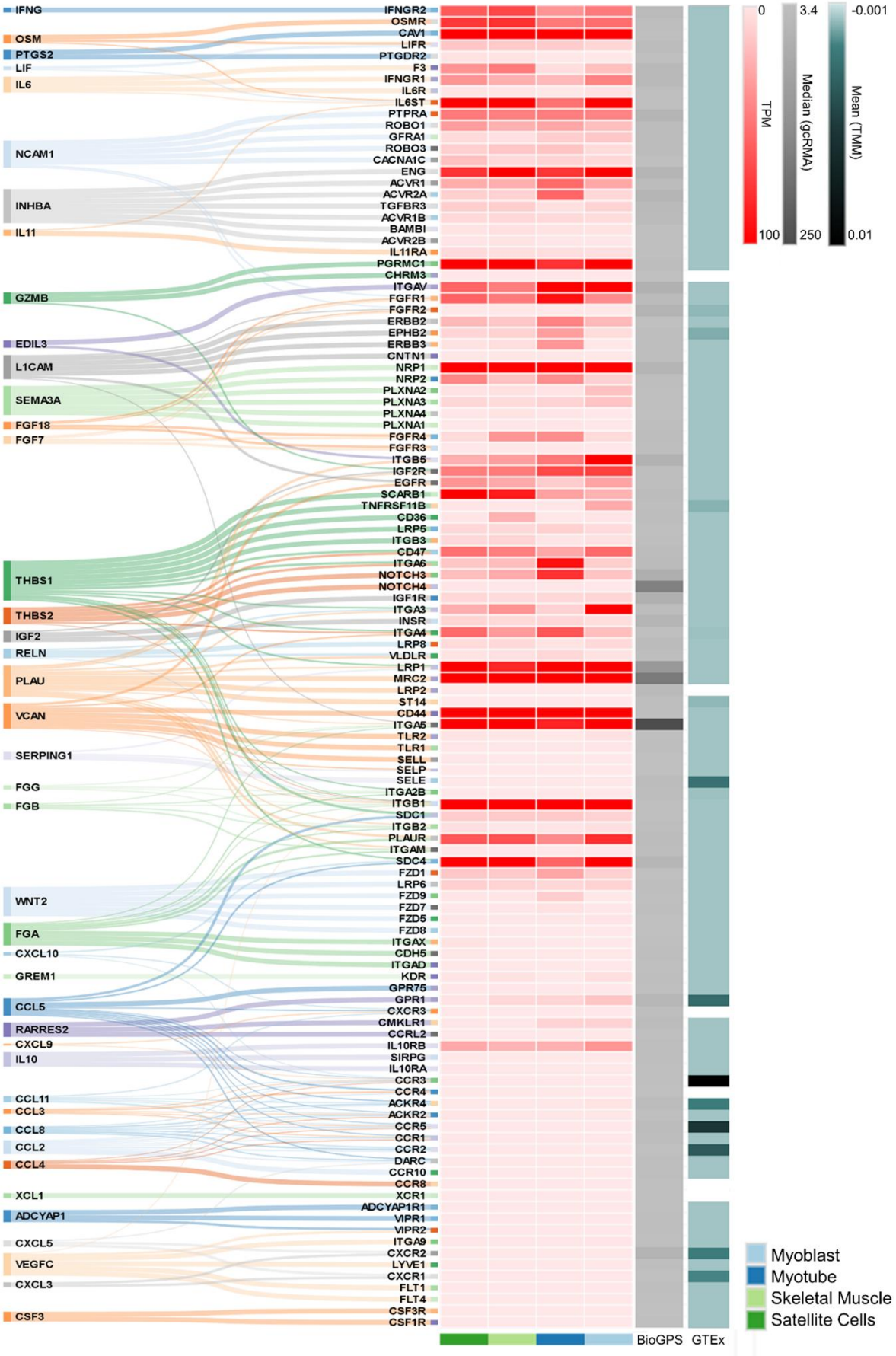
IFNG
OSM
PTGS2
LIF
IL6
NCAM1
INHBA
IL11
GZMB
EDIL3
L1CAM
SEMA3A
FGF18
FGF7
THBS1
THBS2
IGF2
RELN
PLAU
VCAN
SERPING1
FGG
FGB
WNT2
FGA
CXCL10
GREM1
CCL5
RARRES2
CXCL9
IL10
CCL11
CCL3
CCL8
CCL2
CCL4
XCL1
ADCYAP1
CXCL5
VEGFC
CXCL3
CSF3
IFNGR2
OSMR
CAV1
LIFR
PTGDR2
F3
IFNGR1
IL6R
IL6ST
PTPRA
ROBO1
GFRA1
ROBO3
CACNA1C
ENG
ACVR1
ACVR2A
TGFBR3
ACVR1B
BAMBI
ACVR2B
IL11RA
PGRMC1
CHRM3
ITGAV
FGFR1
FGFR2
ERBB2
EPHB2
ERBB3
CNTN1
NRP1
NRP2
PLXNA2
PLXNA3
PLXNA4
PLXNA1
FGFR4
FGFR3
ITGB5
IGF2R
EGFR
SCARB1
TNFRSF11B
CD36
LRP5
ITGB3
CD47
ITGA6
NOTCH3
NOTCH4
IGF1R
ITGA3
INSR
ITGA4
LRP8
VLDLR
LRP1
MRC2
LRP2
ST14
CD44
ITGA5
TLR2
TLR1
SELL
SELP
SELE
ITGA2B
ITGB1
SDC1
ITGB2
PLAUR
ITGAM
SDC4
FZD1
LRP6
FZD9
FZD7
FZD5
FZD8
ITGAX
CDH5
ITGAD
KDR
GPR75
GPR1
CXCR3
CMKLR1
CCRL2
IL10RB
SIRPG
IL10RA
CCR3
CCR4
ACKR4
ACKR2
CCR5
CCR1
CCR2
DARC
CCR10
CCR8
XCR1
ADCYAP1R1
VIPR1
VIPR2
ITGA9
CXCR2
LYVE1
CXCR1
FLT1
FLT4
CSF3R
CSF1R
0
100
TPM
3.4
250
Median (gcRMA)
-0.001
0.01
Mean (TMM)
BioGPS
GTEx
Myoblast
Myotube
Skeletal Muscle
Satellite Cells

Figure 3. Tumor-derived factors and skeletal muscle connectome. Left: alluvial diagram connecting the ligands from the upregulated genes in LM into its matched skeletal muscle receptors. Right: Heatmap of the expression levels of predicted receptors in human primary cell lineages, previously described by Ramilowski et al. 2015[16](red: Transcripts Per Million - TPM), four skeletal muscle tissues from BioGPS (grey: median gcRMA), and 491 skeletal muscle samples from Genotype-Tissue Expression (GTEx) project (green: mean Trimmed Mean of M-values - TMM).

Malignant cells express low levels of secretory genes responsible for inflammation

Once identified a cachexia-like expression profile in LM tumors and confirmed the potential of the tumor secretome in inducing muscle alterations, we next investigated the tumor cell types responsible for producing CIFs. First, to evaluate whether the malignant lung cells express some of the 332 upregulated genes found in the LM, we investigated these DEGs using the expression profile of eight cell lines and lung tumor-derived organoids. We applied k-means clusterization and identified five clusters. We detected two clusters in the secretome genes: cluster A representing the secretory genes expressed in malignant cells and cluster B representing secretory genes expressed at low levels in malignant cells. The genes in cluster A enriched terms related to angiogenesis and leukocyte chemotaxis (*THBS1* and *VEGFC*), and genes present in cluster B are associated with inflammation. Among the genes not predicted to encode secreted proteins, we identified three clusters: clusters C and E, representing genes expressed by malignant cells associated with cell proliferation and mitosis, and cluster D, containing genes expressed at low levels in malignant cells and associated with lymphocyte and T cell biological processes. Noteworthy, cluster E enriched the term "positive regulation of T cell apoptotic process" associated with the high expression of *IDO1* and *CD274* (PDL1) (**Figure 4**).

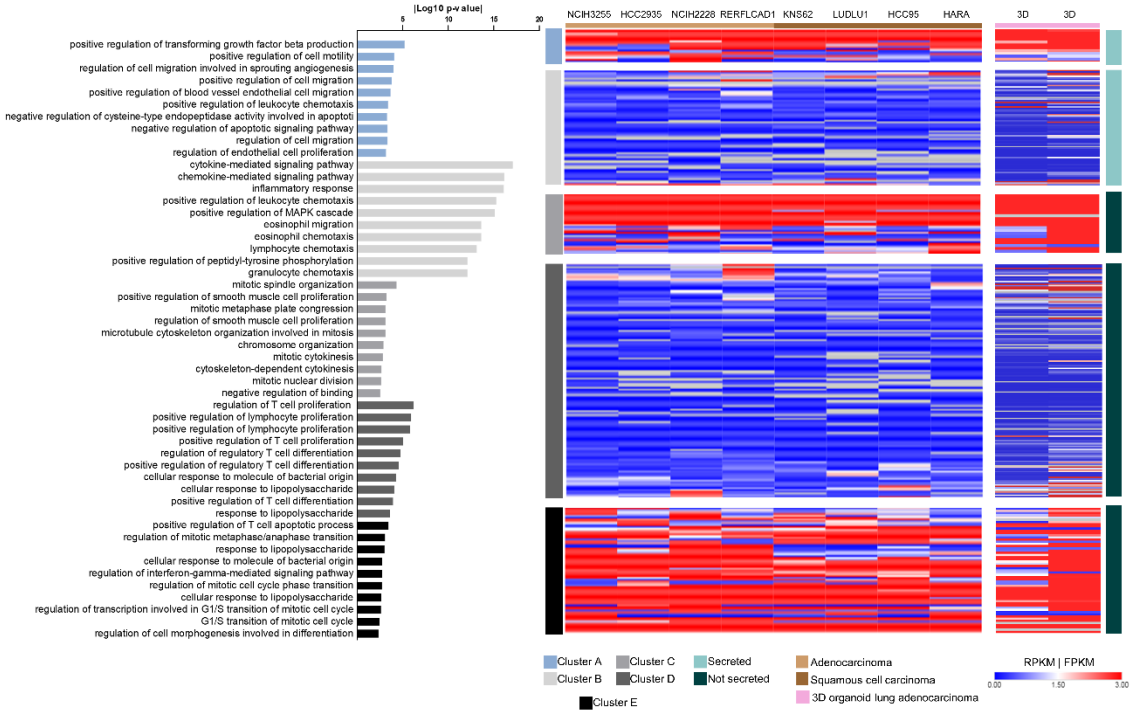

Figure 4. Tumor secretome derived from non-malignant NSCLC cells. Left: Enrichment analysis of top10 terms related to biological processes from each cluster according to EnrichR analysis. Right: Heatmap of gene abundance from cell lines (Reads Per Kilobase Million - RPKM) and lung adenocarcinoma derived-organoid duplicates (Fragment Per Kilobase Million - FPKM) in five clusters generated using k-means clustering analysis of secreted and non-secreted encoding genes.

Global expression profiles of eight cell lines from CCLE (Cancer Cell Line Encyclopedia) were evaluated from adenocarcinoma and squamous cell carcinomas. Global gene expression profiles of 3D organoids were collected from a single patient available in HCMI catalog (Human Cancer Model Initiative).

Low-muscularity patients present high proportions of CD8+T cells.

Since we observed that many inflammation-associated genes are lowly expressed by the lung cancer cells, we used CIBERSORTx to check the TME cellular composition and predict immune cells contribution for the expression of these genes. Low-muscularity patients presented high proportions of CD8+T cells (**Figure 5A**). To understand the molecular profile of CD8+T cells in the TME, we used an independent dataset of NSCLC scRNA-Seq to analyze the expression profile of the 90 secretome genes identified in low-muscularity patients. We found CD8+T cells expressing several of these genes in higher proportions than other immune cells (**Figure 5B**), suggesting that CD8+T cells may be producing factors identified in tumors of LM patients.

When plotting the PCA using the CD8+T cells enriched expression profile, we could better separate the high- from the low-muscularity patients (**Figure 5C**). Cytotoxic and exhausted T cells were prevalent in LM when compared to HM (**Figure 5D**). Investigating the 332 upregulated genes in LM in another scRNA-Seq data from the T cell population of NSCLC using CellphoneDB, we predicted ligands (CCL3L3, CCL5, CCL3, and HLA-G) and receptors (CCR1 and LILRB2) communications among effectors, exhausted, pre-exhausted, and naive CD8+T cells (**Figure 5E**). We observed that exhausted (CD8_C6_LAYN) and pre-exhausted (CD8_C4_GZMK) CD8+T cells presented increased interactions, specifically via CCR1 (exhausted) - CCL3L3 (pre-exhausted) and CCL3 (exhausted) - CCR1 (pre-exhausted) (**Figure S2A and 5E**). Moreover, genes expressed in exhausted tumor-infiltrating CD8+T cells were upregulated in LM patients, such as *GZMB, VCAM1*, *IFNG*, *CCL3, FASLG*, *MYO7A*, *STMN1*, *SAMSN1*, and *ITGAE* (**Table S6**). CD8 and exhaustion scores negatively correlate with PMA (**Figure S2B**). We next evaluated the gene expression of cancer cachexia markers (*Il6* and *Ifng*), *Cd8a*, and exhaustion markers (*Cd274* and *Pdcd1*) in LLC mice with cancer cachexia. We found a slight increase in cachexia and exhaustion marker genes in the CC groups compared to the PC group (**Figure 5F**). These results suggest that the LLC model can recapitulate the immunosuppressive TME found in lung cancer cachexia patients.

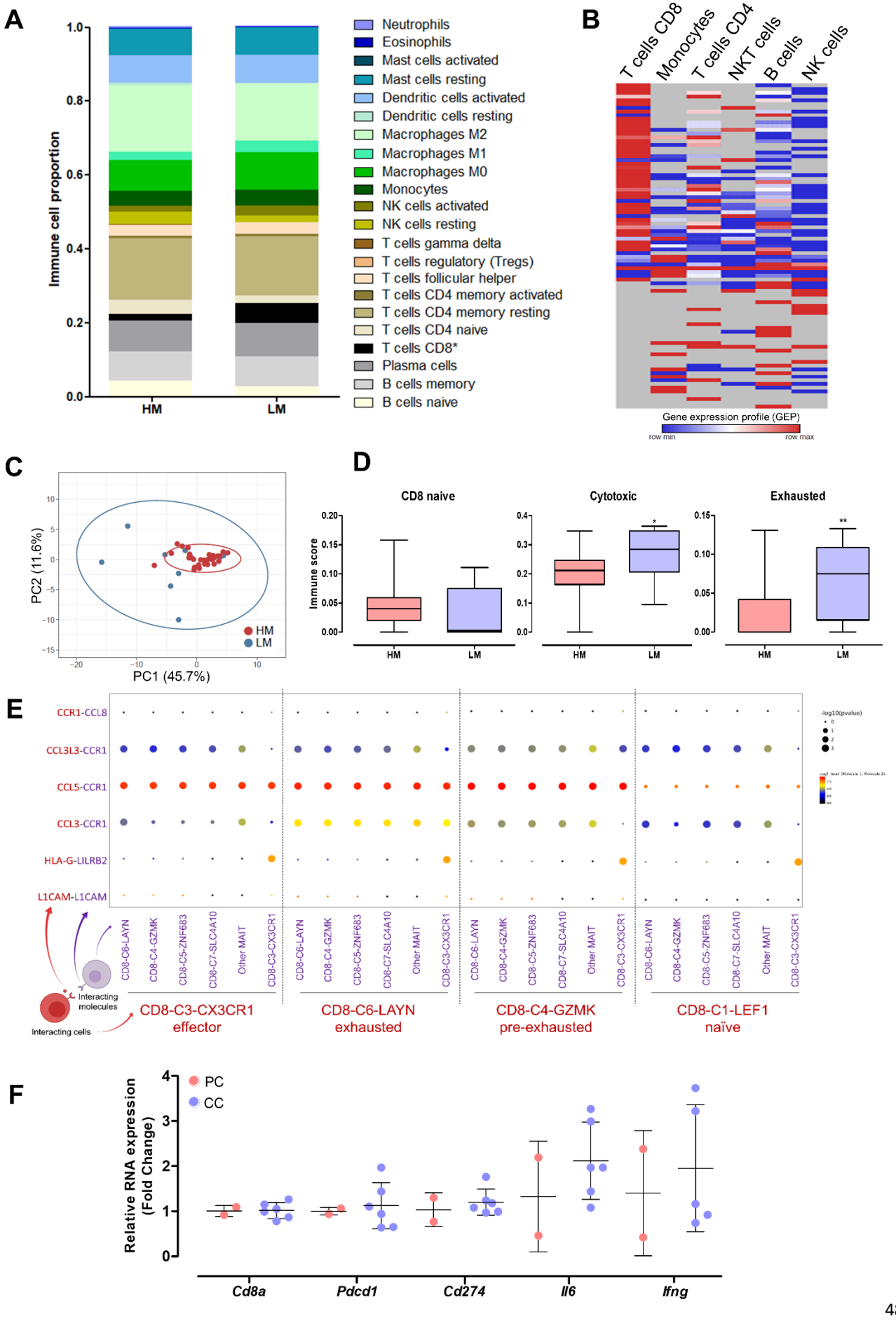
A
Immune cell proportion
HM
LM
Neutrophils
Eosinophils
Mast cells activated
Mast cells resting
Dendritic cells activated
Dendritic cells resting
Macrophages M2
Macrophages M1
Macrophages M0
Monocytes
NK cells activated
NK cells resting
T cells gamma delta
T cells regulatory (Tregs)
T cells follicular helper
T cells CD4 memory activated
T cells CD4 memory resting
T cells CD4 naive
T cells CD8*
Plasma cells
B cells memory
B cells naive
B
T cells CD8
Monocytes
T cells CD4
NKT cells
B cells
NK cells
Gene expression profile (GEP)
row min
row max
C
PC2 (11.6%)
PC1 (45.7%)
HM
LM
D
CD8 naive
Cytotoxic
Exhausted
Immune score
HM
LM
E
CCR1-CCL8
CCL3L3-CCR1
CCL5-CCR1
CCL3-CCR1
HLA-G-LILRB2
L1CAM-L1CAM
CD8-C6-LAYN
CD8-C4-GZMK
CD8-C5-ZNF683
CD8-C7-SLC4A10
Other MAIT
CD8-C3-CX3CR1
Interacting molecules
Interacting cells
CD8-C3-CX3CR1 effector
CD8-C6-LAYN exhausted
CD8-C4-GZMK pre-exhausted
CD8-C1-LEF1 naïve
F
Relative RNA expression (Fold Change)
PC
CC
Cd8a
Pdcd1
Cd274
Il6
Ifng

Figure 5. Digital cytometry based on the gene expression profile revealed that LM patients presented high proportions of CD8+ T cells. A) Bar plot representing 22 immune cells score in LM and HM patients calculated using CIBERSORTx. * *P*-value = 0.03 (Mann-Whitney). **B)** Gene expression profiles (GEP) of secretome genes found upregulated in tumor tissue of LM patients analyzed in single-cell RNA-Seq in peripheral blood mononuclear cells (PBMCs) of NSCLC patients. GEP represents the estimated expression values (log_2) calculated by CIBERSORTx using group mode function**. C)** Principal component analysis (PCA) demonstrating HM and LM clusters generated using the CD8+ T cells enriched expression profile. **D)** Box-plots of CD8 naive, cytotoxic, and exhausted cells scores between LM and HM patients determined using ImmuCellAI. **E)** Cell-cell communications between T cell subsets from NSCLC using the upregulated genes list enriched in LM patients (single-cell data of NSCLC T cell population from GSE99254). *P*-values are indicated by circle size. The average expression level of interacting molecule 1 in CD8 subset red and interacting molecule 2 in CD8 subset purple is indicated by color. Analysis performed using CellPhoneDB. **F)** Dot plot demonstrating gene expression (Fold Change) of cachexia markers (*Il6* and *Ifng*) and CD8 (Cs8a), and exhaustion markers (*Cd274*, and *Pdcd1*) in Lewis Lung Carcinoma (LLC) mice with cachexia compared to non-cachectic animals. LM: low-muscularity; HM: high-muscularity; PC: pre-cachectic (N=2); CC: cancer cachexia (N=7).

Discussion

We demonstrated that lower PMA assessed in CTs used for lung cancer diagnosis before tumor resection predicts worse outcomes in NSCLC patients. We also proposed PMA cutoffs for women and men at young and older ages based on ML analysis. Tumor transcriptome demonstrated that low-muscularity patients present a cachexia-like profile highly expressing CIFs. Digital cytometry based on transcriptomic data revealed that TME is enriched with a suppressive immune microenvironment, mainly composed of CD8+T cells. The prediction of ligand-receptors revealed candidates that may ultimately lead to muscle wasting.

Cancer cachexia classification remains an important clinical challenge. The international consensus proposed as milestones for cachexia classification a weight loss >5% over the past six months or BMI <20 and any degree of weight loss >2% or lumbar SMI determined by CT imaging (men <55 cm^2/m^2; women <39 cm^2/m^2)[4]. However, CTs are often taken in the thoracic region of lung cancer patients[7]. To overcome this limitation, we constructed a cachexia classification model using ML to evaluate clinical parameters routinely available for NSCLC patients. We used PMA, tumor stage, age, and overall survival to construct the model. We found that PMA can predict worse survival. The PMA (z-score) cutoff identified in CART was also validated using independent analysis. These results demonstrated that PMA cutoffs are strong predictors of the poor prognosis of cachectic NSCLC patients. Although not demonstrating an association with worse overall survival, our research group previously demonstrated PMA cutoffs as a potential cachexia predictor in NSCLC patients[9]. The cutoffs found in this study were PMA <32.2 cm^2 and <21 cm^2 for men and women, respectively, similar to those found herein using robust ML analysis. This same ML analysis was recently used to predict cachexia risk-levels in incurable cancer patients with more than 88% of precision and sensibility[24]. These results reinforce the importance of using ML approaches applied in clinical features of cancer patients to classify cachectic states.

We found a high frequency of potentially cachectic patients with smoking habits, corroborating with literature indicating an increase in muscle mass loss in tobacco smokers[25] and confirming the significant role of nicotine in altering the tumor microenvironment and prognosis, as demonstrated for

cachectic patients with pancreatic cancer[26]. Moreover, a high risk of tumor recurrence was found in patients with cancer cachexia and agrees with other studies[27]. *KRAS* mutation was frequently found in our low-muscularity patients, and evidence suggests *KRAS*-mutated tumors are commonly associated with lung cancer cachexia[28]. Since adenocarcinomas - the tumor with the highest prevalence of the *KRAS* mutation[29] - occur at similar rates in LM (72.7%) and HM (85.7%) groups, we confirmed that *KRAS* mutations were associated with cachexia phenotype rather than tumor histopathology. Thus, studies investigating differences in the cachexia phenotype of preclinical models inoculated with KRAS mutated lung cancer cell lines may help to understand the impact of KRAS mutation in the syndrome. These essential features can help guide cancer cachexia definition towards precision medicine in the future.

We found no association between ethnicity and low muscularity in our discovery set, in line with a previous reports showing that cachexia is not related to ethnicity[S1]. By contrast, blacks are suggested to have a higher risk of developing pancreatic cancer-associated cachexia[S2]. Despite the high genetic admixture of ancestry in Brazilians[S3], which challenge to fit this population in the US ethnicity classification[S4] all patients in our validation set classified as black and mixed (N=4) were in the LM group (data not shown). Unfortunately, the low number of samples for this validation set precluded statistical analysis and any precise interpretation regarding ethnicity and lung cancer cachexia.

Our cachexia classification was validated by the increase of CIFs genes in the tumor of LM patients, such as *LIF*, *IL6*, *IFNG*, and *CCL2*[10]. We also identified the increased expression of genes described in NSCLC patients with lower PMA, such as *NCAM1*, *SCG2*, *CSF3*, and *CCL8*[9]. To better understand how the identified factors influence skeletal muscle phenotype and function, we characterized the landscape of cell-cell interaction between tumor and skeletal muscle cells. We predicted the ligand-receptor interactions using transcriptomic data from both tissues to determine the crosstalk. This approach has a higher resolution than proteomics analysis and provides insights into cell and tissue communication[30]. We found receptors for important CIFs expressed at high levels in skeletal muscle cells, such as IFNG receptor (IFNGR2), LIF receptors (LIFR and IL6ST), which can directly trigger atrophy[1]. The gp130 family members, IL-11, IL-6, OSM, and LIF (all highly expressed in the tumors of LM patients) potentially impact skeletal muscle wasting by inducing the STAT3 signaling pathway in a mice model of cancer cachexia[31]. These results confirm the importance of these tumor-derived factors in NSCLC cachexia. Previous studies have inhibited classical CIFs described herein, such as IFN-γ and IL6[S5-S8]. Cachectic patients with non-small cell lung cancer treated with an anti-IL-6 antibody ameliorated weight loss while decreasing anemia and anorexia[S6,S7]. LLC treated with anti-IL-6 demonstrated a improved prognosis and ameliorated the cachexia phenotype[S7]. Antibodies against IFN-γ was also able to decrease body weight loss in LLC mice[S8]. Although preclinical studies inhibiting CIFs have shown some efficiency, these factors have not provided the same benefit in clinical trials[S5,S9]. These previous studies based on CIF inhibitors or immune modulators have shown limited efficiency in treating cancer cachexia, probably because they act on specific targets. Our tumor-muscle interactome analysis revealed a combinatorial action of soluble secreted mediators by cancer cells and cells within the tumor microenvironment that directly acts on skeletal muscle to induce wasting. More studies are needed to describe the role of these ligand-receptors interactions and their combinatorial action in inducing muscle atrophy in patients with lung cancer cachexia.

To investigate the tumor cells responsible for tumor-derived factors' production and secretion, we further evaluated the malignant cell expression profile of NSCLC cell lines that are more representative for NSCLC tumor tissues[32]. We found that inflammation-related genes are low expressed in malignant cells, while genes associated with vessel permeability and T-cell motility, recruitment, and activation are increased[33]. Moreover, we identified enrichment in genes associated with T cell apoptosis, specifically the genes *CD274* (encoding the PDL1 protein) and *IDO1*. The processes involved in tumor immune evasion through IFN-γ (also enriched elevated in LM patients) has been recently reviewed[34]. Anti-tumor cells secrete IFN-γ that induces genomic instability and/or immune evasive gene expression signature in malignant cells (including *PDL1* and *IDO1*)[34]. PDL1 is the ligand of the inhibitory receptor PD-1, responsible for CD8 cell dysfunction in NSCLC[35]. IDO1 can produce local depletion of amino acid tryptophan, contributing to the immunosuppressive microenvironment[34]. These previous results corroborate our digital cytometry analysis that demonstrates an increase in CD8+T cells in TME of LM patients enriched with exhausted cells. Indeed, when analyzing tumors from cachectic mice we found an induction of exhaustion markers compared to pre-cachectic animals. Although cytotoxic CD8+T cells infiltrated in TME are frequently associated with intense anticancer activity[36], the CD8+T cells' signal in tumor tissues is not always related to better outcomes. Using TCGA data, THORSSON et al., 2018 identified six immune subtypes. Subtype 2 (designated as C2) is characterized by IFN-γ predominance and the highest content of M1 macrophages and CD8+T cells. Cancer patients presenting subtype C2 showed less favorable survival despite having the highest lymphocyte infiltration[13]. The authors proposed hypotheses trying to explain this controversy by arguing that these tumors are more aggressive or escaped immune recognition by pre-existing remodeling. However, our results raise the possibility that patients presenting tumors C2 have less favorable survival because they may also be cachectic. In fact, CD8+T cells induce cachexia and adipose tissue wasting in experimental models of chronic infection via type I IFN[37].

Considering the immunosuppressive profile of LM tumors and immunotherapy promises to restore T cell cytotoxicity and its anticancer properties, immunotherapy would probably benefit NSCLC cachectic patients. Cachectic NSCLC patients are resistant to immunotherapy[38], thus restoring the cytotoxicity of CD8+T cells may be crucial for treatment response. Indeed, Bonomi and colleagues reviewed this topic and proposed the urgency of clinical trials testing an agent to reverse cachexia combined with an immune checkpoint inhibitor to treat advanced lung cancer patients, since the treatment with ghrelin analogue have effects in T cell development and proliferation[39]. Therefore, more studies are needed to verify whether immunotherapy combined with targeting drugs of CIFs have the potential to reverse cachexia and increase immunotherapy response.

This study is innovative and valuable for NSCLC cachexia. However, it has limitations. The patients lack information regarding other comorbidities that may influence body composition and clinical outcomes. Considering that LM patients presented a higher frequency of smokers, it is rational to consider that the skeletal muscle alterations identified are triggered by the combination of smoking and CIFs. However, it is difficult to determine the individual impact of each of these variables. We also failed to apply the golden standard definitions of cachexia, such as weight loss, in those patients. Moreover, despite transcriptomic data having high resolution and producing more robust information

than proteomic data, the results should be interpreted carefully considering the complex transcriptional regulation in human cells. Therefore, the results from secretome and ligand-receptor predictions presented in this study need experimental validation in cachectic patients. The causal relationship between the set of CIFs from cancer cells or cells from the tumor microenvironment described herein and muscle atrophy needs to be confirmed in preclinical models. Moreover, the immunosuppressive profile of TME from LM patients also has to be validated using histological examination to check the correlation between CD8 exhaustion and NSCLC cachexia in a higher number of samples.

We used systems biology to classify cachexia in treatment-naive NSCLC patients before surgery and characterized the TME immune fraction from the low-muscularity patients to understand molecular mechanisms by which the tumor induces skeletal muscle atrophy and influences the poor outcomes. These results may contribute to developing future therapeutic strategies aiming to decrease muscle atrophy and immunosuppression, thus increasing the survival and quality of life of patients with NSCLC cachexia. Taken together, the predictive ML model identified patients with lower muscle mass and worse survival (LM patients), who showed a TME with an inflammatory and immunosuppressive profile, expressing cachexia biomarkers and potentially enriched with CD8+T cells.

Acknowledgements

This study was supported by the São Paulo Research Foundation—FAPESP (grant 2020/03854-4 to RFC) and by the National Council for Scientific and Technological Development, CNPq (#41601/2019-1 to SSC and #311530/2019-2 to RFC). Human and animal studies have been performed in accordance with the national laws and ethical standards laid down in the 1964 Declaration of Helsinki and its later amendments. Human and animal studies have been performed in accordance with the national laws and ethical standards laid down in the 1964 Declaration of Helsinki and its later amendments. The datasets presented in this study can be found in online public repositories available under the accession numbers GSE103584 and GSE99254. The results shown here are in part based upon data generated by the Genotype-Tissue Expression project (GTEx) (https://gtexportal.org/). The authors of this manuscript certify that they comply with the ethical guidelines for authorship and publishing in the Journal of Cachexia, Sarcopenia, and Muscle[40].

Conflict of interests

The authors Sarah Santiloni Cury, Diogo de Moraes, Jakeline Oliveira, Paula Paccielli Freire, Patricia P Reis, Miguel Luiz Batista Jr, Érica Nishida Hasimoto, Robson Francisco Carvalho declare that they have no conflicts of interest.

CAPÍTULO 2 - *Tumor secretome factors towards the core of cancer cachexia*

Abstract

Cancer cachexia is a syndrome characterized by skeletal muscle wasting, leading to a significant weight loss that impacts patient morbidity and survival. The action of several cachexia-inducing factors (CIFs), including pro-inflammatory cytokines secreted by cancer cells and cells within the tumor microenvironment, contributes to muscle wasting. Pancreatic ductal adenocarcinoma (PDAC), the cancer type with the highest cachexia prevalence, demonstrates 5–20% neoplastic cellularity and high leukocyte infiltration. However, it remains unclear which cell types in PDAC (cancer cells or cells of the tumor microenvironment) secrete these CIFs. We determined the expression profile of 263 cytokine-cytokine receptor interaction pathway genes using a pan-cancer approach, aiming to identify a core of CIFs specifically and highly expressed in tumor types frequently associated with cachexia. PDAC expressed the highest number of secreted genes from the cytokine-cytokine receptor interaction pathway. We also found that PDAC upregulated 71 cytokine genes shared with at least one cancer type, defined as our core of CIF genes. This analysis also identified 26 genes highly enriched specifically in five cancer types mostly associated with cachexia (gastrointestinal and head and neck cancers). We determined the expression profile of the core-CIF genes in 57,530 pancreatic cells using single-cell RNA sequencing (scRNA-Seq) data from PDAC and normal-like pancreatic tissues (n=27 and n=14, respectively). Our analysis revealed core-CIF genes are mainly expressed by malignant ductal cells, but we also found genes specifically enriched in tumor T cells (*IL2RB*, *CCL5*, *CCL4*, and *CXCL13*) and macrophages (*CCL3*, *CXCL9*, and *CCL18*), suggesting their potential as cachexia mediators. Moreover, we found that core-CIFs have receptors expressed in the main affected organs in cachexia, as adipose, liver, and skeletal muscle. Our findings represent a biological dimension of a core of pro-cachectic factors potentially associated with molecular events identified in cancer cachexia. We found different patterns of core-CIFs expression among the single-cells of PDAC and their potential interactions with adipocytes. This approach provides new insights into the molecular mechanisms behind cachexia development in PDAC.

Keywords: cancer cachexia, pan-cancer, pancreatic cancer, single-cell RNA sequencing, interactome

Introduction

Cancer cachexia is a syndrome characterized by skeletal muscle wasting, leading to a significant weight loss that impacts patient morbidity and survival [1]. Tumor-derived factors, including pro-inflammatory cytokines such as IL-1α, IL-6, IL-8, TNF-α, and INF-γ, contribute to the systemic metabolic alterations in cancer cachexia [2]. The pathogenesis of cachexia-associated cancers is multifactorial, but cytokines and tumor-derived factors have been implicated in alterations in different tissues and organs [3].

Although skeletal muscles are the most affected tissue in cancer cachexia, adipose tissue, liver, brain, and bones are also severely affected by metabolic and molecular disarrangement [4,5]. Tumor-derived factors, including cytokines, reduce skeletal muscle mass and function [6]. Alterations in the respiratory and cardiac muscles in the syndrome may induce respiratory and cardiac failures in cachectic cancer patients, contributing to high death rates [7,8]. Loss of adipose tissues may also be observed in cachectic patients due to increased lipolysis, decreased lipogenesis, depletion of fat depots, and whole-body energy expenditure caused by increased thermogenesis [9]. The liver is stimulated to produce acute-phase proteins and repress drug clearance pathways, which result in excessive toxicity of anticancer therapy [4,10]. In the central nervous system, inflammatory factors affect the neuroendocrine control of appetite leading to anorexia. Finally, bone density loss can also be associated with cancer cachexia, although few studies indicate its association with cachexia [4,5]. Studies addressing the potential crosstalk between tumor and target tissues may help us to understand the pathophysiology of disease and design novel treatment options.

Although previous evidence points to these complex inter-tissue communications existing in cancer cachexia [3], it is still essential to determine whether these tumor-derived factors are produced by the tumor or by the host in response to the carcinoma. Our group has previously shown that the combinatory gene expression of cachexia-inducing factors is positively correlated with high degrees of cachexia prevalence and weight loss among cancer types [11]. We found in pancreatic ductal adenocarcinoma (PDAC), the cancer type with the highest cachexia prevalence and weight loss rates [2], high tumor expression most of the evaluated CIFs [11]. PDAC is also characterized by low tumor purity, demonstrating 5–20% of neoplastic cellularity and high leukocyte infiltration [12,13]. However, it remains unclear which cell types in PDAC (cancer cells or cells of the tumor microenvironment) produce these CIFs. Besides, the extent to which these cells express CIFs needs further analysis.

Our pan-cancer study recently demonstrated that secretory genes (tumor secretome) belonging to the "cytokine-cytokine receptor interaction" pathway are upregulated in tumors highly associated with

cachexia [11]. Considering the potential of this pathway to have other CIFs not previously associated with cachexia, it is crucial to determine a core of genes representative of the pathway in the context of cancer cachexia. Moreover, we expect to distinct the main source of each CIFs by analyzing tumor transcriptomes (bulk and single cells). Therefore, we aimed to address the relevance of the secretome genes related to cytokine-cytokine receptor interaction in the context of cancer cachexia by characterizing the tumor tissues and pancreatic tumor single-cells most expressing these genes and their crosstalk with targeted tissues, as liver, skeletal, adipose tissues. By doing that, we expect to find novel cachexia-associated biomarkers responsible for inflammation that may ultimately serve as molecular treatment targets.

Material and Methods

Transcriptome-based secretome analysis

First, we downloaded the list of cytokine-cytokine receptor interaction genes from The Kyoto Encyclopedia of Genes and Genomes (KEGG) and filtered only the secreted protein-coding genes based on the human secretome list available at The Human Protein Atlas [14] (https://www.proteinatlas.org/humanproteome/secretome). This list of secreted protein-coding genes was predicted by a whole-proteome scan using at least two of the three following signal peptide prediction methods: SignalP4.0, Phobius, and SPOCTOPUS. The original KEGG list had 294 genes, and the final list was composed of 263 genes, which were further analyzed.

Pan-cancer analysis of cytokine-cytokine receptor interaction genes

Using the same strategy previously described [11], we analyzed the transcriptional profiles of 263 cytokine-cytokine receptor interaction selected genes in 12 human cancers from TCGA (https://portal.gdc.cancer. gov/). We compared them with matched normal tissues from TCGA and The Genotype-Tissue Expression (GTEx) Project (http://www. gtexportal.org/). We analyzed the following cancer types ranging from high to low prevalence of cachexia and weight [2,15,16]: invasive breast carcinoma (BRCA); colon adenocarcinoma (COAD); oesophageal carcinoma (ESCA); head and neck squamous cell carcinoma (HNSC); acute myeloid leukemia (LAML); liver hepatocellular carcinoma (LIHC); lung adenocarcinoma (LUAD); lung squamous cell carcinoma (LUSC); pancreatic adenocarcinoma (PAAD); prostate adenocarcinoma (PRAD); rectum adenocarcinoma (READ); stomach adenocarcinoma (STAD). Differentially expressed genes (DEGs) between tumors and normal samples were determined by four-way ANOVA using the web-based tool Gene Expression Profiling

Analysis [17] (http://gepia.cancerpku. cn/). ANOVA measures the strength of the relationship between the log-transformed expression of a gene and all variables mentioned above, between tumour and normal tissues [18]. DEGs were selected using the statistical cutoffs of log2 fold change (FC) > 1 and q value < 0.01.

Definition of a "core" of cachexia inducing factors

The core-CIF represents the most important cytokines in tumor highly associated with cachexia. We identified the core-CIF selecting the secretome genes of cytokine-cytokine receptor interaction pathway from each cancer type shared with PDAC. We next verified the protein-protein interaction network of core-CIF genes upregulated in at least five cancer types highly associated with cachexia. We used STRING tool v.11 considering experiments, databases, co-expression, neighborhood, and co-occurrence as active interaction sources. Only highest confidence interactions were included (interaction score of at least 0.9), and the disconnected nodes were omitted in the network. PPI-enrichment p-value < 0.01 was considered significant. Visualization and data annotation of PPI networks were constructed using Cytoscape (v3.7.2) [19].

Pancreatic ductal adenocarcinoma immune tumor microenvironment (TME)

CIBERSORTx tool [20] was used to assess immune cell type abundance of 22 cell types (LM22 matrix signature) from bulk PDAC available in TCGA and normal pancreatic tissues available in GTEx portal (n=150 and n=165, respectively). We next evaluated the immune cell type differences between PDAC tumors presenting high purity (high neoplastic cellularity) or low purity (low neoplastic cellularity) according to the classification from TCGA research network [12].

Single-cell RNA sequencing from pancreatic adenocarcinoma analysis

We reanalyzed the scRNA-seq data from Peng et al., 2019 [21], aiming to determine the gene expression profile of core-CIFs in 57,530 pancreatic cells using scRNA-Seq data from PDAC and normal-like pancreatic tissues (n=27 and n=14, respectively) publicly available at Genome Sequence Archive (GSA; CRA001160) [22] under project PRJCA001063. We used the same analysis pipeline performed in the original study. The data from raw counts were processed using the Seurat package in R (v.4.0). Next, cell clusters and marker genes were visualized using tSNE or Nebulosa (v.1.7) dimensional reduction plots.

Cancer Cell Line Encyclopedia data analysis

Gene expression data (log2 transformed transcripts per million - TPM, using pseudo-count of 1) of the 71 core-CIFs in 50 pancreatic cancer cell lines from the Cancer Cell Line Encyclopedia (CCLE) portal (https://portals.broadinstitute.org/ccle) [23] were downloaded using the Cancer Dependency Map (DepMap; https://depmap.org/) data portal (Expression 21Q2 Public datasets) [24].

Tumor and targeted tissue communication via core-CIF

To check how the core-CIF from PDAC tumor cells can induce alterations in the distant organs and tissues, we next predicted the ligands existing in the Core-CIF list and the gene expression of their receptors in targeted list cells, tissues, or organs. We used the ligand-receptor consensus list generated by Ramilowski et a., 2015 [25] to verify the expression of the receptors in muscle, adipose, liver, brain, and bone human primary cells from the FANTOM5 project.

KEGG mapper tool (https://www.genome.jp/kegg/mapper/search.html) was used to visualize the Core-CIFs in the cytokine-cytokine receptor interaction pathway and their correspondent receptors. We selected the receptors with more than 3 ligands for further investigation. Furthermore, the microarray data from GSE51931 was used to measure the expression of these selected receptors tissues (skeletal, adipose, and liver) from a pancreatic cancer cachexia model [26]. The gene expression analysis was performed by comparing cachectic tissues and controls using the GEO2R tool (http://www.ncbi.nlm.nih.gov/geo/geo2r/).

Data representation

Secretome genes among all tumor types were displayed using Circos [27] (http://circos.ca/). Heatmaps were created using the web tool Morpheus (https://software.broadinstitute.org/morpheus). Alluvial diagram connecting the ligands into their respective receptor was generated using SankeyMATIC online tool (http://sankeymatic.com/).

Results

Cytokine-cytokine receptor interaction term reveals potential CIFs

PDAC (also called PAAD in TCGA collection) shared most of the secreted cytokines with other cancer types (**Figure 1A**) and was the cancer type most expressing the cytokine-cytokine receptor interaction genes predicted to be secreted by tumor cells (**Figure 1B**). The tumor types highly associated with cachexia, STAD, READ, COAD, ESCA, and HNSC, had in common with PAAD a high number of upregulated cytokine-cytokine receptor interaction secreted genes (**Figure 1B**). We identified the core-

CIF containing 71 genes (all upregulated in PDAC and shared with at least one cancer type), including mostly cytokines and chemokines. The majority was highly expressed in cachexia-associated cancers and absent or downregulated in cancer types where cachexia is not prevalent (**Figure 1C**). Moreover, we constructed the network of protein-protein interaction of 26 core-CIF components upregulated in PAAD, STAD, READ, COAD, ESCA, and HNSC (cachexia associated cancer types). We identified enrichment in Chemokine interleukin-8-like superfamily (**Figure 1D**), suggesting that these factors may be necessary for inflammation in cachexia.

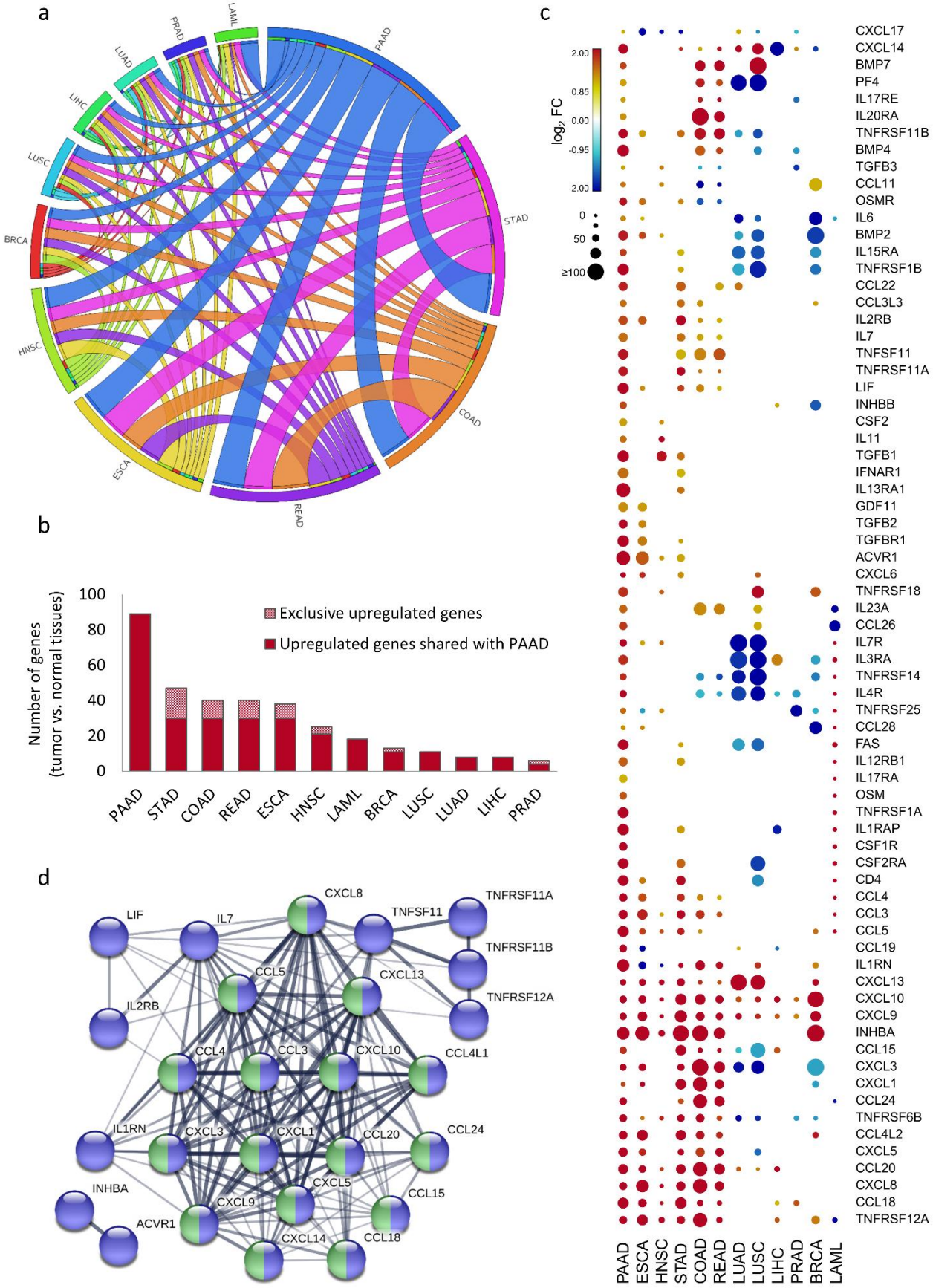
a
PAAD
STAD
COAD
READ
ESCA
HNSC
BRCA
LUSC
LIHC
LUAD
PRAD
LAML
b
Number of genes
(tumor vs. normal tissues)
100
80
60
40
20
0
Exclusive upregulated genes
Upregulated genes shared with PAAD
PAAD
STAD
COAD
READ
ESCA
HNSC
LAML
BRCA
LUSC
LUAD
LIHC
PRAD
c
log2 FC
2.00
0.85
0.00
-0.95
-2.00
0
50
≥100
CXCL17
CXCL14
BMP7
PF4
IL17RE
IL20RA
TNFRSF11B
BMP4
TGFB3
CCL11
OSMR
IL6
BMP2
IL15RA
TNFRSF1B
CCL22
CCL3L3
IL2RB
IL7
TNFSF11
TNFRSF11A
LIF
INHBB
CSF2
IL11
TGFB1
IFNAR1
IL13RA1
GDF11
TGFB2
TGFBR1
ACVR1
CXCL6
TNFRSF18
IL23A
CCL26
IL7R
IL3RA
TNFRSF14
IL4R
TNFRSF25
CCL28
FAS
IL12RB1
IL17RA
OSM
TNFRSF1A
IL1RAP
CSF1R
CSF2RA
CD4
CCL4
CCL3
CCL5
CCL19
IL1RN
CXCL13
CXCL10
CXCL9
INHBA
CCL15
CXCL3
CXCL1
CCL24
TNFRSF6B
CCL4L2
CXCL5
CCL20
CXCL8
CCL18
TNFRSF12A
PAAD
ESCA
HNSC
STAD
COAD
READ
LUAD
LUSC
LIHC
PRAD
BRCA
LAML
d
CXCL8
TNFRSF11A
LIF
IL7
TNFSF11
TNFRSF11B
CCL5
CXCL13
TNFRSF12A
IL2RB
CCL4
CCL3
CXCL10
CCL4L1
IL1RN
CXCL3
CXCL1
CCL20
CCL24
INHBA
CXCL5
CCL15
CXCL9
ACVR1
CXCL14
CCL18

Figure 1. The expression landscape of cytokines-cytokine receptor interaction secreted genes is enriched in cancer highly associated with cachexia. a) The thickness of each link in the Circos plot represents the number of shared upregulated secretome genes among tumor types. **b)** Upregulated genes shared with pancreatic adenocarcinoma (PAAD) and non-shared with pancreatic adenocarcinoma (PAAD). **c)** A heat-scatterplot presenting the results of secretory genes from cytokine-cytokine receptor interaction pathway from each cancer type shared with PAAD. The circles' color corresponds to the log2FC, while circle size is based on the –log10 p-value adjusted in the tumor compared to all healthy tissues. Rows and columns were clustered based on Euclidean distance between log2FC values. **d**) STRING analysis of protein-protein interactions of the 26 secreted proteins that are shared by PAAD, ESCA, STAD, HNSC, COAD, and READ. Edges thickness indicates confidence. Blue circles represent proteins of the cytokine-cytokine receptor interaction pathway, count in the gene set 26 of 263. We observed that the central cluster is enriched by Chemokine interleukin-8-like superfamily, count in the gene set 16 of 26 (green circles). Only proteins significant in at least four tissue sites are presented.

scRNA-seq reveals malignant and infiltrating immune cells in pancreatic tumors highly expressing core-CIF

We further analyzed the expression landscape of core-CIF in scRNA-seq data from pancreatic cancer samples. We found that macrophages, B, and T cells were most abundant in cancer tissues and almost absent in the normal pancreas, especially B cells and T cells (**Figure 2A and B**). Interestingly, T cell and macrophages are also increased in PDAC samples from TCGA when compared to normal pancreas from GTEx (**Figure 2C**). Moreover, we evaluated the expression profile of the 71 core-CIF and identified gene expression enrichment according to cell type, as represented in Nebulosa t-SNE plots and dot plots, however 69 core-CIFs were available in single-cell analysis (**Supplementary figure 1**). Overall, we found that malignant ductal cells (Ductal2) expressed most core-CIFs (57.9%), followed by macrophages (39.1%), fibroblasts (39.1%), and T cells (27.5%) (**Figure 2D**). This result may represent an inflammatory gain of function of malignant ductal cells, considering that normal ductal cells (Ductal1) express less core-CIFs genes (29%) when compared to the neoplastic cells. We verified that the majority of genes were expressed by higher percentages of Ductal2 cells but were also expressed by populations of other cell types from the TME (**Supplementary Figure 2**). *CXCL5*, *CCL15*, and *PF4* were particularly expressed in malignant ductal cells (**Supplementary Figure 2**). We validated the increased expression of some core-CIF genes in pancreatic cancer cell lines from CCLE, including *CXCL8*, *CXCL1*, *CXCL5*, *LIF*, *FAS*, and *TGFB2* (**Supplementary figure 3**). Moreover, we focused this analysis on the 26 genes shared by the cancer types associated with cachexia (PAAD, ESCA, STAD, HNSC, COAD, and READ). In tumor T cells, we found *IL2RB, CCL5, CCL4*, and *CXCL13* enriched expression; in macrophages, we identified *CCL3*, *CXCL9*, and *CCL18*; for malignant ductal cells, we found *CCL15* and *CXCL5*. *CXCL14* was found specifically in fibroblasts, and other genes such as *CCL20*, *CXCL10*, *CCL4L2*, *CXCL1*, and *TNFRF11A* were identified as highly expressed in more than one cell population (**Figure 2E**).

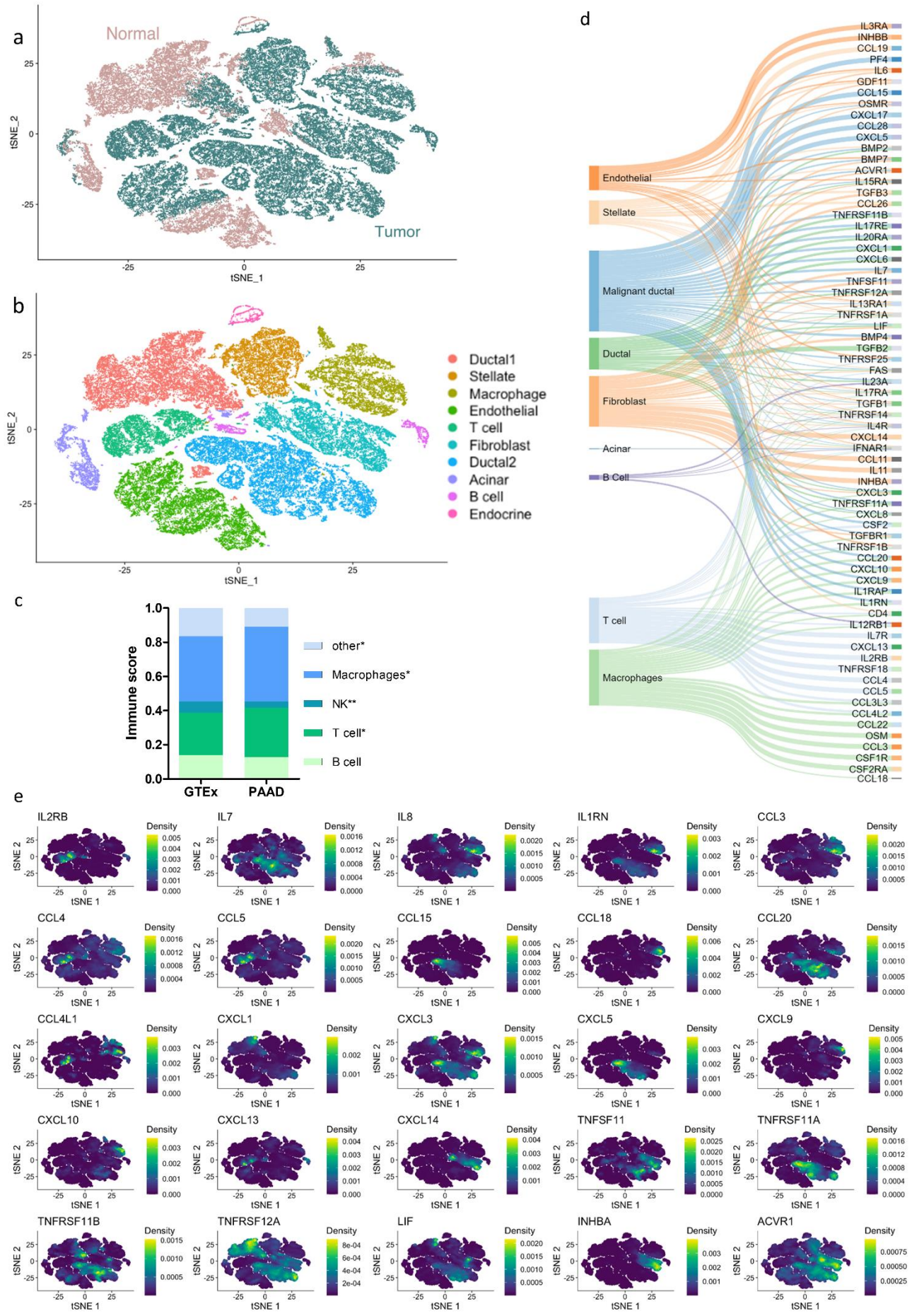
a
Normal
Tumor
tSNE_2
tSNE_1
b
Ductal1
Stellate
Macrophage
Endothelial
T cell
Fibroblast
Ductal2
Acinar
B cell
Endocrine
c
Immune score
other*
Macrophages*
NK**
T cell*
B cell
GTEx
PAAD
d
Endothelial
Stellate
Malignant ductal
Ductal
Fibroblast
Acinar
B Cell
T cell
Macrophages
IL3RA
INHBB
CCL19
PF4
IL6
GDF11
CCL15
OSMR
CXCL17
CCL28
CXCL5
BMP2
BMP7
ACVR1
IL15RA
TGFB3
CCL26
TNFRSF11B
IL17RE
IL20RA
CXCL1
CXCL6
IL7
TNFSF11
TNFRSF12A
IL13RA1
TNFRSF1A
LIF
BMP4
TGFB2
TNFRSF25
FAS
IL23A
IL17RA
TGFB1
TNFRSF14
IL4R
CXCL14
IFNAR1
CCL11
IL11
INHBA
CXCL3
TNFRSF11A
CXCL8
CSF2
TGFBR1
TNFRSF1B
CCL20
CXCL10
CXCL9
IL1RAP
IL1RN
CD4
IL12RB1
IL7R
CXCL13
IL2RB
TNFRSF18
CCL4
CCL5
CCL3L3
CCL4L2
CCL22
OSM
CCL3
CSF1R
CSF2RA
CCL18
e
IL2RB
IL7
IL8
IL1RN
CCL3
CCL4
CCL5
CCL15
CCL18
CCL20
CCL4L1
CXCL1
CXCL3
CXCL5
CXCL9
CXCL10
CXCL13
CXCL14
TNFSF11
TNFRSF11A
TNFRSF11B
TNFRSF12A
LIF
INHBA
ACVR1
Density
tSNE 1
tSNE 2

Figure 2. scRNA-seq analysis reveals core-CIF genes enriched in cell types from PDAC. a) t-SNE plot of 57,530 pancreatic cells using single-cell RNA sequencing (scRNA-Seq) data from PDAC and normal-like pancreatic tissues (n=27 and n=14, respectively). **b)** t-SNE plot of single cells distributed in 10 cell types: acinar, ductal 1, ductal 2 (malignant ductal cell), endothelial, fibroblast, stellate, endocrine, macrophage, B cell, and T cell. **c)** Bar graph representing the cell proportion of Natural Kiler, Macrophages, B, and T cells in PDAC from TCGA and normal pancreatic tissues from GTEx calculated using CIBERSORTx. * p-value < 0.05, and ** p-value < 0.01 **d)** Alluvial plot demonstrating the gene expression of core-CIFs per cell type. e) t-SNE expression plots from genes belonging to the core-CIF most expressed in the tumor types associated with cachexia prevalence (result demonstrated in Figure 1D). **e)** Expression density of 26 genes belonging to the core-CIF demonstrated in Nebulosa tSNE plots in all cell types identified in single-cell analysis.

Crosstalk between tumor cells and distant organs

We found that adipose cells followed by liver cells express a higher number of core-CIF receptors (85.5% and 62%, respectively). Neurons and bone cells express the lowest quantity of core-CIF receptors (31% and 18.3%, respectively). Skeletal muscle cells expressed 43% of core-CIF receptors. Mature adipocytes and hepatocytes represented the cells with a higher number of expressed receptors (66.2%), suggesting the direct effect of core-CIF in these cell types (**Figure 3**). CXCR1, CXCR2, CXCR3, CCR5, and CCR1 presented more than three ligands from the core-CIF list as demonstrated in KEGG database (**Supplementary Figure 4A**) *Ccr1* and *Ccr5* are differentially expressed in skeletal muscle, white adipose, and liver samples from pancreatic cancer-induced model of cachexia when compared to controls (Log2FC > 1.15 and p-value < 0.05) **Supplementary Figure 4B**). While *Cxcr2* is significantly overexpressed only in liver from cachectic animals (**Supplementary Figure 4B**). Considering these results, we suggest *Ccr1* and *CCr5* as potential targets for future studies trying to restore tissues homeostasis.

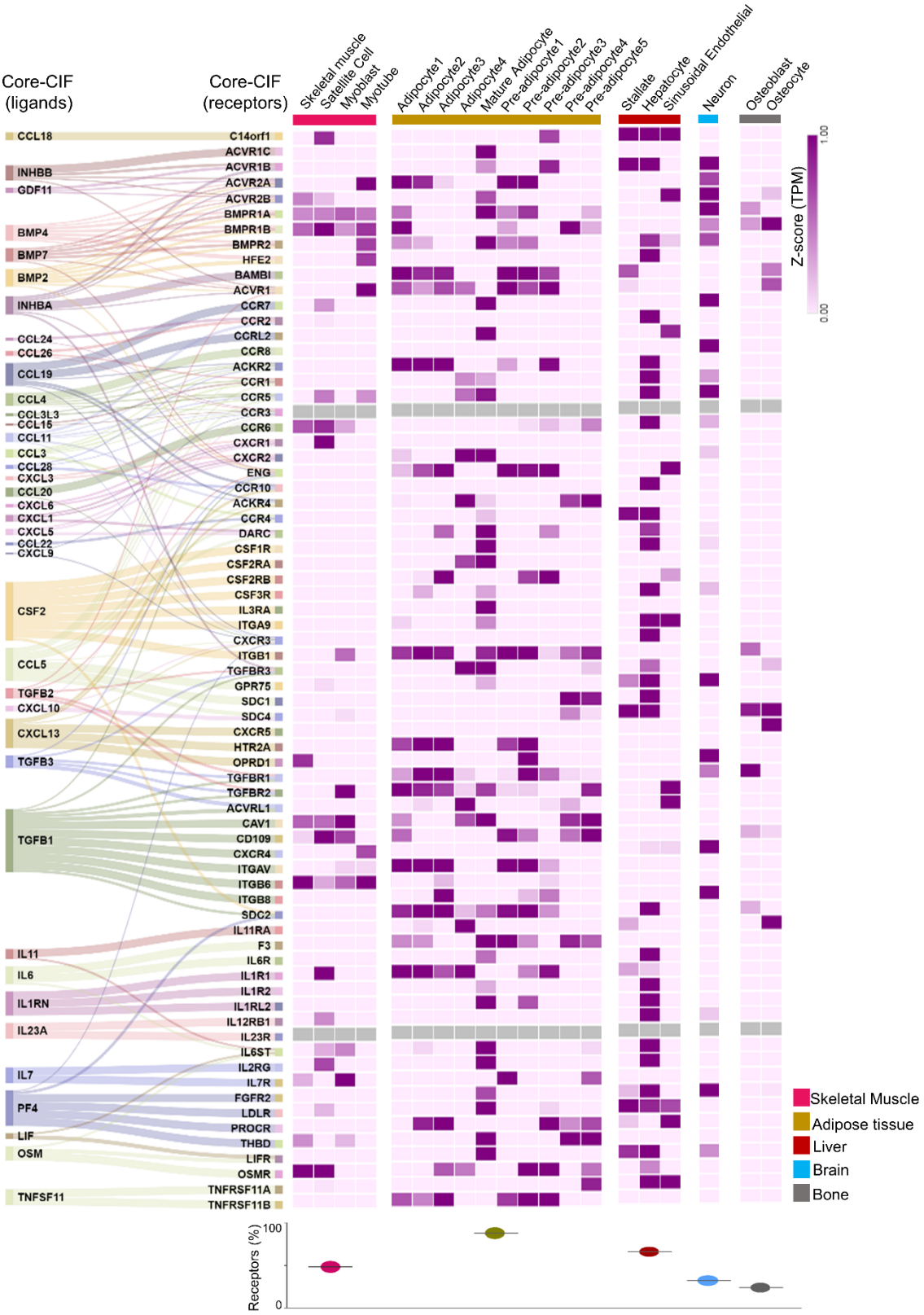
Core-CIF (ligands)
Core-CIF (receptors)
Skeletal muscle
Satellite Cell
Myoblast
Myotube
Adipocyte1
Adipocyte2
Adipocyte3
Adipocyte4
Mature Adipocyte
Pre-adipocyte1
Pre-adipocyte2
Pre-adipocyte3
Pre-adipocyte4
Pre-adipocyte5
Stallate
Hepatocyte
Sinusoidal Endothelial
Neuron
Osteoblast
Osteocyte
Z-score (TPM)
1.00
0.00
CCL18
INHBB
GDF11
BMP4
BMP7
BMP2
INHBA
CCL24
CCL26
CCL19
CCL4
CCL3L3
CCL15
CCL11
CCL3
CCL28
CXCL3
CCL20
CXCL6
CXCL1
CXCL5
CCL22
CXCL9
CSF2
CCL5
TGFB2
CXCL10
CXCL13
TGFB3
TGFB1
IL11
IL6
IL1RN
IL23A
IL7
PF4
LIF
OSM
TNFSF11
C14orf1
ACVR1C
ACVR1B
ACVR2A
ACVR2B
BMPR1A
BMPR1B
BMPR2
HFE2
BAMBI
ACVR1
CCR7
CCR2
CCRL2
CCR8
ACKR2
CCR1
CCR5
CCR3
CCR6
CXCR1
CXCR2
ENG
CCR10
ACKR4
CCR4
DARC
CSF1R
CSF2RA
CSF2RB
CSF3R
IL3RA
ITGA9
CXCR3
ITGB1
TGFBR3
GPR75
SDC1
SDC4
CXCR5
HTR2A
OPRD1
TGFBR1
TGFBR2
ACVRL1
CAV1
CD109
CXCR4
ITGAV
ITGB6
ITGB8
SDC2
IL11RA
F3
IL6R
IL1R1
IL1R2
IL1RL2
IL12RB1
IL23R
IL6ST
IL2RG
IL7R
FGFR2
LDLR
PROCR
THBD
LIFR
OSMR
TNFRSF11A
TNFRSF11B
Receptors (%)
100
0
Skeletal Muscle
Adipose tissue
Liver
Brain
Bone

Figure 4. Pan-tissue connectome of the core-CIF and its receptors. Left: alluvial diagram connecting the ligands from the core-cachexia inducing factors (CIF) into its matched receptors. Right: Heat map of the expression levels (z-score normalized Transcripts Per Million - TPM) of predicted receptors in human primary cell lineages, previously described by Ramilowski et al., 2015. Bottom: Scatter plot showing the percentage of core-CIF receptors expressed in each tissue. Muscle: 31 out of 71 receptors (43.7%); Adipose tissue: 60 out of 71 receptors (85.5%); Liver: 44 out of 71 receptors (62%); Brain: 22 out of 71 receptors (31%); Bone: 13 out of 71 receptors (18.3%). Adipocyte1: Breast adipocyte; Adipocyte2: Omental adipocyte; Adipocyte3: Perirenal adipocyte; Preadipocyte1: Breast preadipocyte; Preadipocyte2: Omental preadipocyte; Preadipocyte3: Perirenal preadipocyte; Preadipocyte4: Subcutaneous preadipocyte; Preadipocyte5: Visceral preadipocyte.

Discussion

We demonstrate, using a pan-cancer analysis, that a core of pro-cachectic factors (associated with the cytokine-cytokine receptor interaction pathway) are enriched in the tumor types where cachexia prevalence is higher. By analyzing PDAC tumor tissues, the cancer type with higher risk of cachexia, we confirmed the increase of cellularity using both bulk and single-cells samples from publicly available datasets. However, the malignant subtype of ductal cells was responsible for the expression of the majority of genes belonging to the core, followed by stromal and immune cells within the TME. Moreover, we found that the core-CIF genes can interact with myocytes, hepatocytes, and adipocytes via receptors expressed in those cells, especially in mature adipocytes. These results show novel potential pro-cachectic biomarkers that can trigger wasting in the targeted tissues most altered in cancer cachexia. Besides, we demonstrate that neoplastic ductal cells as the main source of core-CIFs production in the tumor tissue of PDAC patients. These results open new possibilities to target cancer cachexia either through tumor released factor or pathways activated in distant organs.

Tumor promoting-inflammation is a hallmark of cancer [28]. The complexity of inflammation in cancer initiation and progression is still intriguing scientists, especially in the context of cancer cachexia, where the tumor-induced inflammation plays a critical role in the syndrome development [29]. It was previously demonstrated using transcriptomics that cytokine-cytokine receptor interaction pathway is enriched in the tumor tissues of cancer types with higher risks of developing cachexia [11]. Indeed, cytokines and chemokines belonging to these pathways are extensively associated with cachexia [29]. However, these factors are often studied separately in individual cancer types. Here, we showed for the first time a set of 71 genes, belonging to the cited pathway, that are increased in tumor tissues of several cancer types associated with cachexia using a pan-cancer strategy. We denominated this gene set as a core of cachexia-inducing factors or core-CIFs. Interestingly, we found 26 genes highly enriched in cachexia associated cancer (gastrointestinal cancers and head and neck cancers). PPI analysis showed the gene CXCL8 (also known as interleukin-8, IL8) having the highest centrality,

interacting with other genes associated with Chemokine Interleukin-8-like Superfamily. IL8 is a tumor derived factor already associated with muscle wasting in pancreatic and lung cancer [30–32].

Studies demonstrated that the TME contributes to the production of inflammatory factors [30,33]. In PDAC, the increased expression of CIFs was associated with associated with the low tumor purity and high TME cellularity [11]. We found at a single-cell resolution that pancreatic tumor tissues show an increase in immune cells compared with to normal-like pancreas where T cell, B cells and macrophages were almost absent. This observation was confirmed using digital cytometry in PDAC samples and normal pancreas from the databases TCGA and GTEx, respectively. Evidence show that high tumor cellularity is related to more aggressive PDAC with poorer prognosis [34,35]. Therefore, low purity PDAC tumors with a dense TME composed with stromal and immune cells can be associated with cachexia. In fact, pancreatic cancer cells secret cytokines that attract immunosuppressive cells [36].

We found that malignant ductal cells express more than half of the core-CIF genes. Considering that severity of PDAC, this result may indicate that cancer cells induce immune evasion by producing factors that allow the inhibition of effector T cells [36]. The genes *IL6*, *CXCL1*, and *CSF2*, among the core-CIFs, are involved in the recruitment of suppressive myeloid cells in PDAC [36,37]. Another evidence of immunosuppression in PDAC is the expression of *CXCL14* in fibroblasts (normal and cancer-associated), which is already demonstrated to induce immune evasion [38]. Fibroblasts are the main source of CXCL14 production, while cancer cells exhibit low or absent expression of this chemokine [39], corroborating our finding.

We found that adipose cells express the majority of core-CIF receptors (85.5%). This result may indicate that adipose tissue is most responsive to cachexia stimulus than skeletal muscle. This greater response of adipose tissue than muscle was previous demonstrated when comparing the gene expression alteration of rectus abdominis muscle and subcutaneous adipose tissue of PDAC cachectic patients [40]. Moreover, brain and bone cells seems to interact less with the core-CIFs, however these organs can also interact with core-CIF factors, which may explain the neuro-inflammation and bone density loss observed in cachexia [5]. Hepatic cells also showed expression of core-CIF receptors in high proportions (62%) and the liver is demonstrated to be greatly affected by pro-inflammatory cytokines that promotes the organ disfunction [5].

The receptors CCR1, CCR5, CXCR1, CXCR2, and CXCR3 interact with more than three core-CIFs demonstrating its potential relevance in trigger alterations in cancer cachexia. When analyzing tissues from cachectic mice, we found that *Ccr1* and *Ccr5* are upregulated in skeletal muscle, liver, and adipose tissue. Myoblasts treated with CCL3 (ligand protein MIP-1α) demonstrated increased

proliferation and expression of *Ccr1* and *Ccr5* [41]. Indeed, CCR5 activates proliferation, migration, metastasis, and NF-kβ signaling [42]. Contrarily, CCR5 inhibition completely reversed the myogenic differentiation stimulated by recombinant CCL11 in C2C12 cells [43]. However, clearly CCR1/CCR5 participates in inflammatory signaling and the treatment with the anti-inflammatory quercetin demonstrated a suppression of adipose tissue inflammation by downregulating MIP-1α and CCR1/CCR5 [44]. Antagonists of CCR1 and CCR5 receptors are potential therapeutic option for cancer and HIV patients [45,46]. Therefore, future studies need to determine the potential of CCR1 and CCR5 as targets for cachexia.

This is an exploratory study that opens new perspectives for cancer cachexia therapy and molecular mechanisms, however, it has limitations. We failed to classify cachexia status in the included patients, but considering the prevalence of cachexia in PDAC patients, it is likely that the majority of patients included are cachectic. Moreover, the validation of tumor-tissues interaction needs further validation in cachectic samples at protein level. Overall, we demonstrated novel potential pro-cachectic factors expressed by cachexia-related tumor types that can interact with tissues most altered in cancer cachexia with different degrees. Besides, we demonstrate that neoplastic ductal cells as the main source of core-CIFs production in the tumor tissue of PDAC patients.

4. Considerações finais

O transcriptoma tumoral nos revela uma gama bastante rica de informações que podem ser extraídas, ou até mesmo preditas a partir de seus dados. Aqui, vimos seu potencial para decompor e quantificar os componentes do microambiente imune tumoral. Essa estratégia se mostrou eficaz na identificação de moléculas secretadas pelo tumor e que podem contribuir para o estado caquético em pacientes com câncer de pulmão ou pâncreas. No capítulo 1 demonstramos que a área dos músculos peitorais sozinha é eficaz na identificação de pacientes potencialmente caquéticos (corroborado por dados clínicos e moleculares), bem como, demonstramos a relevância do microambiente tumoral enriquecido por células T CD8 potencialmente exauridas. No capítulo 2 demonstramos o relevante papel dos genes que compõe a via de interação entre citocinas, os quais são comumente encontrados em tumores com alta prevalência de caquexia, especialmente no câncer de pâncreas. Investigando a expressão desses genes (classificados como "core" ou cerne de fatores indutores de caquexia) em sequenciamento de células únicas de amostras de ADP, identificamos as células neoplásicas ductais pancreáticas como principais fontes desses fatores. Além disso, esses fatores interagem com diversos receptores expressos em órgãos-alvo na caquexia, como o músculo esquelético, fígado e tecido adiposo. Esses achados abrem novas perspectivas na identificação de mediadores e biomarcadores de caquexia com caráter célula tumoral-específica para câncer de pulmão e pâncreas, bem como suas principais vias de atuação sistêmica. Futuramente, esperamos que esses resultados possam servir como base para geração de tratamentos eficazes para a caquexia em pacientes com câncer de pulmão e pâncreas.

5. Conclusões

A caracterização do perfil transcricional tumoral do secretoma permitiu a definição da composição celular do microambiente tumoral e revelou potenciais mediadores de caquexia derivados do tumor.

Nos pacientes com câncer de pulmão, a baixa muscularidade, aferida pela área dos músculos peitorais em tomografias computadorizadas, está relacionada ao prognóstico desfavorável (menor sobrevida e maior frequência de recorrência tumoral). A análise do secretoma tumoral desses pacientes demonstrou enriquecimento de perfil inflamatório com aumento de expressão de biomarcadores de caquexia, provenientes de células do microambiente imune tumoral, principalmente por células T CD8+. Além disso, observamos um aumento da citotoxicidade e exaustão de células T em pacientes potencialmente caquéticos. Análises de transcriptomas musculares revelaram expressão de receptores que interagem com genes do secretoma aumentados nos pacientes com baixa muscularidade, demonstrando potenciais vias de comunicação tumor-músculo.

No câncer de pâncreas, análise pan-câncer de dados do TCGA revelou novos potenciais fatores pró-caquéticos centrais em cânceres associados à alta prevalência de caquexia, que participam da via de interação citocina receptor de citocina. Nós demonstramos que esses fatores participam na indução de caquexia por interagirem com tecidos alterados, em diferentes graus, durante a caquexia. Adipócitos apresentaram maior frequência de expressão de receptores para os fatores centrais identificados, enquanto células do tecido ósseo possuem expressão de poucos receptores. Além disso, a reanálise de dados de scRNA-seq demonstrou que as células neoplásicas ductais pancreáticas são as principais produtoras desses fatores.

5. Referências bibliográficas

Introdução:

1. Fearon K, Strasser F, Anker SD, et al. Definition and classification of cancer cachexia: An international consensus. *The Lancet Oncology*. 2011;12(5):489-495. doi:10.1016/S1470-2045(10)70218-7

2. Evans WJ, Morley JE, Argilés J, et al. Cachexia: A new definition. *Clinical Nutrition*. 2008;27(6):793-799. doi:10.1016/j.clnu.2008.06.013

3. von Haehling S, Anker SD. Cachexia as a major underestimated and unmet medical need: Facts and numbers. *Journal of Cachexia, Sarcopenia and Muscle*. 2010;1(1):1-5. doi:10.1007/s13539-010-0002-6

4. Cohen S, Nathan JA, Goldberg AL. Muscle wasting in disease : molecular mechanisms and promising therapies. *Nature Publishing Group*. 2015;14(1):58-74. doi:10.1038/nrd4467

5. Busquets S, Stemmler B, Lo FJ. Cachexia and sarcopenia : mechanisms and potential targets for intervention. *Curr Opin Pharmacol*. 2015;22:100-106. doi:10.1016/j.coph.2015.04.003

6. Haehling S Von, Anker MS, Anker SD. Prevalence and clinical impact of cachexia in chronic illness in Europe , USA , and Japan : facts and numbers update 2016. *J Cachexia Sarcopenia Muscle*. 2016;7(5):507-509. doi:10.1002/jcsm.12167

7. Fearon KCH, Glass DJ, Guttridge DC. Cancer cachexia: mediators, signaling, and metabolic pathways. *Cell metabolism*. 2012;16(2):153-166. doi:10.1016/j.cmet.2012.06.011

8. Harimoto N, Shirabe K, Yamashita YI, et al. Sarcopenia as a predictor of prognosis in patients following hepatectomy for hepatocellular carcinoma. *British Journal of Surgery*. 2013;100(11):1523-1530. doi:10.1002/bjs.9258

9. Pressoir M, Desné S, Berchery D, et al. Prevalence, risk factors and clinical implications of malnutrition in french comprehensive cancer centres. *British Journal of Cancer*. 2010;102(6):966-971. doi:10.1038/sj.bjc.6605578

10. Bozzetti F. Screening the nutritional status in oncology: A preliminary report on 1,000 outpatients. *Supportive Care in Cancer*. 2009;17(3):279-284. doi:10.1007/s00520-008-0476-3

11. Segura A, Pardo J, Jara C, et al. An epidemiological evaluation of the prevalence of malnutrition in Spanish patients with locally advanced or metastatic cancer. *Clinical Nutrition*. 2005;24(5):801-814. doi:10.1016/j.clnu.2005.05.001

12. Hébuterne X, Lemarié E, Michallet M, De Montreuil CB, Schneider SM, Goldwasser F. Prevalence of malnutrition and current use of nutrition support in patients with cancer. *Journal of Parenteral and Enteral Nutrition*. 2014;38(2):196-204. doi:10.1177/0148607113502674

13. Baracos VE, Martin L, Korc M, Guttridge DC, Fearon KCH. Cancer-associated cachexia. *Nature Publishing Group*. 2018;4:1-18. doi:10.1038/nrdp.2017.105

14. Anker MS, Holcomb R, Muscaritoli M, et al. Orphan disease status of cancer cachexia in the USA and in the European Union: a systematic review. *Journal of cachexia, sarcopenia and muscle*. 2019;10(1):22-34. doi:10.1002/jcsm.12402

15. Donohoe CL, Ryan AM, Reynolds J V. Cancer Cachexia : Mechanisms and Clinical Implications. *Gastroenterol Res Pract*. 2011;2011:601430. doi:10.1155/2011/601434

16. Tisdale MJ. Biology of cachexia. *Journal of the National Cancer Institute*. 1997;89(23):1763-1773.

17. Tisdale MJ. Cachexia in cancer patients. *Nature reviews cancer*. 2002;3(11):883-889. doi:10.1038/nrg927

18. Tsoli M, Robertson G. Cancer cachexia : malignant inflammation, tumorkines, and metabolic mayhem. *Trends Endocrinol Metab*. 2013;24(4):174-183. doi:10.1016/j.tem.2012.10.006

19. Baracos VE, Reiman T, Mourtzakis M, Gioulbasanis I, Antoun S. Body composition in patients with non-small cell lung cancer: a contemporary view of cancer cachexia with the use of computed tomography image analysis. *Am J Clin Nutr*. 2010;91(4):1133-1137. doi:10.3945/ajcn.2010.28608C.INTRODUCTION

20. Sung H, Ferlay J, Siegel RL, et al. Global cancer statistics 2020: GLOBOCAN estimates of incidence and mortality worldwide for 36 cancers in 185 countries. *CA A Cancer J Clin*. Published online February 4, 2021:caac.21660. doi:10.3322/caac.21660

21. Instituto Nacional de Cancer José Alencar Gomes da Silva. *Estimativa 2020: Incidência de Câncer No Brasil*. Vol 66. Ministério da Saúde Instituto Nacional de Câncer José Alencar Gomes da Silva (INCA); 2019.

22. Herbst RS, Morgensztern D, Boshoff C. The biology and management of non-small cell lung cancer. *Nature Publishing Group*. 2018;553(7689):446-454. doi:10.1038/nature25183

23. Mitchell G, Mitchell C. Lung cancer. *Aust Fam Physician*. 2004;33(5):321-325.

24. Wahbah M, Boroumand N, Castro C, El-zeky F, Eltorky M. Changing trends in the distribution of the histologic types of lung cancer : a review of 4439 cases. *Ann Diagn Pathol*. 2007;11(2):89-96. doi:10.1016/j.anndiagpath.2006.04.006

25. Hecht SS. Tobacco Smoke Carcinogens and Lung Cancer. *J Natl Cancer Inst*. 1999;91(14):1194-1210.

26. Travis WD, Brambilla E, Nicholson AG, et al. The 2015 World Health Organization Classification of Lung Tumors. *Journal of Thoracic Oncology*. 2015;10(9):1243-1260. doi:10.1097/JTO.0000000000000630

27. Garraway LA. Genomics-Driven Oncology: Framework for an Emerging Paradigm. *JCO*. 2013;31(15):1806-1814. doi:10.1200/JCO.2012.46.8934

28. Saito M, Suzuki H, Kono K, Takenoshita S, Kohno T. Treatment of lung adenocarcinoma by molecular-targeted therapy and immunotherapy. *Surg Today*. 2018;48(1):1-8. doi:10.1007/s00595-017-1497-7

29. Del Ferraro C, Grant M, Koczywas M, Dorr-Uyemura LA. Management of Anorexia-Cachexia in Late-Stage Lung Cancer Patients: *Journal of Hospice & Palliative Nursing*. 2012;14(6):397-402. doi:10.1097/NJH.0b013e31825f3470

30. Cury SS, de Moraes D, Freire PP, et al. Tumor Transcriptome Reveals High Expression of IL-8 in Non-Small Cell Lung Cancer Patients with Low Pectoralis Muscle Area and Reduced Survival. *Cancers (Basel)*. 2019;11(9). doi:10.3390/cancers11091251

31. Unit L, Hospital RM, Road D. Do patients with weight loss have a worse outcome when undergoing chemotherapy for lung cancers ? *Br J Cancer*. 2004;90(10):1905-1911. doi:10.1038/sj.bjc.6601781

32. Del Ferraro C, Grant M, Koczywas M, Dorr-Uyemura L. Management of Anorexia-Cachexia in Late Stage Lung Cancer Patients. *J Hosp Palliat Nurs*. 2012;14(6). doi:10.1097/NJH.0b013e31825f3470

33. Miller A, Mcleod L, Alhayyani S, et al. Blockade of the IL-6 trans-signalling / STAT3 axis suppresses cachexia in Kras-induced lung adenocarcinoma. *Oncogene*. 2016;36(21):3059-3066. doi:10.1038/onc.2016.437

34. Mytelka DS, Li L, Benoit K. Post-diagnosis weight loss as a prognostic factor in non-small cell lung cancer. *Journal of Cachexia, Sarcopenia and Muscle*. 2018;9(1):86-92. doi:10.1002/jcsm.12253

35. Dahlberg SE, Schiller JH, Bonomi PB, et al. Body mass index and its association with clinical outcomes for advanced non-small-cell lung cancer patients enrolled on eastern cooperative oncology group clinical trials. *Journal of Thoracic Oncology*. 2013;8(9):1121-1127. doi:10.1097/JTO.0b013e31829cf942

36. Martin L, Birdsell L, MacDonald N, et al. Cancer cachexia in the age of obesity: Skeletal muscle depletion is a powerful prognostic factor, independent of body mass index. *Journal of Clinical Oncology*. 2013;31(12):1539-1547. doi:10.1200/JCO.2012.45.2722

37. Stene GB, Helbostad JL, Amundsen T, et al. Changes in skeletal muscle mass during palliative chemotherapy in patients with advanced lung cancer. *Acta Oncol*. 2015;54(3):340-348. doi:10.3109/0284186X.2014.953259

38. Prado CMM, Lieff JR, Mccargar LJ, et al. Prevalence and clinical implications of sarcopenic obesity in patients with solid tumours of the respiratory and gastrointestinal tracts : a population-based study. :629-635. doi:10.1016/S1470-2045(08)70153-0

39. Arrieta O, De la Torre-Vallejo M, López-Macías D, et al. Nutritional Status , Body Surface , and Low Lean Body Mass / Body Mass Index Are Related to Dose Reduction and Severe Gastrointestinal Toxicity Induced by Afatinib in Patients With Non-Small Cell Lung Cancer. *Oncologist*. Published online 2015:967-974.

40. Fløtten Ø, Hjermstad MJ, Aass N, Jordhøy M. Low muscle mass is associated with chemotherapy-induced haematological toxicity in advanced non-small cell lung cancer. Published online 2015:1-7. doi:10.1016/j.lungcan.2015.07.001

41. Kinsey CM, San Jose Estepar R, Van der Velden J, et al. Lower Pectoralis Muscle Area Is Associated with a Worse Overall Survival in Non – Small. *Cancer Epidemiology Biomarkers & Prevention*. 2017;26(January):38-44. doi:10.1158/1055-9965.EPI-15-1067

42. Bye A, Sjøblom B, Wentzel-Larsen T, et al. Muscle mass and association to quality of life in non-small cell lung cancer patients. *Journal of Cachexia, Sarcopenia and Muscle*. 2017;8(5):759-767. doi:10.1002/jcsm.12206

43. Kilgour RD, Vigano A, Trutschnigg B, et al. Cancer-related fatigue: The impact of skeletal muscle mass and strength in patients with advanced cancer. *Journal of Cachexia, Sarcopenia and Muscle*. 2010;1(2):177-185. doi:10.1007/s13539-010-0016-0

44. Collins J, Noble S, Chester J, Coles B, Byrne A. The assessment and impact of sarcopenia in lung cancer : a systematic literature review. *BMJ Open*. 2014;4(1):e003697. doi:10.1136/bmjopen-2013-003697

45. Fong ZV, Winter JM. Biomarkers in Pancreatic Cancer. *The Cancer Journal*. 2012;18(6):530-538. doi:10.1097/PPO.0b013e31827654ea

46. Kleeff J, Korc M, Apte M, et al. Pancreatic cancer. *Nature Reviews Disease Primers*. 2016;2(1):16022. doi:10.1038/nrdp.2016.22

47. Siegel RL, Miller KD, Jemal A. Cancer statistics, 2020. *CA: A Cancer Journal for Clinicians*. 2020;70(1):7-30. doi:10.3322/caac.21590

48. Bray F, Ferlay J, Soerjomataram I, Siegel RL, Torre L, Jemal A. Global Cancer Statistics 2018: GLOBOCAN estimates of incidence and mortality worldwide for 36 cancers in 185 countries. *CA Cancer J Clin*. 2018;68(6):394-424. doi:10.3322/caac.21492

49. Ferlay J, Partensky C, Bray F. More deaths from pancreatic cancer than breast cancer in the EU by 2017. *Acta Oncologica*. 2016;55(9-10):1158-1160. doi:10.1080/0284186X.2016.1197419

50. Pausch T, Hartwig W, Hinz U, et al. Cachexia but not obesity worsens the postoperative outcome after pancreatoduodenectomy in pancreatic cancer. *Surgery*. 2012;152(3):S81-S88. doi:10.1016/j.surg.2012.05.028

51. Bachmann J, Heiligensetzer M, Krakowski-Roosen H, Büchler MW, Friess H, Martignoni ME. Cachexia Worsens Prognosis in Patients with Resectable Pancreatic Cancer. *Journal of Gastrointestinal Surgery*. 2008;12(7):1193-1201. doi:10.1007/s11605-008-0505-z

52. Talbert EE, Lewis HL, Farren MR, et al. Circulating monocyte chemoattractant protein-1 (MCP-1) is associated with cachexia in treatment-naïve pancreatic cancer patients. *Journal of Cachexia, Sarcopenia and Muscle*. 2018;1. doi:10.1002/jcsm.12251

53. Gilabert M, Calvo E, Airoldi A, et al. Pancreatic cancer-induced cachexia is Jak2-dependent in mice. *Journal of cellular physiology*. 2014;229(10):1437-1443. doi:10.1002/jcp.24580

54. Delitto D, Judge SM, George TJ, et al. A clinically applicable muscular index predicts long-term survival in resectable pancreatic cancer. *Surgery (United States)*. 2017;161(4):930-938. doi:10.1016/j.surg.2016.09.038

55. Zhong X, Pons M, Poirier C, et al. The systemic activin response to pancreatic cancer: implications for effective cancer cachexia therapy. *Journal of Cachexia, Sarcopenia and Muscle*. 2019;10(5):1083-1101. doi:10.1002/jcsm.12461

56. Judge SM, Nosacka RL, Delitto D, et al. Skeletal Muscle Fibrosis in Pancreatic Cancer Patients with Respect to Survival. *JNCI Cancer Spectrum*. 2018;2(3). doi:10.1093/jncics/pky043

57. Armstrong VS, Fitzgerald LW, Bathe OF. Cancer-Associated Muscle Wasting—Candidate Mechanisms and Molecular Pathways. *IJMS*. 2020;21(23):9268. doi:10.3390/ijms21239268

58. Freire PP, Fernandez GJ, de Moraes D, et al. The expression landscape of cachexia-inducing factors in human cancers. *Journal of Cachexia, Sarcopenia and Muscle*. 2020;11(4):947-961. doi:10.1002/jcsm.12565

59. Twelkmeyer B, Tardif N, Rooyackers O. Omics and cachexia. *Curr Opin Clin Nutr Metab Care*. 2017;20(3):181-185. doi:10.1097/MCO.0000000000000363

60. Argilés JM, Stemmler B, López-Soriano FJ, Busquets S. Inter-tissue communication in cancer cachexia. *Nature Reviews Endocrinology*. Published online 2018. doi:10.1038/s41574-018-0123-0

61. Penafuerte CA, Gagnon B, Sirois J, Murphy J, Macdonald N, Tremblay ML. Identification of neutrophil-derived proteases and angiotensin II as biomarkers of cancer cachexia. *British Journal of Cancer*. 2016;114(6):680-687. doi:10.1038/bjc.2016.3

62. Lerner L, Hayes TG, Tao N, et al. Plasma growth differentiation factor 15 is associated with weight loss and mortality in cancer patients. *Journal of Cachexia, Sarcopenia and Muscle*. 2015;6(4):317-324. doi:10.1002/jcsm.12033

63. Lerner L, Tao J, Liu Q, et al. MAP3K11/GDF15 axis is a critical driver of cancer cachexia. *Journal of Cachexia, Sarcopenia and Muscle*. 2016;7(4):467-482. doi:10.1002/jcsm.12077

64. Fukawa T, Yan-Jiang BC, Min-Wen JC, et al. Excessive fatty acid oxidation induces muscle atrophy in cancer cachexia. *Nature Medicine*. 2016;22(6):666-671. doi:10.1038/nm.4093

65. McLean JB, Moylan JS, Horrell EMW, Andrade FH. Proteomic analysis of media from lung cancer cells reveals role of 14-3-3 proteins in cachexia. *Frontiers in Physiology*. 2015;6(APR):1-8. doi:10.3389/fphys.2015.00136

66. Laine A, Iyengar P, Pandita T. The role of inflammatory pathways in cancer-associated cachexia and radiation resistance. *Mol Cancer Res*. 2013;11(9):967-972. doi:10.1158/1541-7786.MCR-13-0189

67. Petruzzelli M, Wagner EF. Mechanisms of metabolic dysfunction in cancer-associated cachexia. *Genes Dev*. 2016;30(5):489-501. doi:10.1101/gad.276733.115.GENES

68. Han J, Meng Q, Shen L, Wu G. Interleukin-6 induces fat loss in cancer cachexia by promoting white adipose tissue lipolysis and browning. *Lipids in Health and Disease*. 2018;17(1):14. doi:10.1186/s12944-018-0657-0

69. Haddad F, Zaldivar F, Cooper DM, Adams GR. IL-6-induced skeletal muscle atrophy. *Journal of applied physiology (Bethesda, Md : 1985)*. 2005;98(3):911-917. doi:10.1152/japplphysiol.01026.2004

70. Bonetto A, Aydogdu T, Jin X, et al. JAK/STAT3 pathway inhibition blocks skeletal muscle wasting downstream of IL-6 and in experimental cancer cachexia. *American Journal of Physiology-Endocrinology and Metabolism*. 2012;303(3):E410-E421. doi:10.1152/ajpendo.00039.2012

71. Soda K, Kawakami M, Kashii A, Miyata M. Manifestations of cancer cachexia induced by colon 26 adenocarcinoma are not fully ascribable to interleukin-6. *International journal of cancer Journal international du cancer*. 1995;62(3):332-336.

72. Strassmann G, Fong M, Kenney JS, Jacob CO. Evidence for the involvement of interleukin 6 in experimental cancer cachexia. *The Journal of clinical investigation*. 1992;89(5):1681-1684. doi:10.1172/JCI115767

73. White JP, Baynes JW, Welle SL, et al. The regulation of skeletal muscle protein turnover during the progression of cancer cachexia in the Apc(Min/+) mouse. *PloS one*. 2011;6(9):e24650. doi:10.1371/journal.pone.0024650

74. Tamura S, Ouchi KF, Mori K, et al. Involvement of human interleukin 6 in experimental cachexia induced by a human uterine cervical carcinoma xenograft. *Clinical cancer research : an official journal of the American Association for Cancer Research*. 1995;1(11):1353-1358.

75. Prado BL, Qian Y. Anti-cytokines in the treatment of cancer cachexia. *Annals of Palliative Medicine*. 2019;8(1):67-79. doi:10.21037/apm.2018.07.06

76. Schuster M, Rigas JR, Orlov S V., et al. ALD518, a humanized anti-IL-6 antibody, treats anemia in patients with advanced non-small cell lung cancer (NSCLC): Results of a phase II, randomized, double-blind, placebo-controlled trial. *Journal of Clinical Oncology*. 2010;28:15_supp:7631-7631.

77. Bayliss TJ, Smith JT, Schuster M, Dragnev KH, Rigas JR. A humanized anti-IL-6 antibody (ALD518) in non-small cell lung cancer. *Expert Opinion on Biological Therapy*. 2011;11(12):1663-1668. doi:10.1517/14712598.2011.627850

78. Cao Z, Scott AM, Hoogenraad NJ, Osellame LD. Mediators and clinical treatment for cancer cachexia: a systematic review. *JCSM Rapid Communications*. 2021;4(2):166-186. doi:10.1002/rco2.30

79. Anker SD, Coats AJS, Morley JE. Evidence for partial pharmaceutical reversal of the cancer anorexia-cachexia syndrome: the case of anamorelin. *J Cachexia Sarcopenia Muscle*. 2015;6(4):275-277. doi:10.1002/jcsm.12063

80. Wakabayashi H, Arai H, Inui A. The regulatory approval of anamorelin for treatment of cachexia in patients with non-small cell lung cancer, gastric cancer, pancreatic cancer, and colorectal cancer in Japan: facts and numbers. *J Cachexia Sarcopenia Muscle*. 2021;12(1):14-16. doi:10.1002/jcsm.12675

81. Gerber MH, Underwood PW, Judge SM, et al. Local and Systemic Cytokine Profiling for Pancreatic Ductal Adenocarcinoma to Study Cancer Cachexia in an Era of Precision Medicine. *International Journal of Molecular Sciences*. 2018;19(12):3836. doi:10.3390/ijms19123836

82. Hou YC, Wang CJ, Chao YJ, et al. Elevated Serum Interleukin-8 Level Correlates with Cancer-Related Cachexia and Sarcopenia: An Indicator for Pancreatic Cancer Outcomes. *Journal of Clinical Medicine*. 2018;7(12):502. doi:10.3390/jcm7120502

83. Maman S, Witz IP. A history of exploring cancer in context. *Nature reviews Cancer*. 2018;18(6):359-376. doi:10.1038/s41568-018-0006-7

84. Balkwill FR, Capasso M, Hagemann T. The tumor microenvironment at a glance. *Journal of cell science*. 2012;125(Pt 23):5591-5596. doi:10.1242/jcs.116392

85. Quail DF, Joyce JA. Microenvironmental regulation of tumor progression and metastasis. *Nature Medicine*. 2013;19(11):1423-1437. doi:10.1038/nm.3394

86. Hanahan D, Coussens LM. Accessories to the crime: functions of cells recruited to the tumor microenvironment. *Cancer cell*. 2012;21(3):309-322. doi:10.1016/j.ccr.2012.02.022

87. Lau AN, Vander Heiden MG. Metabolism in the Tumor Microenvironment. *Annu Rev Cancer Biol*. 2020;4(1):17-40. doi:10.1146/annurev-cancerbio-030419-033333

88. Bailey P, Chang DK, Nones K, et al. Genomic analyses identify molecular subtypes of pancreatic cancer. *Nature*. 2016;531(7592):47-52. doi:10.1038/nature16965

89. Cancer Genome Atlas Network. Genomic Classification of Cutaneous Melanoma. *Cell*. 2015;161(7):1681-1696. doi:10.1016/j.cell.2015.05.044

90. Cancer Genome Atlas Research Network. Integrated genomic analyses of ovarian carcinoma. *Nature*. 2011;474(7353):609-615. doi:10.1038/nature10166

91. Iglesia MD, Parker JS, Hoadley KA, Serody JS, Perou CM, Vincent BG. Genomic Analysis of Immune Cell Infiltrates Across 11 Tumor Types. *Journal of the National Cancer Institute*. 2016;108(11). doi:10.1093/jnci/djw144

92. Bindea G, Mlecnik B, Tosolini M, et al. Spatiotemporal dynamics of intratumoral immune cells reveal the immune landscape in human cancer. *Immunity*. 2013;39(4):782-795. doi:10.1016/j.immuni.2013.10.003

93. Brown SD, Raeburn LA, Holt RA. Profiling tissue-resident T cell repertoires by RNA sequencing. *Genome Medicine*. 2015;7(1):1-8. doi:10.1186/s13073-015-0248-x

94. Charoentong P, Finotello F, Angelova M, et al. Pan-cancer Immunogenomic Analyses Reveal Genotype-Immunophenotype Relationships and Predictors of Response to Checkpoint Blockade. *Cell Reports*. 2017;18(1):248-262. doi:10.1016/j.celrep.2016.12.019

95. S. D. Brown, R. L. Warren, E. A. Gibb, et al. Neo-antigens predicted by tumor genome meta-analysis correlate with increased patient survival. *Genome research*. 2014;24(5):743-750. doi:10.1101/gr.165985.113

96. Gentles AJ, Newman AM, Liu CL, et al. The prognostic landscape of genes and infiltrating immune cells across human cancers. *Nature Medicine*. 2015;21(8):938-945. doi:10.1038/nm.3909

97. Iglesia MD, Parker JS, Hoadley KA, Serody JS, Perou CM, Vincent BG. Genomic Analysis of Immune Cell Infiltrates Across 11 Tumor Types. 2016;108:1-11. doi:10.1093/jnci/djw144

98. Li B, Severson E, Pignon JC, et al. Comprehensive analyses of tumor immunity: Implications for cancer immunotherapy. *Genome Biology*. 2016;17(1):1-16. doi:10.1186/s13059-016-1028-7

99. Porta-Pardo E, Godzik A. Mutation Drivers of Immunological Responses to Cancer. *Cancer Immunology Research*. 2016;4(9):789-798. doi:10.1158/2326-6066.cir-15-0233

100. Rooney MS, Shukla SA, Wu CJ, Getz G, Hacohen N. Molecular and genetic properties of tumors associated with local immune cytolytic activity. *Cell*. 2015;160(1-2):48-61. doi:10.1016/j.cell.2014.12.033

101. Thorsson V, Gibbs DL, Brown SD, et al. The Immune Landscape of Cancer. *Immunity*. 2018;48(4):812-830.e14. doi:10.1016/j.immuni.2018.03.023

102. Yoshihara K, Shahmoradgoli M, Martínez E, et al. Inferring tumour purity and stromal and immune cell admixture from expression data. *Nature Communications*. 2013;4. doi:10.1038/ncomms3612

103. Carter SL, Cibulskis K, Helman E, et al. Absolute quantification of somatic DNA alterations in human cancer. *Nature Biotechnology*. 2012;30(5):413-421. doi:10.1038/nbt.2203

104. Oesper L, Mahmoody A, Raphael BJ. THetA: inferring intra-tumor heterogeneity from high-throughput DNA sequencing data. *Genome biology*. 2013;14(7):R80. doi:10.1186/gb-2013-14-7-r80

105. Chen H, Bell JM, Zavala NA, Ji HP, Zhang NR. Allele-specific copy number profiling by next-generation DNA sequencing. *Nucleic Acids Research*. 2015;43(4):1-14. doi:10.1093/nar/gku1252

106. Andor N, Harness J V., Müller S, Mewes HW, Petritsch C. Expands: Expanding ploidy and allele frequency on nested subpopulations. *Bioinformatics*. 2014;30(1):50-60. doi:10.1093/bioinformatics/btt622

107. Zheng X, Zhao Q, Wu HJ, et al. MethylPurify: tumor purity deconvolution and differential methylation detection from single tumor DNA methylomes. *Genome biology*. 2014;15(8):419. doi:10.1186/s13059-014-0419-x

108. Aran D, Sirota M, Butte AJ. Systematic pan-cancer analysis of tumour purity. *Nature Communications*. 2015;6:1-11. doi:10.1038/ncomms9971

109. Raphael BJ, Hruban RH, Aguirre AJ, et al. Integrated Genomic Characterization of Pancreatic Ductal Adenocarcinoma. *Cancer Cell*. 2017;32(2):185-203.e13. doi:10.1016/j.ccell.2017.07.007

110. Matsuyama T, Ishikawa T, Okayama T, et al. Tumor inoculation site affects the development of cancer cachexia and muscle wasting. *International Journal of Cancer*. 2015;137(11):2558-2565. doi:10.1002/ijc.29620

111. de Matos-Neto EM, Lima JDCC, de Pereira WO, et al. Systemic inflammation in cachexia - Is tumor cytokine expression profile the culprit? *Frontiers in Immunology*. 2015;6(DEC):1-11. doi:10.3389/fimmu.2015.00629

112. Akkın S, Varan G, Bilensoy E. A Review on Cancer Immunotherapy and Applications of Nanotechnology to Chemoimmunotherapy of Different Cancers. *Molecules*. 2021;26(11):3382. doi:10.3390/molecules26113382

113. Ohaegbulam KC, Assal A, Lazar-Molnar E, Yao Y, Zang X. Human cancer immunotherapy with antibodies to the PD-1 and PD-L1 pathway. *Trends in Molecular Medicine*. 2015;21(1):24-33. doi:10.1016/j.molmed.2014.10.009

114. Fujii H, Araki A, Iihara H, et al. Cancer cachexia as a determinant of efficacy of first-line pembrolizumab in patients with advanced non-small cell lung cancer. *Mol Clin Oncol*. 2022;16(4):91. doi:10.3892/mco.2022.2524

115. Peng J, Sun BF, Chen CY, et al. Single-cell RNA-seq highlights intra-tumoral heterogeneity and malignant progression in pancreatic ductal adenocarcinoma. *Cell Research*. 2019;(June). doi:10.1038/s41422-019-0195-y

116. Ligorio M, Sil S, Malagon-Lopez J, et al. Stromal Microenvironment Shapes the Intratumoral Architecture of Pancreatic Cancer. *Cell*. 2019;178(1):160-175.e27. doi:10.1016/j.cell.2019.05.012

117. Puram S V., Tirosh I, Parikh AS, et al. Single-Cell Transcriptomic Analysis of Primary and Metastatic Tumor Ecosystems in Head and Neck Cancer. *Cell*. 2017;171(7):1611-1624.e24. doi:10.1016/j.cell.2017.10.044

118. Zheng C, Zheng L, Yoo JK, et al. Landscape of Infiltrating T Cells in Liver Cancer Revealed by Single-Cell Sequencing. *Cell*. 2017;169(7):1342-1356.e16. doi:10.1016/j.cell.2017.05.035

119. Ho DWH, Tsui YM, Sze KMF, et al. Single-cell transcriptomics reveals the landscape of intra-tumoral heterogeneity and stemness-related subpopulations in liver cancer. *Cancer Letters*. 2019;459(March):176-185. doi:10.1016/j.canlet.2019.06.002

120. Zheng H, Pomyen Y, Hernandez MO, et al. Single-cell analysis reveals cancer stem cell heterogeneity in hepatocellular carcinoma. *Hepatology*. 2018;68(1):127-140. doi:10.1002/hep.29778

121. Zilionis R, Engblom C, Pfirschke C, et al. Single-Cell Transcriptomics of Human and Mouse Lung Cancers Reveals Conserved Myeloid Populations across Individuals and Species Resource Single-Cell Transcriptomics of Human and Mouse Lung Cancers Reveals Conserved Myeloid Populations across Individuals . *Immunity*. Published online 2019:1-18. doi:10.1016/j.immuni.2019.03.009

122. Guo X, Zhang Y, Zheng L, et al. Global characterization of T cells in non-small-cell lung cancer by single-cell sequencing. *Nature Medicine*. 2018;24(7):978-985. doi:10.1038/s41591-018-0045-3

123. Lavin Y, Kobayashi S, Leader A, et al. Innate Immune Landscape in Early Lung Adenocarcinoma by Paired Single-Cell Analyses. *Cell*. 2017;169(4):750-765.e17. doi:10.1016/j.cell.2017.04.014

124. Lin W, Noel P, Borazanci EH, et al. Single-cell transcriptome analysis of tumor and stromal compartments of pancreatic ductal adenocarcinoma primary tumors and metastatic lesions. *Genome Medicine*. 2020;12(1):80. doi:10.1186/s13073-020-00776-9

125. Schlesinger Y, Yosefov-Levi O, Kolodkin-Gal D, et al. Single-cell transcriptomes of pancreatic preinvasive lesions and cancer reveal acinar metaplastic cells' heterogeneity. *Nature Communications*. 2020;11(1):4516. doi:10.1038/s41467-020-18207-z

126. Uhlen M, Fagerberg L, Hallstrom BM, et al. Tissue-based map of the human proteome. *Science*. 2015;347(6220):1260419-1260419. doi:10.1126/science.1260419

127. Thul PJ, Akesson L, Wiking M, et al. A subcellular map of the human proteome. *Science*. 2017;356(6340):eaal3321. doi:10.1126/science.aal3321

128. Lonsdale J, Thomas J, Salvatore M, et al. The Genotype-Tissue Expression (GTEx) project. *Nature Genetics*. 2013;45(6):580-585. doi:10.1038/ng.2653

129. Treutlein B, Brownfield DG, Wu AR, et al. Reconstructing lineage hierarchies of the distal lung epithelium using single-cell RNA-seq. *Nature*. 2014;509(7500):371-375. doi:10.1038/nature13173

130. Angelidis I, Simon LM, Fernandez IE, et al. An atlas of the aging lung mapped by single cell transcriptomics and deep tissue proteomics. *Nature Communications*. 2019;10(1):963. doi:10.1038/s41467-019-08831-9

131. Enge M, Arda HE, Mignardi M, et al. Single-Cell Analysis of Human Pancreas Reveals Transcriptional Signatures of Aging and Somatic Mutation Patterns. *Cell*. 2017;171(2):321-330.e14. doi:10.1016/j.cell.2017.09.004

132. Halpern KB, Shenhav R, Matcovitch-Natan O, et al. Single-cell spatial reconstruction reveals global division of labour in the mammalian liver. *Nature*. 2017;542(7641):352-356. doi:10.1038/nature21065

133. Muraro MJ, Dharmadhikari G, Grün D, et al. A Single-Cell Transcriptome Atlas of the Human Pancreas. *Cell Systems*. 2016;3(4):385-394.e3. doi:10.1016/j.cels.2016.09.002

134. Shapiro E, Biezuner T, Linnarsson S. Single-cell sequencing-based technologies will revolutionize whole-organism science. *Nature reviews Genetics*. 14(9):618-630. doi:10.1038/nrg3542

135. Racle J, de Jonge K, Baumgaertner P, Speiser DE, Gfeller D. Simultaneous enumeration of cancer and immune cell types from bulk tumor gene expression data. *eLife*. 2017;6:1-25. doi:10.7554/eLife.26476

136. Aran D, Hu Z, Butte AJ. xCell: Digitally portraying the tissue cellular heterogeneity landscape. *Genome Biology*. 2017;18(1):1-14. doi:10.1186/s13059-017-1349-1

137. Newman AM, Liu CL, Green MR, et al. Robust enumeration of cell subsets from tissue expression profiles. *Nature Methods*. 2015;12(5):453-457. doi:10.1038/nmeth.3337

138. Newman AM, Steen CB, Liu CL, et al. Determining cell type abundance and expression from bulk tissues with digital cytometry. *Nature Biotechnology*. Published online 2019. doi:10.1038/s41587-019-0114-2

139. Patel S, Ngounou Wetie A, Darie C, Clarkson B. Cancer secretomes and their place in supplementing other hallmarks of cancer. *Adv Exp Med Biol*. 2014;806:409-442. doi:10.1007/978-3-319-06068-2_20

140. Makridakis M, Vlahou A. Secretome proteomics for discovery of cancer biomarkers. *Proteomics, J*. 2010;73(12):2291-2305. doi:10.1016/j.jprot.2010.07.001

141. Tjalsma H, Bolhuis A, Jongbloed J, Bron S, van Dijl J. Signal peptide-dependent protein transport in Bacillus subtilis: a genome-based survey of the secretome. *Microbiol Mol Biol Rev*. 2000;64:515-547.

142. Schaaij-visser TBM, Wit M De, Lam SW, Jiménez CR. The cancer secretome, current status and opportunities in the lung , breast and colorectal cancer context. *BBA - Proteins and Proteomics*. 2013;1834(11):2242-2258. doi:10.1016/j.bbapap.2013.01.029

143. Mukherjee P, Mani S. Methodologies to decipher the cell secretome. *Biochim Biophys Acta*. 2013;1834(11):2226-2232. doi:10.1016/j.bbapap.2013.01.022

144. Rapoport TA. Protein translocation across the eukaryotic endoplasmic reticulum and bacterial plasma membranes. *Nature*. 2007;450(7170):663-669. doi:10.1038/nature06384

145. Burdukiewicz M, Sobczyk P, Chilimoniuk J, Gagat P, Mackiewicz P. Prediction of Signal Peptides in Proteins from Malaria Parasites. *IJMS*. 2018;19(12):3709. doi:10.3390/ijms19123709

146. Bhattacharya A, Prakash YS, Eissa NT. Secretory function of autophagy in innate immune cells: Secretory function of autophagy. *Cell Microbiol*. 2014;16(11):1637-1645. doi:10.1111/cmi.12365

147. Bendtsen JD, Jensen LJ, Blom N, von Heijne G, Brunak S. Feature-based prediction of non-classical and leaderless protein secretion. *Protein Engineering Design and Selection*. 2004;17(4):349-356. doi:10.1093/protein/gzh037

148. Sullivan DP, Winsnes CF, Åkesson L, et al. Deep learning is combined with massive-scale citizen science to improve large-scale image classification. *Nat Biotechnol*. 2018;36(9):820-828. doi:10.1038/nbt.4225

149. Mukherjee P, Mani S. Methodologies to decipher the cell secretome. *Biochimica et Biophysica Acta (BBA) - Proteins and Proteomics*. 2013;1834(11):2226-2232. doi:10.1016/j.bbapap.2013.01.022

150. Welsh JB, Sapinoso LM, Kern SG, et al. Large-scale delineation of secreted protein biomarkers overexpressed in cancer tissue and serum. Published online 2010.

151. Canto LM do, Cury SS, Barros-Filho MC, et al. Locally advanced rectal cancer transcriptomic-based secretome analysis reveals novel biomarkers useful to identify patients according to neoadjuvant chemoradiotherapy response. *Scientific Reports*. 2019;9(1):1-11. doi:10.1038/s41598-019-45151-w

152. Cury SS, Lapa RML, de Mello JBH, et al. Increased DSG2 plasmatic levels identified by transcriptomic-based secretome analysis is a potential prognostic biomarker in laryngeal carcinoma. *Oral Oncology*. 2020;103. doi:10.1016/j.oraloncology.2020.104592

153. Armingol E, Officer A, Harismendy O, Lewis NE. Deciphering cell–cell interactions and communication from gene expression. *Nature Reviews Genetics*. Published online 2020. doi:10.1038/s41576-020-00292-x

154. Penna F, Busquets S, Argilés JM. Experimental cancer cachexia : Evolving strategies for getting closer to the human scenario. *Seminars in Cell and Developmental Biology*. 2016;54:20-27. doi:10.1016/j.semcdb.2015.09.002

155. Rung J, Brazma A. Reuse of public genome-wide gene expression data. *Nature Reviews Genetics*. 2013;14(2):89-99. doi:10.1038/nrg3394

156. Perez-Riverol Y, Zorin A, Dass G, et al. Quantifying the impact of public omics data. *Nature Communications*. 2019;10(1):3512. doi:10.1038/s41467-019-11461-w

157. Tomczak K, Czerwińska P, Wiznerowicz M. The Cancer Genome Atlas (TCGA): an immeasurable source of knowledge. *Contemp Oncol (Pozn)*. 2015;19(1A):A68-77. doi:10.5114/wo.2014.47136

158. Barretina J, Caponigro G, Stransky N, et al. The Cancer Cell Line Encyclopedia enables predictive modelling of anticancer drug sensitivity. *Nature*. 2012;483(7391):603-607. doi:10.1038/nature11003

159. Robinson JL, Feizi A, Uhlén M, Nielsen J. A Systematic Investigation of the Malignant Functions and Diagnostic Potential of the Cancer Secretome. *Cell Reports*. 2019;26(10):2622-2635.e5. doi:10.1016/j.celrep.2019.02.025

160. Bakr S, Gevaert O, Echegaray S, et al. Data for NSCLC Radiogenomics Collection. Published online 2017. doi:10.7937/K9/TCIA.2017.7HS46ERV

161. Su AI, Wiltshire T, Batalov S, et al. A gene atlas of the mouse and human protein-encoding transcriptomes. *Proceedings of the National Academy of Sciences*. 2004;101(16):6062-6067. doi:10.1073/pnas.0400782101

162. Budczies J, Klauschen F, Sinn BV, et al. Cutoff Finder: A Comprehensive and Straightforward Web Application Enabling Rapid Biomarker Cutoff Optimization. van Diest P, ed. *PLoS ONE*. 2012;7(12):e51862. doi:10.1371/journal.pone.0051862

163. Goksuluk D, Korkmaz S, Zararsiz G, Karaagaoglu A Ergun. easyROC: An Interactive Web-tool for ROC Curve Analysis Using R Language Environment. *The R Journal*. 2016;8(2):213. doi:10.32614/RJ-2016-042

164. Thul PJ, Åkesson L, Wiking M, et al. A subcellular map of the human proteome. *Science*. 2017;356(6340):eaal3321. doi:10.1126/science.aal3321

165. Shannon P. Cytoscape: A Software Environment for Integrated Models of Biomolecular Interaction Networks. *Genome Research*. 2003;13(11):2498-2504. doi:10.1101/gr.1239303

166. Tang Y, Li M, Wang J, Pan Y, Wu FX. CytoNCA: A cytoscape plugin for centrality analysis and evaluation of protein interaction networks. *Biosystems*. 2015;127:67-72. doi:10.1016/j.biosystems.2014.11.005

167. Robinson MD, Oshlack A. A scaling normalization method for differential expression analysis of RNA-seq data. *Genome Biol*. 2010;11(3):R25. doi:10.1186/gb-2010-11-3-r25

168. Clark K, Vendt B, Smith K, et al. The Cancer Imaging Archive (TCIA): Maintaining and Operating a Public Information Repository. *J Digit Imaging*. 2013;26(6):1045-1057. doi:10.1007/s10278-013-9622-7

169. Wu C, Orozco C, Boyer J, et al. BioGPS: an extensible and customizable portal for querying and organizing gene annotation resources. *Genome Biol*. 2009;10(11):R130. doi:10.1186/gb-2009-10-11-r130

170. Barretina J, Caponigro G, Stransky N, et al. The Cancer Cell Line Encyclopedia enables predictive modelling of anticancer drug sensitivity. *Nature*. 2012;483(7391):603-607. doi:10.1038/nature11003

171. Yu K, Chen B, Aran D, et al. Comprehensive transcriptomic analysis of cell lines as models of primary tumors across 22 tumor types. *Nat Commun*. 2019;10(1):3574. doi:10.1038/s41467-019-11415-2

172. Chen B, Khodadoust MS, Liu CL, Newman AM, Alizadeh AA. Profiling Tumor Infiltrating Immune Cells with CIBERSORT. In: von Stechow L, ed. *Cancer Systems Biology*. Vol 1711. Methods in Molecular Biology. Springer New York; 2018:243-259. doi:10.1007/978-1-4939-7493-1_12

173. Miao Y, Zhang Q, Lei Q, et al. ImmuCellAI: A Unique Method for Comprehensive T-Cell Subsets Abundance Prediction and its Application in Cancer Immunotherapy. *Adv Sci*. 2020;7(7):1902880. doi:10.1002/advs.201902880

174. Efremova M, Vento-Tormo M, Teichmann SA, Vento-Tormo R. CellPhoneDB: inferring cell–cell communication from combined expression of multi-subunit ligand–receptor complexes. *Nat Protoc*. 2020;15(4):1484-1506. doi:10.1038/s41596-020-0292-x

175. Chen EY, Tan CM, Kou Y, et al. Enrichr: interactive and collaborative HTML5 gene list enrichment analysis tool. *BMC Bioinformatics*. 2013;14(1):128. doi:10.1186/1471-2105-14-128

176. Kuleshov MV, Jones MR, Rouillard AD, et al. Enrichr: a comprehensive gene set enrichment analysis web server 2016 update. *Nucleic Acids Res*. 2016;44(W1):W90-W97. doi:10.1093/nar/gkw377

177. Torre D, Lachmann A, Ma'ayan A. BioJupies: Automated Generation of Interactive Notebooks for RNA-Seq Data Analysis in the Cloud. *Cell Systems*. 2018;7(5):556-561.e3. doi:10.1016/j.cels.2018.10.007

178. Metsalu T, Vilo J. ClustVis: a web tool for visualizing clustering of multivariate data using Principal Component Analysis and heatmap. *Nucleic Acids Res*. 2015;43(W1):W566-W570. doi:10.1093/nar/gkv468

Capítulo 1:

1. Baracos VE, Martin L, Korc M, Guttridge DC, Fearon KCH. Cancer-associated cachexia. *Nat Rev Dis Primer* 2018;**4**:17105.

2. Kimura M, Naito T, Kenmotsu H, Taira T, Wakuda K, Oyakawa T *et al.* Prognostic impact of cancer cachexia in patients with advanced non-small cell lung cancer. *Support Care Cancer* 2015;**23**:1699–1708.

3. Herbst RS, Morgensztern D, Boshoff C. The biology and management of non-small cell lung cancer. *Nature* 2018;**553**:446–454.

4. Fearon K, Strasser F, Anker SD, Bosaeus I, Bruera E, Fainsinger RL *et al.* Definition and classification of cancer cachexia: an international consensus. *Lancet Oncol* 2011;**12**:489–495.

5. Buckinx F, Landi F, Cesari M, Fielding RA, Visser M, Engelke K *et al.* Pitfalls in the measurement of muscle mass: a need for a reference standard: Measurement of muscle mass. *J Cachexia Sarcopenia Muscle* 2018;**9**:269–278.

6. Prado CM, Birdsell LA, Baracos VE. The emerging role of computerized tomography in assessing cancer cachexia: *Curr Opin Support Palliat Care* 2009;**3**:269–275.

7. Swensen SJ, Jett JR, Hartman TE, Midthun DE, Sloan JA, Sykes A-M *et al.* Lung Cancer Screening with CT: Mayo Clinic Experience. *Radiology* 2003;**226**:756–761.

8. Kinsey CM, San José Estépar R, van der Velden J, Cole BF, Christiani DC, Washko GR. Lower Pectoralis Muscle Area Is Associated with a Worse Overall Survival in Non–Small Cell Lung Cancer. *Cancer Epidemiol Biomarkers Prev* 2017;**26**:38–43.

9. Cury SS, de Moraes D, Freire PP, de Oliveira G, Marques DVP, Fernandez GJ *et al.* Tumor Transcriptome Reveals High Expression of IL-8 in Non-Small Cell Lung Cancer Patients with Low Pectoralis Muscle Area and Reduced Survival. *Cancers* 2019;**11**.

10. Freire PP, Fernandez GJ, Moraes D, Cury SS, Dal Pai-Silva M, Reis PP *et al.* The expression landscape of cachexia-inducing factors in human cancers. *J Cachexia Sarcopenia Muscle* 2020;**11**:947–961.

11. Sørensen J. Lung Cancer Cachexia: Can Molecular Understanding Guide Clinical Management? *Integr Cancer Ther* 2018;**17**:1000–1008.

12. Argilés JM, Stemmler B, López-Soriano FJ, Busquets S. Inter-tissue communication in cancer cachexia. *Nat Rev Endocrinol* 2019;**15**:9–20.

13. Thorsson V, Gibbs DL, Brown SD, Wolf D, Bortone DS, Ou Yang T-H *et al.* The Immune Landscape of Cancer. *Immunity* 2018;**48**:812-830.e14.

14. Bakr S, Gevaert O, Echegaray S, Ayers K, Zhou M, Shafiq M *et al.* A radiogenomic dataset of non-small cell lung

cancer. *Sci Data* 2018;**5**:180202.

15. Gevaert O, Xu J, Hoang CD, Leung AN, Xu Y, Quon A *et al.* Non–Small Cell Lung Cancer: Identifying Prognostic Imaging Biomarkers by Leveraging Public Gene Expression Microarray Data—Methods and Preliminary Results. *Radiology* 2012;**264**:387–396.

16. Ramilowski JA, Goldberg T, Harshbarger J, Kloppmann E, Lizio M, Satagopam VP *et al.* A draft network of ligand–receptor-mediated multicellular signalling in human. *Nat Commun* 2015;**6**:7866.

17. Kim M, Mun H, Sung CO, Cho EJ, Jeon H-J, Chun S-M *et al.* Patient-derived lung cancer organoids as in vitro cancer models for therapeutic screening. *Nat Commun* 2019;**10**:3991.

18. Newman AM, Steen CB, Liu CL, Gentles AJ, Chaudhuri AA, Scherer F *et al.* Determining cell type abundance and expression from bulk tissues with digital cytometry. *Nat Biotechnol* 2019;**37**:773–782.

19. Guo X, Zhang Y, Zheng L, Zheng C, Song J, Zhang Q *et al.* Global characterization of T cells in non-small-cell lung cancer by single-cell sequencing. *Nat Med* 2018;**24**:978–985.

20. Henriques F, Lopes MA, Franco FO, Knobl P, Santos KB, Bueno LL *et al.* Toll-Like Receptor-4 Disruption Suppresses Adipose Tissue Remodeling and Increases Survival in Cancer Cachexia Syndrome. *Sci Rep* 2018;**8**:18024.

21. Beluzi M, Peres SB, Henriques FS, Sertié RAL, Franco FO, Santos KB *et al.* Pioglitazone Treatment Increases Survival and Prevents Body Weight Loss in Tumor–Bearing Animals: Possible Anti-Cachectic Effect. *PLOS ONE* 2015;**10**:e0122660.

22. Livak KJ, Schmittgen TD. Analysis of Relative Gene Expression Data Using Real-Time Quantitative PCR and the 2−ΔΔCT Method. *Methods* 2001;**25**:402–408.

23. Vandesompele J, De Preter K, Pattyn F, Poppe B, Van Roy N, De Paepe A *et al.* Accurate normalization of real-time quantitative RT-PCR data by geometric averaging of multiple internal control genes. *Genome Biol* 2002;**3**:research0034.1.

24. Vagnildhaug OM, Brunelli C, Hjermstad MJ, Strasser F, Baracos V, Wilcock A *et al.* A prospective study examining cachexia predictors in patients with incurable cancer. *BMC Palliat Care* 2019;**18**:46.

25. Derksen JWG, Kurk SA, Oskam MJ, Peeters PHM, Punt CJA, Koopman M *et al.* Factors Contributing to Cancer-Related Muscle Wasting During First-Line Systemic Treatment for Metastatic Colorectal Cancer. *JNCI Cancer Spectr* 2019;**3**:pkz014.

26. Underwood PW, Zhang DY, Cameron ME, Gerber MH, Delitto D, Maduka MU *et al.* Nicotine Induces IL-8 Secretion from Pancreatic Cancer Stroma and Worsens Cancer-Induced Cachexia. *Cancers* 2020;**12**:329.

27. Marhold M, Topakian T, Unseld M. Sarcopenia in cancer—a focus on elderly cancer patients. *Memo - Mag Eur Med Oncol* 2020 doi:10.1007/s12254-020-00637-6.

28. Shiono M, Huang K, Downey RJ, Consul N, Villanueva N, Beck K *et al.* An analysis of the relationship between metastases and cachexia in lung cancer patients. *Cancer Med* 2016;**5**:2641–2648.

29. Garrido P, Olmedo ME, Gómez A, Paz Ares L, López-Ríos F, Rosa-Rosa JM *et al.* Treating KRAS-mutant NSCLC: latest evidence and clinical consequences. *Ther Adv Med Oncol* 2017;**9**:589–597.

30. Armingol E, Officer A, Harismendy O, Lewis NE. Deciphering cell–cell interactions and communication from gene expression. *Nat Rev Genet* 2020 doi:10.1038/s41576-020-00292-x.

31. Seto DN, Kandarian SC, Jackman RW. A Key Role for Leukemia Inhibitory Factor in C26 Cancer Cachexia. *J Biol Chem* 2015;**290**:19976–19986.

32. Yu K, Chen B, Aran D, Charalel J, Yau C, Wolf DM *et al.* Comprehensive transcriptomic analysis of cell lines as models of primary tumors across 22 tumor types. *Nat Commun* 2019;**10**:3574.

33. Kadambi A, Mouta Carreira C, Yun CO, Padera TP, Dolmans DE, Carmeliet P *et al.* Vascular endothelial growth factor (VEGF)-C differentially affects tumor vascular function and leukocyte recruitment: role of VEGF-receptor 2 and host VEGF-A. *Cancer Res* 2001;**61**:2404–2408.

34. Mojic M, Takeda K, Hayakawa Y. The Dark Side of IFN-γ: Its Role in Promoting Cancer Immunoevasion. *Int J Mol Sci* 2017;**19**.

35. Zhang Y, Huang S, Gong D, Qin Y, Shen Q. Programmed death-1 upregulation is correlated with dysfunction of tumor-infiltrating CD8+ T lymphocytes in human non-small cell lung cancer. *Cell Mol Immunol* 2010;**7**:389–395.

36. Raskov H, Orhan A, Christensen JP, Gögenur I. Cytotoxic CD8+ T cells in cancer and cancer immunotherapy. *Br J Cancer* 2020 doi:10.1038/s41416-020-01048-4.

37. Baazim H, Schweiger M, Moschinger M, Xu H, Scherer T, Popa A *et al.* CD8+ T cells induce cachexia during chronic viral infection. *Nat Immunol* 2019;**20**:701–710.

38. Philip M, Fairchild L, Sun L, Horste EL, Camara S, Shakiba M *et al.* Chromatin states define tumour-specific T cell dysfunction and reprogramming. *Nature* 2017;**545**:452–456.

39. Bonomi P, Fidler MJ, Shah P, Borgia J. Theoretical and Practical Implications of Treating Cachexia in Advanced Lung Cancer Patients. *Cancers* 2019;**11**:1619.

40. Haehling S, Coats AJS, Anker SD. Ethical guidelines for publishing in the *Journal of Cachexia, Sarcopenia and Muscle* : update 2021. *J Cachexia Sarcopenia Muscle* 2021;**12**:2259–2261.

S1. Hendifar AE, Chang JI, Huang BZ, Tuli R, Wu BU. Cachexia, and not obesity, prior to pancreatic cancer diagnosis worsens survival and is negated by chemotherapy. J Gastrointest Oncol 2018;9:17–23.

S2. Permuth JB, Clark Daly A, Jeong D, Choi JW, Cameron ME, Chen D et al. Racial and ethnic disparities in a state-wide registry of patients with pancreatic cancer and an exploratory investigation of cancer cachexia as a contributor to observed inequities. Cancer Med 2019;8:3314–3324.

S3. Cardena MMSG, Ribeiro-dos-Santos Â, Santos S, Mansur AJ, Pereira AC, Fridman C. Assessment of the Relationship between Self-Declared Ethnicity, Mitochondrial Haplogroups and Genomic Ancestry in Brazilian Individuals. PLoS ONE 2013;8:e62005

S4. Marrow H. To be or not to be (Hispanic or Latino): Brazilian Racial and Ethnic Identity in the United States. Ethnicities 2003;3:427–464.

S5. Cao Z, Scott AM, Hoogenraad NJ, Osellame LD. Mediators and clinical treatment for cancer cachexia: a systematic review. JCSM Rapid Commun 2021;4:166–186.S6. Bayliss TJ, Smith JT, Schuster M, Dragnev KH, Rigas JR. A humanized anti-IL-6 antibody (ALD518) in non-small cell lung cancer. Expert Opin Biol Ther 2011;11:1663–1668.

S7. Ando K, Takahashi F, Kato M, Kaneko N, Doi T, Ohe Y et al. Tocilizumab, a Proposed Therapy for the Cachexia of Interleukin6-Expressing Lung Cancer. PLoS ONE 2014;9:e102436

S8. Matthys P, Heremans H, Opdenakker G, Billiau A. Anti-interferon-γ antibody treatment, growth of Lewis lung tumours in mice and tumour-associated cachexia. Eur J Cancer Clin Oncol 1991;27:182–187.

S9. Talbert EE, Guttridge DC. Emerging signaling mediators in the anorexia–cachexia syndrome of cancer. Trends Cancer 2022;8:397–403.

Capítulo 2:

1. Fearon K, Strasser F, Anker SD, Bosaeus I, Bruera E, Fainsinger RL et al. Definition and classification of cancer cachexia: an international consensus. Lancet Oncol 2011;12:489–495.

2. Baracos VE, Martin L, Korc M, Guttridge DC, Fearon KCH. Cancer-associated cachexia. Nat Rev Dis Primer 2018;4:17105.

3. Argilés JM, Stemmler B, López-Soriano FJ, Busquets S. Inter-tissue communication in cancer cachexia. Nat Rev Endocrinol 2019;15:9–20.

4. Tsoli M, Robertson G. Cancer cachexia: malignant inflammation, tumorkines, and metabolic mayhem. Trends Endocrinol Metab 2013;24:174–183.

5. Wyart E, Bindels LB, Mina E, Menga A, Stanga S, Porporato PE. Cachexia, a Systemic Disease beyond Muscle Atrophy. Int J Mol Sci 2020;21:8592.

6. Webster JM, Kempen LJAP, Hardy RS, Langen RCJ. Inflammation and Skeletal Muscle Wasting During Cachexia. Front Physiol 2020;11:597675.

7. Barkhudaryan A, Scherbakov N, Springer J, Doehner W. Cardiac muscle wasting in individuals with cancer cachexia: Cardiac wasting in cancer. ESC Heart Fail 2017;4:458–467.

8. Feathers LSB, Wilcock A, Manderson C, Rgn, Weller R, Rgn et al. Measuring Inspiratory Muscle Weakness in Patients with Cancer and Breathlessness. J Pain Symptom Manage 2003;25:305–306.

9. Dahlman I, Mejhert N, Linder K, Agustsson T, Mutch DM, Kulyte A et al. Adipose tissue pathways involved in weight loss of cancer cachexia. Br J Cancer 2010;102:1541–1548.

10. Bonetto A, Aydogdu T, Kunzevitzky N, Guttridge DC, Khuri S, Koniaris LG et al. STAT3 Activation in Skeletal Muscle Links Muscle Wasting and the Acute Phase Response in Cancer Cachexia. PLoS ONE 2011;6:e22538.

11. Freire PP, Fernandez GJ, Moraes D, Cury SS, Dal Pai-Silva M, Reis PP et al. The expression landscape of cachexia-inducing factors in human cancers. J Cachexia Sarcopenia Muscle 2020;11:947–961.

12. Raphael BJ, Hruban RH, Aguirre AJ, Moffitt RA, Yeh JJ, Stewart C et al. Integrated Genomic Characterization of Pancreatic Ductal Adenocarcinoma. Cancer Cell 2017;32:185-203.e13.

13. Wood LD, Hruban RH. Pathology and Molecular Genetics of Pancreatic Neoplasms: Cancer J 2012;18:492–501.

14. Thul PJ, Åkesson L, Wiking M, Mahdessian D, Geladaki A, Ait Blal H et al. A subcellular map of the human proteome. Science 2017;356:eaal3321.

15. Hébuterne X, Lemarié E, Michallet M, de Montreuil CB, Schneider SM, Goldwasser F. Prevalence of Malnutrition and Current Use of Nutrition Support in Patients With Cancer. J Parenter Enter Nutr 2014;38:196–204.

16. Pressoir M, Desné S, Berchery D, Rossignol G, Poiree B, Meslier M et al. Prevalence, risk factors and clinical implications of malnutrition in French Comprehensive Cancer Centres. Br J Cancer 2010;102:966–971.

17. Tang Z, Li C, Kang B, Gao G, Li C, Zhang Z. GEPIA: a web server for cancer and normal gene expression profiling and interactive analyses. Nucleic Acids Res 2017;45:W98–W102.

18. Malod-Dognin N, Petschnigg J, Windels SFL, Povh J, Hemingway H, Ketteler R et al. Towards a data-integrated cell. Nat Commun 2019;10:805.

19. Shannon P. Cytoscape: A Software Environment for Integrated Models of Biomolecular Interaction Networks. Genome Res 2003;13:2498–2504.

20. Chen B, Khodadoust MS, Liu CL, Newman AM, Alizadeh AA. Profiling Tumor Infiltrating Immune Cells with CIBERSORT. In: von Stechow L, editor. Cancer Systems Biology. Springer New York: New York, NY; 2018. pp. 243–259.

21. Peng J, Sun B-F, Chen C-Y, Zhou J-Y, Chen Y-S, Chen H et al. Single-cell RNA-seq highlights intra-tumoral heterogeneity and malignant progression in pancreatic ductal adenocarcinoma. Cell Res 2019;29:725–738.

22. Wang Y, Song F, Zhu J, Zhang S, Yang Y, Chen T et al. GSA: Genome Sequence Archive *. Genomics Proteomics Bioinformatics 2017;15:14–18.

23. Barretina J, Caponigro G, Stransky N, Venkatesan K, Margolin AA, Kim S et al. The Cancer Cell Line Encyclopedia enables predictive modelling of anticancer drug sensitivity. Nature 2012;483:603–607.

24. Ghandi M, Huang FW, Jané-Valbuena J, Kryukov GV, Lo CC, McDonald ER et al. Next-generation characterization of the Cancer Cell Line Encyclopedia. Nature 2019;569:503–508.

25. Ramilowski JA, Goldberg T, Harshbarger J, Kloppmann E, Lizio M, Satagopam VP et al. A draft network of ligand–receptor-mediated multicellular signalling in human. Nat Commun 2015;6:7866.

26. Gilabert M, Calvo E, Airoldi A, Hamidi T, Moutardier V, Turrini O et al. Pancreatic Cancer-Induced Cachexia Is Jak2-Dependent in Mice: Jak2-DEPENDENT CACHEXIA. J Cell Physiol 2014;229:1437–1443.

27. Krzywinski M, Schein J, Birol I, Connors J, Gascoyne R, Horsman D et al. Circos: An information aesthetic for comparative genomics. Genome Res 2009;19:1639–1645.

28. Hanahan D. Hallmarks of Cancer: New Dimensions. Cancer Discov 2022;12:31–46.

29. Singh SK, Singh R. Cytokines and Chemokines in Cancer Cachexia and Its Long-Term Impact on COVID-19. Cells 2022;11:579.

30. Callaway CS, Delitto AE, D'Lugos AC, Patel R, Nosacka RL, Delitto D et al. IL-8 Released from Human Pancreatic Cancer and Tumor-Associated Stromal Cells Signals through a CXCR2-ERK1/2 Axis to Induce Muscle Atrophy. Cancers 2019;11:1863.

31. Cury SS, de Moraes D, Freire PP, de Oliveira G, Marques DVP, Fernandez GJ et al. Tumor Transcriptome Reveals High Expression of IL-8 in Non-Small Cell Lung Cancer Patients with Low Pectoralis Muscle Area and Reduced Survival. Cancers 2019;11.

32. Hou Y-C, Wang C-J, Chao Y-J, Chen H-Y, Wang H-C, Tung H-L et al. Elevated Serum Interleukin-8 Level Correlates with Cancer-Related Cachexia and Sarcopenia: An Indicator for Pancreatic Cancer Outcomes. J Clin Med 2018;7:502.

33. Mace TA, Shakya R, Pitarresi JR, Swanson B, McQuinn CW, Loftus S et al. IL-6 and PD-L1 antibody blockade combination therapy reduces tumour progression in murine models of pancreatic cancer. Gut 2018;67:320–332.

34. Heid I, Steiger K, Trajkovic-Arsic M, Settles M, Eßwein MR, Erkan M et al. Co-clinical Assessment of Tumor Cellularity in Pancreatic Cancer. Clin Cancer Res 2017;23:1461–1470.

35. Jungmann F, Kaissis GA, Ziegelmayer S, Harder F, Schilling C, Yen H-Y et al. Prediction of Tumor Cellularity in Resectable PDAC from Preoperative Computed Tomography Imaging. Cancers 2021;13:2069.

36. Yao W, Maitra A, Ying H. Recent insights into the biology of pancreatic cancer. EBioMedicine 2020;53:102655.

37. Dougan SK. The Pancreatic Cancer Microenvironment. Cancer J 2017;23:321–325.

38. Gunaydin G. CAFs Interacting With TAMs in Tumor Microenvironment to Enhance Tumorigenesis and Immune Evasion. Front Oncol 2021;11:668349.

39. Geismann, Schäfer, Gundlach, Hauser, Egberts, Schneider et al. NF-κB Dependent Chemokine Signaling in Pancreatic Cancer. Cancers 2019;11:1445.

40. Narasimhan A, Zhong X, Au EP, Ceppa EP, Nakeeb A, House MG et al. Profiling of Adipose and Skeletal Muscle in Human Pancreatic Cancer Cachexia Reveals Distinct Gene Profiles with Convergent Pathways. Cancers 2021;13:1975.

41. Yahiaoui L, Gvozdic D, Danialou G, Mack M, Petrof BJ. CC family chemokines directly regulate myoblast responses to skeletal muscle injury: CC chemokines regulate myoblast behaviour. J Physiol 2008;586:3991–4004.

42. Zeng Z, Lan T, Wei Y, Wei X. CCL5/CCR5 axis in human diseases and related treatments. Genes Dis 2022;9:12–27.

43. Kim DA, Park SJ, Lee JY, Kim JH, Lee S, Lee E et al. Effect of CCL11 on In Vitro Myogenesis and Its Clinical Relevance for Sarcopenia in Older Adults. Endocrinol Metab 2021;36:455–465.

44. Noh H-J, Kim C-S, Kang J-H, Park J-Y, Choe S-Y, Hong S-M et al. Quercetin Suppresses MIP-1α–Induced Adipose Inflammation by Downregulating Its Receptors CCR1/CCR5 and Inhibiting Inflammatory Signaling. J Med Food 2014;17:550–557.

45. Gilchrist A, Echeverria SL. Targeting Chemokine Receptor CCR1 as a Potential Therapeutic Approach for Multiple Myeloma. Front Endocrinol 2022;13:846310.

46. Westby M, van der Ryst E. CCR5 Antagonists: Host-Targeted Antivirals for the Treatment of HIV Infection. Antivir Chem Chemother 2005;16:339–354.

Capítulo 1.

1.1. Material Suplementar

Supplementary material. Information regarding the software, tools, and databases used in the methodology.

Software, tools, and databases	Web page	Version	Reference
NSCLC-Radiogenomics collection	https://wiki.cancerimagingarchive.net/display/Public/NSCLC+Radiogenomics		[160]
gcrma human dataset			[161]
Slice-O-Matic	https://www.tomovision.com/products/sliceomatic.html	v.5.0	
Cutoff Finder		v1.0	[162]
rpart	https://cran.r-project.org/web/packages/rpart/index.html	v4.1	
RStudio	https://www.rstudio.com/	v.4.1.0	
R	https://cran.r-project.org/	v3.5.1	
easyROC	http://www.biosoft.hacettepe.edu.tr/easyROC/	v. 1.3.1	[163]
Human Protein Atlas	http://www.proteinatlas.org	v18.1	[164]
Cytoscape	https://cytoscape.org/	v3.7.2	[165]
CytoNCA	https://apps.cytoscape.org/apps/cytonca	v2.1.6	[166]
GTEx portal	https://www.gtexportal.org/	V8	[167]
cellxgene Data Portal	https://cellxgene.cziscience.com	v0.16.0	
The Cancer Imaging Archive	http://cancerimagingarchive.net		[168]
BioGPS	http://biogps.org/		[169]
SankeyMATIC	http://sankeymatic.com/		
Cancer Cell Line	https://portals.broadinstitute.org/ccle		[170]

Encyclopedia portal		
TCGA-110CL Cell Line Panel	https://comphealth.ucsf.edu/app/tcga-110	171
Human Cancer Model Initiative catalog	https://ocg.cancer.gov/programs/hcmi/	
CIBERSORTx	https://cibersortx.stanford.edu/	172
Immune Cell Abundance Identifier	http://bioinfo.life.hust.edu.cn/ImmuCellAI#!/	173
CellPhoneDB	https://www.cellphonedb.org/	174
EnrichR	https://maayanlab.cloud/Enrichr/	175,176
Biojupies	https://amp.pharm.mssm.edu/biojupies/	177
ClustVis	https://biit.cs.ut.ee/clustvis/	178

References

1. Bakr S, Gevaert O, Echegaray S, Ayers K, Zhou M, Shafiq M *et al.* Data for NSCLC Radiogenomics Collection. 2017 doi:10.7937/K9/TCIA.2017.7HS46ERV.

2. Su AI, Wiltshire T, Batalov S, Lapp H, Ching KA, Block D *et al.* A gene atlas of the mouse and human protein-encoding transcriptomes. *Proceedings of the National Academy of Sciences* 2004;**101**:6062–6067.

3. Budczies J, Klauschen F, Sinn BV, Győrffy B, Schmitt WD, Darb-Esfahani S *et al.* Cutoff Finder: A Comprehensive and Straightforward Web Application Enabling Rapid Biomarker Cutoff Optimization. *PLoS ONE* 2012;**7**:e51862.

4. Goksuluk D, Korkmaz S, Zararsiz G, Karaagaoglu A Ergun. easyROC: An Interactive Web-tool for ROC Curve Analysis Using R Language Environment. *The R Journal* 2016;**8**:213.

5. Thul PJ, Åkesson L, Wiking M, Mahdessian D, Geladaki A, Ait Blal H *et al.* A subcellular map of the human proteome. *Science* 2017;**356**:eaal3321.

6. Shannon P. Cytoscape: A Software Environment for Integrated Models of Biomolecular Interaction Networks. *Genome Research* 2003;**13**:2498–2504.

7. Tang Y, Li M, Wang J, Pan Y, Wu F-X. CytoNCA: A cytoscape plugin for centrality analysis and evaluation of protein interaction networks. *Biosystems* 2015;**127**:67–72.

8. Robinson MD, Oshlack A. A scaling normalization method for differential expression analysis of RNA-seq data. *Genome Biol* 2010;**11**:R25.

9. Clark K, Vendt B, Smith K, Freymann J, Kirby J, Koppel P *et al.* The Cancer Imaging Archive (TCIA): Maintaining and Operating a Public Information Repository. *J Digit Imaging* 2013;**26**:1045–1057.

10. Wu C, Orozco C, Boyer J, Leglise M, Goodale J, Batalov S *et al.* BioGPS: an extensible and customizable portal for querying and organizing gene annotation resources. *Genome Biol* 2009;**10**:R130.

11. Barretina J, Caponigro G, Stransky N, Venkatesan K, Margolin AA, Kim S *et al.* The Cancer Cell Line Encyclopedia enables predictive modelling of anticancer drug sensitivity. *Nature* 2012;**483**:603–607.

12. Yu K, Chen B, Aran D, Charalel J, Yau C, Wolf DM *et al.* Comprehensive transcriptomic analysis of cell lines as models of primary tumors across 22 tumor types. *Nat Commun* 2019;**10**:3574.

13. Chen B, Khodadoust MS, Liu CL, Newman AM, Alizadeh AA. Profiling Tumor Infiltrating Immune Cells with CIBERSORT. In: von Stechow L, editor. *Cancer Systems Biology*. Springer New York: New York, NY; 2018. pp. 243–259.

14. Miao Y, Zhang Q, Lei Q, Luo M, Xie G, Wang H *et al.* ImmuCellAI: A Unique Method for Comprehensive T-Cell Subsets Abundance Prediction and its Application in Cancer Immunotherapy. *Adv Sci* 2020;**7**:1902880.

1.2. Figuras Suplementares

Supplementary Figure 1. Pectoralis muscle area (PMA) cut-offs predict cachexia. A) Boxplot of PMA (mm²) from 38 young males, 97 old males, 34 young females, and 42 old females. B) Boxplot of the same measurements from panel A z-score normalized for gender and age. C) AUC-ROC curve demonstrating the specificity and sensitivity of PMA cut-offs in indicating cachexia.

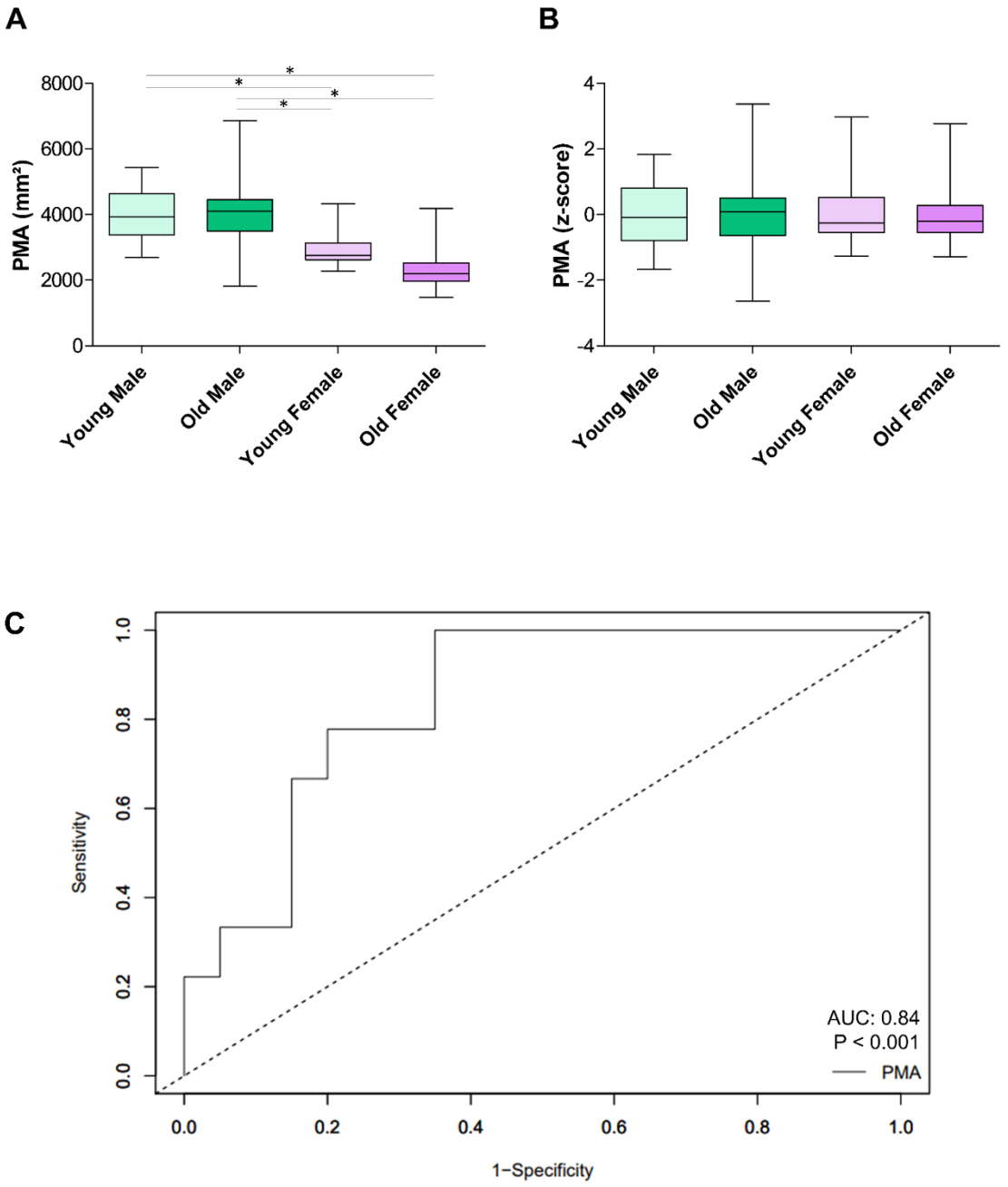

Supplementary Figure 2. Exhausted CD8+T cells interacts with pre-exhausted CD8+T cells through tumor-derived factors identified in low-muscularity patients and negativelly correlates with pectoralis muscle areas (PMA). A) Heatmap demonstrating the number of interactions between each CD8 cell subsets. CD8_C6-LAYN is the exhausted subtype while CD8_C4-GZMK correspond to the pre-exhausted subtype. Analysis performed using CellPhoneDB using the single-cell RNAseq data publicly available at GSE99254. B) Pearson correlation plot showing negative correlation between CD8 and exhaustion scores (identified in the digital cytometry analysis) and PMA. BMI: body mass index.

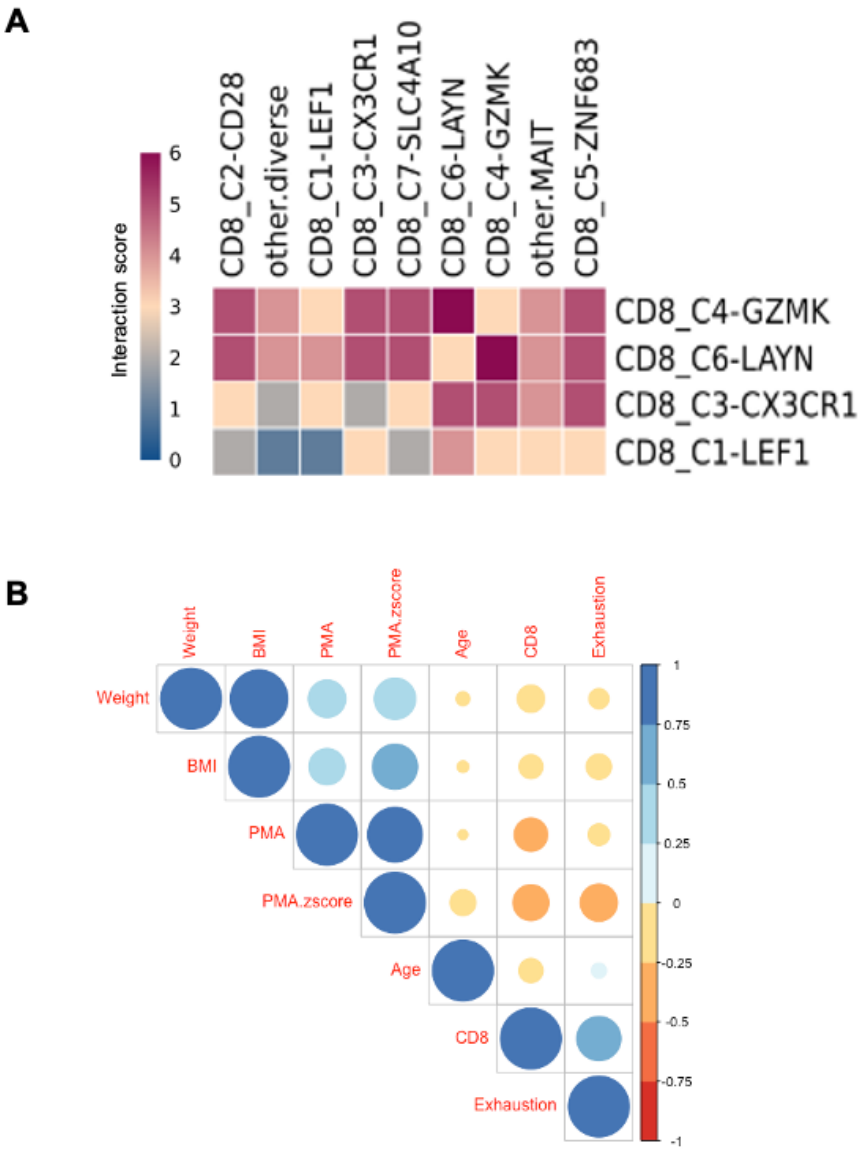

1.3.Tabelas Suplementares

Acesso:
https://docs.google.com/spreadsheets/d/1iQ_R471EFp38LG2-Ra0UghdOl6hXn5YU/edit?usp=sharing&ouid=104102016426115001672&rtpof=true&sd=true

Capítulo 2.

2.1. Figuras Suplementares

Supplementary Figure 1. Core-CIF expression landscape in human pancreatic cells from normal and tumor samples. Dotplot with expression values of core-CIF genes in PDAC and normal-like pancreas samples.

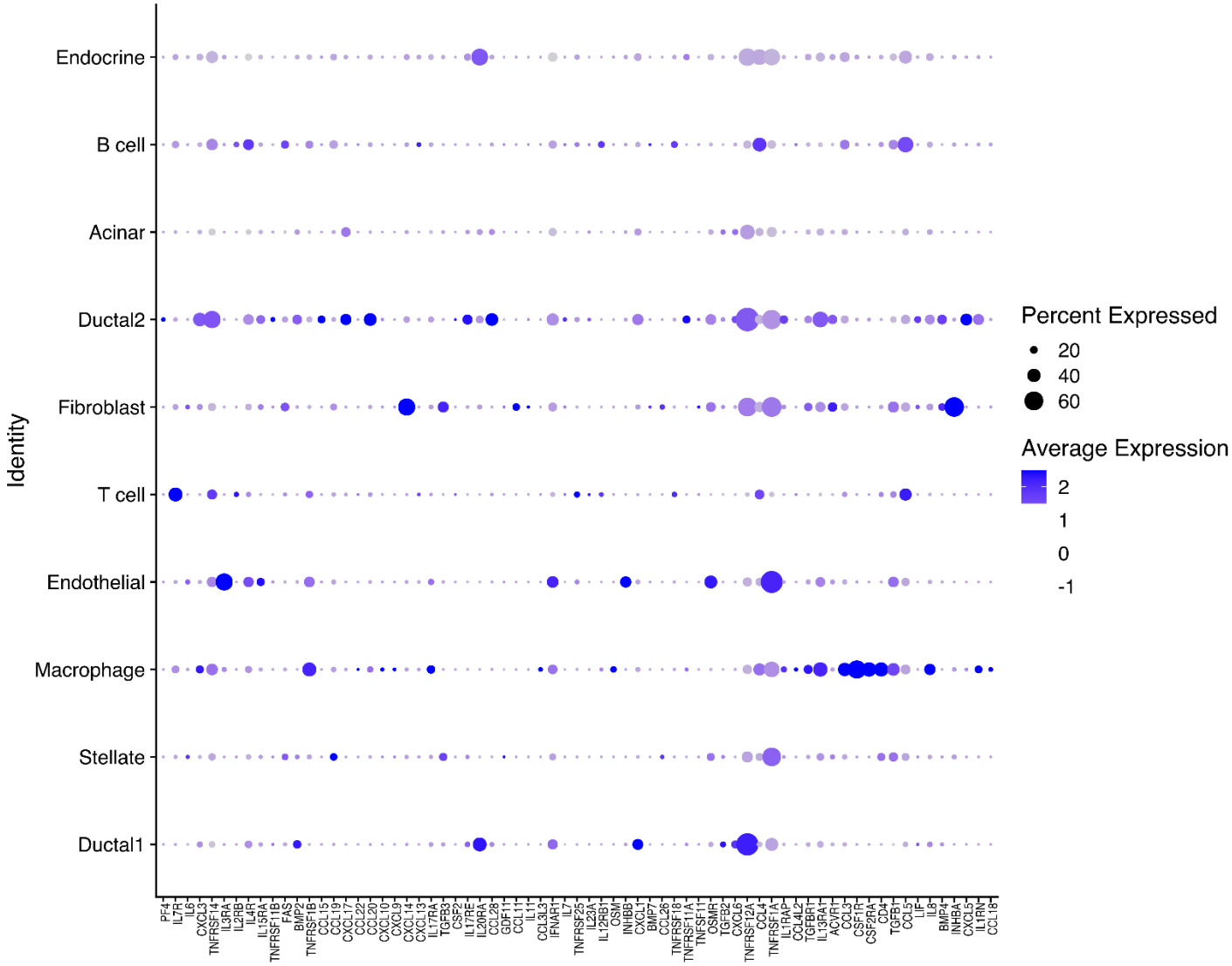

Supplementary Figure 2. Malignant ductal cells (Ductal2) are the major source of Core-CIF expression. Bar graph demonstrating the percentage of cells expressing Core-CIFs in each cell type.

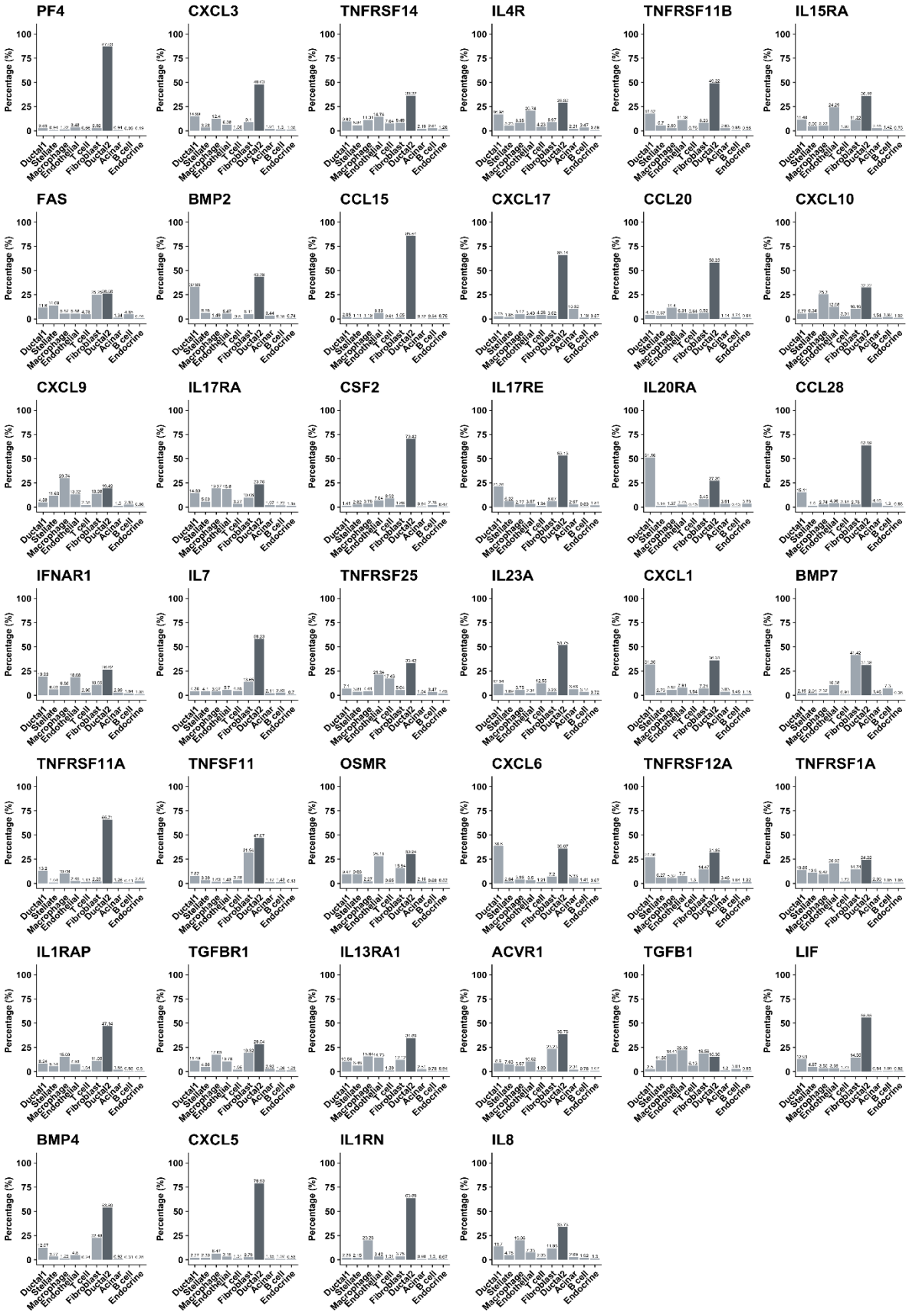
PF4
CXCL3
TNFRSF14
IL4R
TNFRSF11B
IL15RA
FAS
BMP2
CCL15
CXCL17
CCL20
CXCL10
CXCL9
IL17RA
CSF2
IL17RE
IL20RA
CCL28
IFNAR1
IL7
TNFRSF25
IL23A
CXCL1
BMP7
TNFRSF11A
TNFSF11
OSMR
CXCL6
TNFRSF12A
TNFRSF1A
IL1RAP
TGFBR1
IL13RA1
ACVR1
TGFB1
LIF
BMP4
CXCL5
IL1RN
IL8
Percentage (%)
Ductal1
Stellate
Macrophage
Endothelial
T cell
Fibroblast
Ductal2
Acinar
B cell
Endocrine

Supplementary Figure 3. Core-CIF expression landscape in human pancreatic cells lines from Cancer Cell Line Enciclopedia data. Heatmap of core-CIF gene z-scored expression values [log2(TPM+1)] from 50 pancreatic cancer cell lines available in Cancer Cell Line Encyclopedia (CCLE) database. The data were obtained from the Cancer Dependency Map (DepMap; https://depmap.org/). Columns represent the cell lines and rows represent gene expression of 71 core-CIF genes. Rows and collumns were clustered using Euclidean distance. K-means analysis applied in the rows yielded two gene clusters.

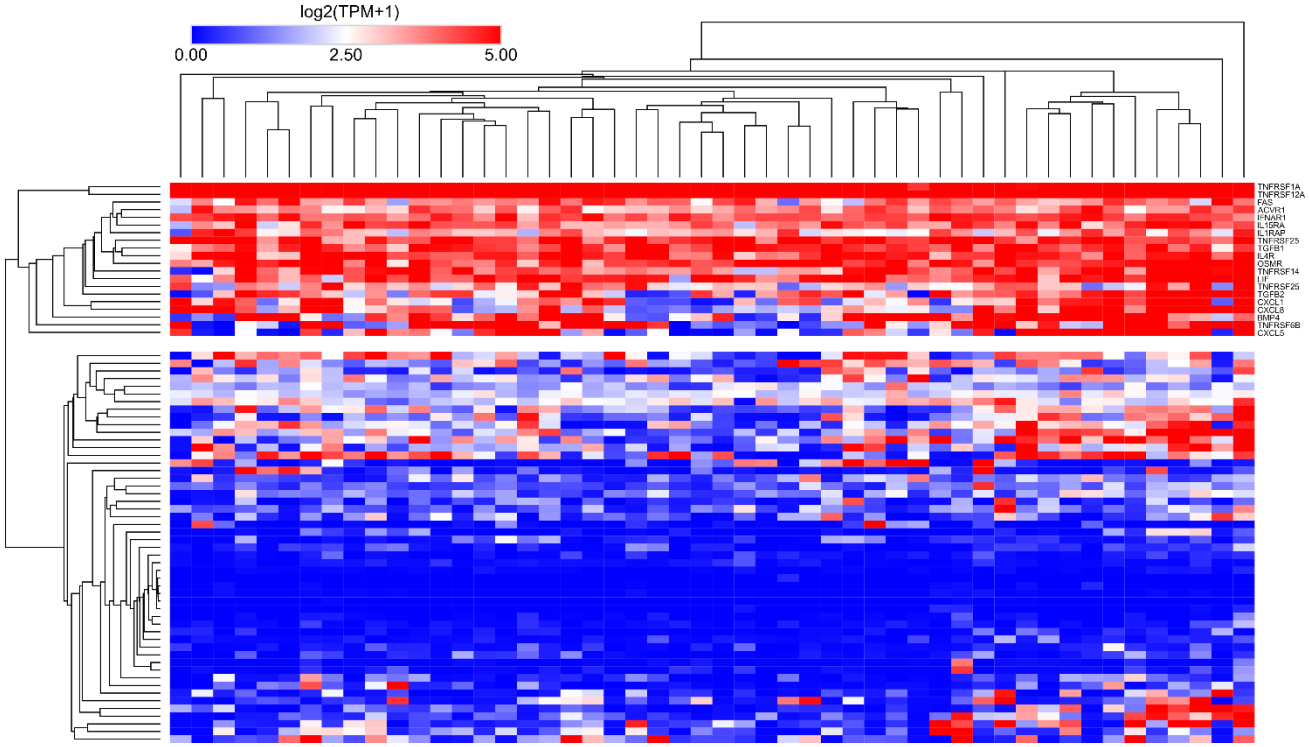

Supplementary Figure 4. Core-CIF receptors CCR1 and CCR5 are increased in cachectic tissues. a) Cytokine-cytokine receptor interaction (hsa04060) performed by KEGG mapper (https://www.genome.jp/kegg/mapper/). The red box indicates the genes belonging to the core-CIFs. **b)** Geoprofiles (https://www.ncbi.nlm.nih.gov/geoprofiles/) expression bar graphs demonstrating the expression of *Ccr1*, *Ccr2*, *Cxcr1*, *Cxcr2*, and *Cxcr3* in white adipose tissue, liver, and skeletal muscle from pancreatic cancer-induced cachexia mice and controls. Log2 Fold change (FC) and p-values were calculated using GEO2R tool using publicly expression data GSE51931.

a

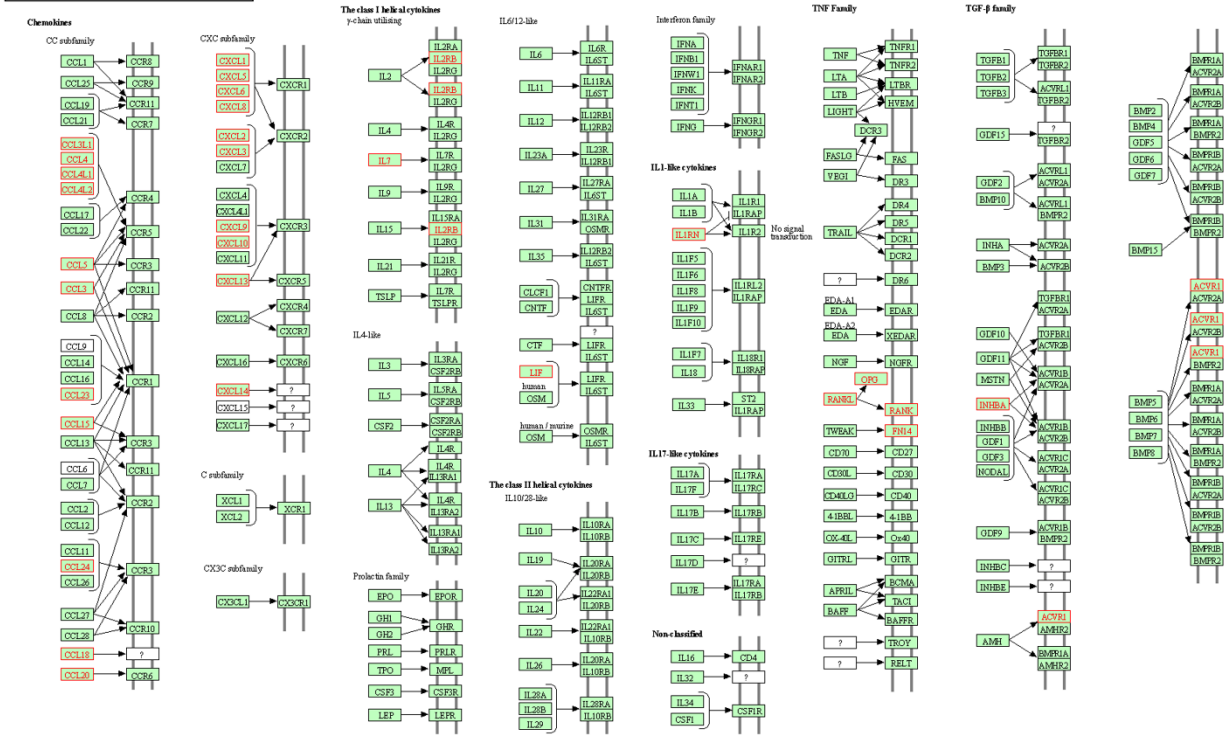

b

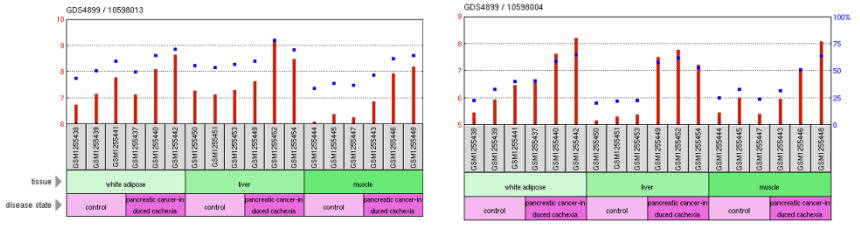

P = 0.15 FC = 0.74 | P = 0.01 FC = 1.21 | P = 0.005 FC = 1.44

P = 0.01 FC = 1.15 | P < 0.001 FC = 2.21 | P = 0.03 FC = 1.42

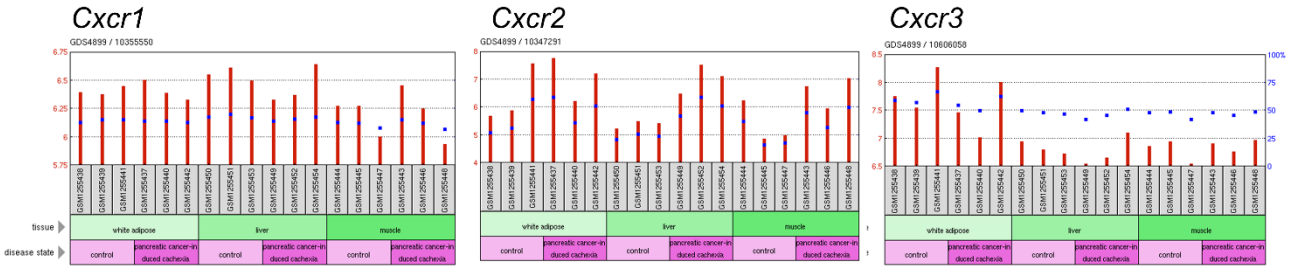

P= 0.99 FC = -0.0002 | P = 0.40 FC = -0.11 | P = 0.87 FC = 0.03

P = 0.31 FC = 0.68 | P < 0.001 FC = 1.65 | P = 0.03 FC = 1.22

P = 0.29 FC = -0.36 | P = 0.71 FC = -0.06 | P = 0.51 FC = 0.09

7. Anexos

Anexo 1. Parecer de aprovação do estudo pelo Comitê de Ética em Pesquisa em seres humanos.

PARECER CONSUBSTANCIADO DO CEP

DADOS DO PROJETO DE PESQUISA

Título da Pesquisa: Predição de caquexia em pacientes com câncer de pulmão de células não pequenas.

Pesquisador: Erica Nishida Hasimoto
Área Temática:
Versão: 2
CAAE: 45723921.0.0000.5411
Instituição Proponente: Departamento de Cirurgia e Ortopedia
Patrocinador Principal: Financiamento Próprio

DADOS DO PARECER

Número do Parecer: 4.836.559

Apresentação do Projeto:
As informações descritas nos campos “Apresentação do Projeto”, “Objetivo da Pesquisa” e “Avaliação dos Riscos e Benefícios” foram retiradas dos documentos e arquivo - Informações Básicas da Pesquisa.

A caquexia é uma síndrome frequentemente encontrada em pacientes com câncer de pulmão. Essa síndrome é definida por uma perda de massa muscular, com consequente perda involuntária de peso, que leva a um comprometimento funcional sistêmico devido a alterações fisiológicas, metabólicas e imunológicas. No entanto, ainda é um desafio definir o estado caquético em pacientes com câncer de pulmão. Nosso grupo de pesquisa construiu um modelo de predição de caquexia, utilizando aprendizado de máquina, que se mostrou promissor para identificar pacientes com câncer de pulmão potencialmente caquéticos. Entretanto, é necessário validar o modelo preditivo em um conjunto independente de pacientes.
Portanto, nosso objetivo é validar o modelo de predição e classificação de caquexia baseando-se na integração das análises de tomografias computadorizadas (TCs) e dados clínicos. Nossa proposta é selecionar o corte transversal da TC contendo os músculos peitorais e analisar a área dos músculos peitorais (AMP) utilizando o software Slice-O-Matic. Dados de muscularidade serão comparados aos dados clínicos dos pacientes,
para avaliarmos a relação de baixa muscularidade e prognóstico desfavorável nos pacientes com

Endereço: Chácara Butignolli , s/n
Bairro: Rubião Junior **CEP:** 18.618-970
UF: SP **Município:** BOTUCATU
Telefone: (14)3880-1609 **E-mail:** cep@fmb.unesp.br

câncer de pulmão. A validação do modelo de predição de caquexia deve contribuir para a classificação da caquexia com potencial utilização clínica para diagnóstico precoce da caquexia e melhoria no tratamento desses pacientes.

Critério de Inclusão:
Serão aplicados os seguintes critérios: pacientes maiores de 18 anos, diagnosticados com tumores primários do pulmão, de subtipos histológicos adenocarcinoma ou carcinoma de células escamosas, de qualquer estadiamento, tendo cirurgia como tratamento primário e não tratados anteriormente com quimioterapia e/ou radioterapia.
Critério de Exclusão:
Presença de doença secundária metastática no pulmão, devido a outros tumores e história prévia de câncer, de qualquer tipo.

tamanho da amostra: 50 participantes.

Objetivo da Pesquisa:
Objetivo Primário:
Validar o modelo de predição de caquexia, gerado previamente, em um conjunto independente de pacientes com CPCNP

Avaliação dos Riscos e Benefícios:
Riscos mínimos
Benefícios:
O presente projeto utilizará de metodologia não-invasivas para classificar pacientes caquéticos. A predição de caquexia será feita avaliando apenas dados clínicos de prontuário e imagens de tomografias computadorizadas já realizadas. A validação do modelo de predição de caquexia deve contribuir para a classificação da caquexia com potencial utilização clínica para diagnóstico precoce da caquexia e melhoria no tratamento desses pacientes.

Comentários e Considerações sobre a Pesquisa:
Estudo observacional. Cronograma de execução: a coleta de dados deverá ser iniciada após aprovação do CEP. Encerramento da pesquisa consta: 01/09/2021.

Considerações sobre os Termos de apresentação obrigatória:

Termos encontram-se inseridos na Plataforma: folha de rosto, anuencia institucional (HCFMB e FMB), projeto de pesquisa. Os pesquisadores incluíram TCLE para os pacientes que ainda se encontrarem em seguimento médico no serviço. O TCLE está adequado ao estudo, em linguagem apropriada.

Recomendações:

-

Conclusões ou Pendências e Lista de Inadequações:

Após análise em REUNIÃO ORDINÁRIA, o Colegiado deliberou APROVAÇÃO do PROJETO de Pesquisa apresentado.

Considerações Finais a critério do CEP:

Conforme deliberação do Colegiado, em REUNIÃO ORDINÁRIA do Comitê de Ética em Pesquisa FMB/UNESP, realizada em 05/07/2021, do PROJETO de Pesquisa apresentado encontra-se APROVADO. Ao final da execução da pesquisa, o Pesquisador deverá enviar o Relatório Final de Atividades, na forma de Notificação, via Plataforma Brasil.

Atenciosamente,

Comitê de Ética em Pesquisa FMB/UNESP

Este parecer foi elaborado baseado nos documentos abaixo relacionados:

Tipo Documento	Arquivo	Postagem	Autor	Situação
Informações Básicas do Projeto	PB_INFORMAÇÕES_BÁSICAS_DO_PROJETO_1713229.pdf	18/05/2021 00:30:22		Aceito
TCLE / Termos de Assentimento / Justificativa de Ausência	TCLECaquexia.docx	18/05/2021 00:29:55	Erica Nishida Hasimoto	Aceito
Outros	CartaRespostaCaquexia.docx	18/05/2021 00:29:18	Erica Nishida Hasimoto	Aceito
Folha de Rosto	FolhaDeRostoAssinadaCaquexia.pdf	21/03/2021 15:16:56	Erica Nishida Hasimoto	Aceito

Outros	AnaliseDeViabilidadeDoProjetoDePesquisaCaquexia.pdf	16/03/2021 11:57:07	Erica Nishida Hasimoto	Aceito
Outros	AnuenciaHcfmb.pdf	16/03/2021 11:52:51	Erica Nishida Hasimoto	Aceito
Outros	TermoDeAnuenciaInstitucionalEAPCaquexia.pdf	16/03/2021 11:52:14	Erica Nishida Hasimoto	Aceito
Projeto Detalhado / Brochura Investigador	Projeto_CEP_caquexia.pdf	06/03/2021 15:06:55	Erica Nishida Hasimoto	Aceito

Situação do Parecer:
Aprovado

Necessita Apreciação da CONEP:
Não

BOTUCATU, 08 de Julho de 2021

Assinado por:
SILVANA ANDREA MOLINA LIMA

(Coordenador(a))

Anexo 2.

Outras publicações como primeira autora durante o doutoramento.

1. **CURY, SS**; DE MORAES, D; FREIRE, PP; DE OLIVEIRA, G; MARQUES, DVP ; FERNANDEZ, GJ ; DAL-PAI-SILVA, M; HASIMOTO, ÉN; REIS, PP; ROGATTO, SR; CARVALHO, RF. Tumor Transcriptome Reveals High Expression of IL-8 in Non-Small Cell Lung Cancer Patients with Low Pectoralis Muscle Area and Reduced Survival. *Cancers*, v. 11, p. 1251, 2019. IF: 6.575

2. DE BIAGI, CAO*; **CURY, SS***; ALVES, CP; RABHI, N; SILVA, WA; FARMER, SR; CARVALHO, RF; BATISTA, ML. Multidimensional Single-Nuclei RNA-Seq Reconstruction of Adipose Tissue Reveals Adipocyte Plasticity Underlying Thermogenic Response. *Cells*, v. 10, p. 3073, 2021. *Sharing first authorship. IF: 7.666

3. **CURY, SS**; KUASNE, H; SOUZA, JS; MUÑOZ, JJM; DA SILVA, JP; LOPES, A; SCAPULATEMPO-NETO, C; FARIA, EF; DELAISSÉ, J; MARCHI, FA; ROGATTO, SR. Interplay Between Immune and Cancer-Associated Fibroblasts: A Path to Target Metalloproteinases in Penile Cancer. *Frontiers in oncology*, v. 12, p. 935093, 2022. IF: 6.244.

4. **CURY, SS;** MIRANDA, PM; MARCHI, FA; CANTO, LM; CHULAM, TC; PETERSEN, AH; AAGAARD, MM; PINTO, CAL; KOWALSKI, LP; ROGATTO, SR. Germline variants in DNA

repair genes are associated with young-onset head and neck cancer. *Oral oncology*, v. 122, p. 105545, 2021. IF: 5.337

5. CURY, SS; LAPA, RML; DE MELLO, JBH; MARCHI, FA; DOMINGUES, MAC; PINTO, CAL; CARVALHO, RF; DE CARVALHO, GB; KOWALSKI, LP; ROGATTO, SR. Increased DSG2 plasmatic levels identified by transcriptomic-based secretome analysis is a potential prognostic biomarker in laryngeal carcinoma. *Oral oncology*, v. 103, p. 104592, 2020. IF: 5.337

6. CONSTANTINO, FB*; **CURY, SS***; NOGUEIRA, CR; CARVALHO, RF; JUSTULIN, LA. Prediction of Non-canonical Routes for SARS-CoV-2 Infection in Human Placenta Cells. *Frontiers in molecular biosciences*, v. 8, p. 614728, 2021. *Sharing first authorship. IF:4.615

Outras publicações como coautora durante o doutoramento.

Freire PP, Fernandez GJ, de Moraes D, **Cury SS**, Dal Pai-Silva M, Dos Reis PP, Rogatto SR, Carvalho RF. The expression landscape of cachexia-inducing factors in human cancers. J Cachexia Sarcopenia Muscle. 2020; 11(4):947-961. (IF = 12.063)

Beltrami, CM; do Canto, LM; Villacis, RAR; Petersen, AH; Aagaard, MM; **Cury, SS**; Formiga, MNC; Junior, SA; Rogatto, SR. The repertoire of germline variants in patients with early-onset rectal cancer. Cancer Communications, v. 1, p. 1-5, 2022. (IF = 15.283)

de Moraes D, Paiva BVB, **Cury SS**, Ludwig RG, Junior JPA, Mori MADS, Carvalho RF. Prediction of SARS-CoV Interaction with Host Proteins during Lung Aging Reveals a Potential Role for TRIB3 in COVID-19. Aging Dis. 2021; 12(1):42-49. (IF = 9.968)

Martinucci B, Cucielo MS, Minatel BC, **Cury SS**, Caxali GH, Aal MCE, Felisbino SL, Pinhal D, Carvalho RF, Delella FK. Fibronectin Modulates the Expression of miRNAs in Prostate Cancer Cell Lines. Front Vet Sci. 2022 Jul 11;9:879997.

Rodrigues BM, Mathias LS, Deprá IC, **Cury SS**, de Oliveira M, Olimpio RMC, De Sibio MT, Gonçalves BM, Nogueira CR. Effects of Triiodothyronine on Human Osteoblast-Like Cells: Novel Insights From a Global Transcriptome Analysis. Front Cell Dev Biol. 2022 Jun 17;10:886136.

Guiraldelli GG, Prado MCM, de F Lainetti P, Leis-Filho AF, Kobayashi PE, **Cury SS**, Fonseca-Alves CE, Laufer-Amorim R. Pathways Involved in the Development of Vasculogenic Mimicry in Canine Mammary Carcinoma Cell Cultures. J Comp Pathol. 2022 Apr;192:50-60.

Freire PP, **Cury SS**, Lopes LO, Fernandez GJ, Liu J, de Moraes LN, de Oliveira G, Oliveira JS, de Moraes D, Cabral-Marques O, Dal-Pai-Silva M, Hu X, Wang DZ, Carvalho RF. Decreased miR-497-5p Suppresses IL-6 Induced Atrophy in Muscle Cells. Cells. 2021 Dec 14;10(12):3527.

Carvalho RF, do Canto LM, **Cury SS**, Frøstrup Hansen T, Jensen LH, Rogatto SR. Drug Repositioning Based on the Reversal of Gene Expression Signatures Identifies TOP2A as a Therapeutic Target for Rectal Cancer. Cancers (Basel). 2021 Oct 31;13(21):5492.

Martins JRB, Moraes LN, **Cury SS**, Capannacci J, Carvalho RF, Nogueira CR, Hokama NK, Hokama POM. MiR-125a-3p and MiR-320b Differentially Expressed in Patients with Chronic Myeloid Leukemia Treated with Allogeneic Hematopoietic Stem Cell Transplantation and Imatinib Mesylate.

Mariano TB, de Souza Castilho AC, de Almeida Sabela AKD, de Oliveira AC, **Cury SS**, Aguiar AF, Dias RJD, Cicogna AC, Okoshi K, Junior LAJ, Carvalho RF, Pacagnelli FL. Preventive training does not interfere with mRNA-encoding myosin and collagen expression during pulmonary arterial hypertension. PLoS One. 2021 Sep 8;16(9):e0244768.

Kobayashi PE, Lainetti PF, Leis-Filho AF, Delella FK, Carvalho M, **Cury SS**, Carvalho RF, Fonseca-Alves CE, Laufer-Amorim R. Transcriptome of Two Canine Prostate Cancer Cells Treated With Toceranib Phosphate Reveals Distinct Antitumor Profiles Associated With the PDGFR Pathway. Front Vet Sci. 2020 Nov26;7:561212.

Martins JRB, de Moraes LN, **Cury SS**, Dadalto J, Capannacci J, Carvalho RF, Nogueira CR, Hokama NK, Hokama POM. Comparison of microRNA Expression Profile in Chronic Myeloid Leukemia Patients Newly Diagnosed and Treated by Allogeneic Hematopoietic Stem Cell Transplantation.

Faldoni FLC, Villacis RAR, Canto LM, Fonseca-Alves CE, **Cury SS**, Larsen SJ, Aagaard MM, Souza CP, Scapulatempo-Neto C, Osório CABT, Baumbach J, Marchi FA, Rogatto SR. Inflammatory Breast Cancer: Clinical Implications of Genomic Alterations and Mutational Profiling. Cancers (Basel). 2020 Sep 30;12(10):2816.

Freire PP, Fernandez GJ, de Moraes D, **Cury SS**, Dal Pai-Silva M, Dos Reis PP, Rogatto SR, Carvalho RF. The authors reply: Comment on "The expression landscape of cachexia-inducing factors in human cancers" by Freire et al. J Cachexia Sarcopenia Muscle. 2020 Dec;11(6):1854-1857.

Chuffa LGA, Carvalho RF, Justulin LA, **Cury SS**, Seiva FRF, Jardim-Perassi BV, Zuccari DAPC, Reiter RJ. A meta-analysis of microRNA networks regulated by melatonin in cancer: Portrait of potential candidates for breast cancer treatment. J Pineal Res. 2020 Nov;69(4):e12693.

Fernandez GJ, Ferreira JH, Vechetti IJ Jr, de Moraes LN, **Cury SS**, Freire PP, Gutiérrez J, Ferretti R, Dal-Pai-Silva M, Rogatto SR, Carvalho RF. MicroRNA-mRNA Co-sequencing Identifies Transcriptional and Post-transcriptional Regulatory Networks Underlying Muscle Wasting in Cancer Cachexia. Front Genet. 2020 May 29;11:541.

de Oliveira G, Freire PP, **Cury SS**, de Moraes D, Oliveira JS, Dal-Pai-Silva M, Reis PP, Carvalho RF. An Integrated Meta-Analysis of Secretome and Proteome Identify Potential Biomarkers of Pancreatic Ductal Adenocarcinoma. Cancers (Basel). 2020 Mar 18;12(3):716.

Canto LMD, **Cury SS**, Barros-Filho MC, Kupper BEC, Begnami MDFS, Scapulatempo-Neto C, Carvalho RF, Marchi FA, Olsen DA, Madsen JS, Havelund BM, Aguiar S Jr, Rogatto SR. Locally advanced rectal cancer transcriptomic-based secretome analysis reveals novel biomarkers useful to identify patients according to neoadjuvant chemoradiotherapy response. Sci Rep. 2019 Jun 18;9(1):8702.

Freire PP, Fernandez GJ, **Cury SS**, de Moraes D, Oliveira JS, de Oliveira G, Dal-Pai-Silva M, Dos Reis PP, Carvalho RF. The Pathway to Cancer Cachexia: MicroRNA-Regulated Networks in Muscle Wasting Based on Integrative Meta-Analysis. Int J Mol Sci. 2019 Apr 22;20(8):1962.

Publicações em revisão.

Sarah Santiloni Cury, Diogo de Moraes, Jakeline Oliveira, Paula Paccielli Freire, Patricia P Reis, Miguel Luiz Batista Jr, Érica Nishida Hasimoto, Robson Francisco Carvalho. Lung cancer cachexia is associated with an inflammatory and immunosuppressive tumor microenvironment. Journal of Cachexia, Sarcopenia and Muscle.

Cury SS, Oliveira J, Biagi-Júnior CAO, Silva Jr WA, Reis PP, Hasimoto EN, Freire PP, Carvalho RF. Transcriptional profiles and common genes link lung cancer with the development and severity of COVID-19. Gene.

Diogo de Moraes, Felippe Mousovich-Neto, **Sarah Santiloni Cury**, Jakeline Oliveira, Jeferson dos Santos Souza, Paula Paccielli Freire, Maeli Dal Pai, Marcelo A. Mori, Geysson Javier Fernandez, Robson Francisco Carvalho. The transcriptomic landscape of age-induced changes in human visceral fat and the predicted omentum-liver connectome in males. Aging Cell.